Supporting Information

Exploring the substitution effect on the magnetic coupling of tetrazinyl-bridged Ln_2 single-molecule magnets

Niki Mavragani,[a] Alexandros A. Kitos,[a] Rezeda Gayfullina,[b] Akseli Mansikkamäki,*[c] Jani O. Moilanen,*[b] and Muralee Murugesu*[a]

Table of Contents:

[a] *Department of Chemistry and Biomolecular Sciences, University of Ottawa, 10 Marie Curie, Ottawa, Ontario, K1N 6N5, Canada.*
[b] *Department of Chemistry, Nanoscience Centre, University of Jyväskylä, P.O. Box 35, FI-40014, Finland.*
[c] *NMR Research Unit, University of Oulu, P.O. Box 8000, Oulu FI-90014, Finland.*
E-mail: akseli.mansikkamaki@oulu.fi; jani.o.moilanen@jyu.fi; m.murugesu@uottawa.ca

1. Experimental Section

General Procedures and Materials: All operations were performed in a Mbraun glovebox under an N_2 atmosphere. Solvents were dried using a J. C. Meyer solvent system, degassed by free-pump-thaw method and stored over activated 4 Å molecular sieves prior to use. The 3,6-dimethyl-1,2,4,5-tetrazine (dmtz), 3,6-dimethoxy-1,2,4,5-tetrazine (dmeotz), 1,2,4,5-tetrazine (tz) and 3,6-dichloro-1,2,4,5-tetrazine ligands were prepared according to the literature.[1–4] The 3,6-bis(3,5-dimethyl-pyrazolyl)-1,2,4,5-tetrazine (bpytz), which was used as a precursor for the synthesis of dmeotz and dctz, was prepared according to the literature.[5] $[Cp^*_2Ln][BPh_4]$ (Ln = Gd^{III}, Dy^{III}) starting materials were prepared according to the literature.[6] All reagents were purchased from TCI, Alfa Aesar, or Strem Chemicals and used without further purification. HCp* (99+%) was purchased from Alfa Aesar and was degassed/dried as previously described prior to use. FT-IR spectra were recorded on an Agilent Technologies Cary 630 FTIR spectrometer in the transmission window of 600-4000 cm^{-1}. Elemental Analysis was performed by Midwest Microlab.

Synthesis of $[(Cp^*_2Gd)_2(dmtz^{\bullet-})(THF)_2][BPh_4]\cdot THF$ (1-Gd): In 8 mL THF, one equivalent of dmtz (0.125 mmol, 14 mg) was combined with one equivalent of $[Cp^*_2Gd][BPh_4]$ (0.125 mmol, 93 mg). The colour of the solution gradually became dark purple (almost black) upon stirring. The reaction solution was left to stir for 3 hours and then was filtered. Upon slow diffusion with Et_2O at low temperature, dark purple crystals of **1-Gd** were isolated after one week in 45% yield. Elemental Analysis (**1-Gd** was analyzed as solvent free): Calcd: C, 63.88 %; H, 7.19 %; N, 3.92%, Found: C, 63.49%; H, 6.86%; N, 3.51%.

Synthesis of $[(Cp^*_2Dy)_2(dmtz^{\bullet-})(THF)_2][BPh_4]\cdot THF$ (1-Dy):This complex was prepared in a similar manner as **1-Gd** by simply replacing $[Cp^*_2Gd][BPh_4]$ with $[Cp^*_2Dy][BPh_4]$ (0.125 mmol, 94 mg) in **1-Dy.** Yield = 48%. Elemental Analysis (**1-Dy** was analyzed as solvent free): Calcd: C, 63.41%; H, 7.14%; N, 3.89%, Found: C, 63.06%; H, 7.07%; N, 3.66%

Synthesis of $[(Cp^*_2Gd)_2(dmeotz^{\bullet-})(THF)][BPh_4]$ (2-Gd): In 4 mL THF,one equivalent of dmeotz (0.125 mmol, 16 mg) was added to one equivalent of Cp_2Co (0.125 mmol, 24 mg), changing the colour of the ligand to dark red. The dark red solution was added to a THF (4 mL) solution of two equivalents of $[Cp^*_2Gd][BPh_4]$ (0.25 mmol, 187mg), resulting in a dark red-brown slurry. The reaction was left to stir for 2 hours and then filtered. Upon slow diffusion with Et_2O, dark red-green (dichroic) crystals of **2-Gd** were isolated over the period of one week in 55% yield. Elemental Analysis: Calcd: C, 62.27%; H, 6.82%; N, 4.03%, Found: C, 62.02%; H, 6.38%; N, 3.91%.

Synthesis of $[(Cp^*_2Dy)_2(dmeotz^{\bullet-})(THF)][BPh_4]$ (2-Dy): This complex was prepared in a similar manner as **2-Gd** by simply replacing $[Cp^*_2Gd][BPh_4]$ with $[Cp^*_2Dy][BPh_4]$ (0.25 mmol, 188 mg) in **2-Dy.** Yield = 53%. Elemental Analysis: Calcd: C, 61.80%; H, 6.77%; N, 4.00%, Found: C, 61.52%; H, 6.76%; N, 3.57%

UV-Vis Spectroscopy: UV-visible spectra were recorded on samples dissolved in dichloromethane (DCM) at ambient temperature using an Agilent Cary 5000 UV-Vis-NIR spectrophotometer. Measurements were completed in the range of 250-800 nm with solutions occupying standard 10 mm pathlength cuvettes.

Electrochemical Analysis: Cyclic voltammetry (CV) was performed using a Princeton Applied Research Versastat 3 potentiostat employing a glass cell, platinum auxiliary wires for the counter and pseudo-reference electrodes, and a glassy carbon electrode as a working electrode. The measurements were carried out in dichloromethane (DCM) solutions (dried by J. C. Meyer solvent system and stored over molecular sieves for several days prior to use) containing 0.1 M tetrabutylammonium hexafluorophosphate (Sigma Aldrich) as supporting electrolyte with a scan rate of 100 mV/s. The experiments were referenced to the Fc/Fc^{+} redox couple of ferrocene (Sigma Aldrich) at +0.48 V vs. SCE.

Single Crystal X-ray Diffraction: Suitable crystals of **1-Gd**, **1-Dy**, **2-Gd** and **2-Dy** for single-crystal X-ray diffraction (SCXRD) analysis were covered in parabar oil and mounted on a MiTeGen MicroLoop. Full data (Table S2) were collected on a Bruker KAPPA APEX-II CCD single-crystal diffractometer (graphite monochromated Mo-Kα radiation, λ = 0.71073 Å), at 213 K (**1-Gd**) and 200 K (**1-Dy**, **2-Gd** and **2-Dy**) temperatures. Absorption corrections were applied by using multi-scan of the SADABS[7] program. All structures were solved using direct methods with SHELXT[8] and refined by the full-matrix least-squares methods on F^2 with SHELXL-2018/3[9] in anisotropic approximation for all non-hydrogen atoms. All carbon-bound hydrogen atoms were generated geometrically and were included in the refinement in the riding model approximation. The temperature factors of all H atoms were set to multiple of the equivalent isotropic temperature factors of the parent site (aromatic and methylene 1.2 times; methyl 1.5 times the factor). In structures **2-Gd** and **2-Dy**, there is a positional disorder on one and two Cp* ligands and the coordinated THF solvent molecules, respectively. After careful refinement, the ratio was found to be close to 52:48 % for the THF molecules and 75:25 % for the Cp* ligands, where the disordered components were left to refine with free variables. Soft restraints were used to handle the disorder groups (SIMU, SADI, ISOR, DFIX etc). A few discordant reflections with error/esd > 10 (1 reflection for **1-Gd**; 10 reflections for **1-Dy** and **2-Gd**; 4 reflections for **2-Dy**) have been omitted from the refinement. All geometric/crystallographic calculations were carried out using PLATON[10] and WINGX[11] packages while the molecular/packing graphics were prepared with DIAMOND[12] and MERCURY.[13]

Magnetic Measurements: Magnetic susceptibility measurements were obtained using a Quantum Design SQUID magnetometer MPMS-XL7 operating between 1.8 and 300 K. Direct current (dc) measurements were performed on 14 mg (**1-Gd**), 13 mg (**1-Dy**), 21 mg (**2-Gd**) and 16 mg (**2-Dy**) of crushed polycrystalline samples, which were restrained with silicon grease and sealed in a polyethylene membrane, under an inert atmosphere, for which diamagnetic corrections were applied. The samples were subjected to dc fields of 70 to -70 kOe, while alternating current (ac) measurements took place in the absence of a static dc field (H_{dc} = 0 Oe).

2. Cyclic voltammetry and UV-Vis absorption spectroscopy

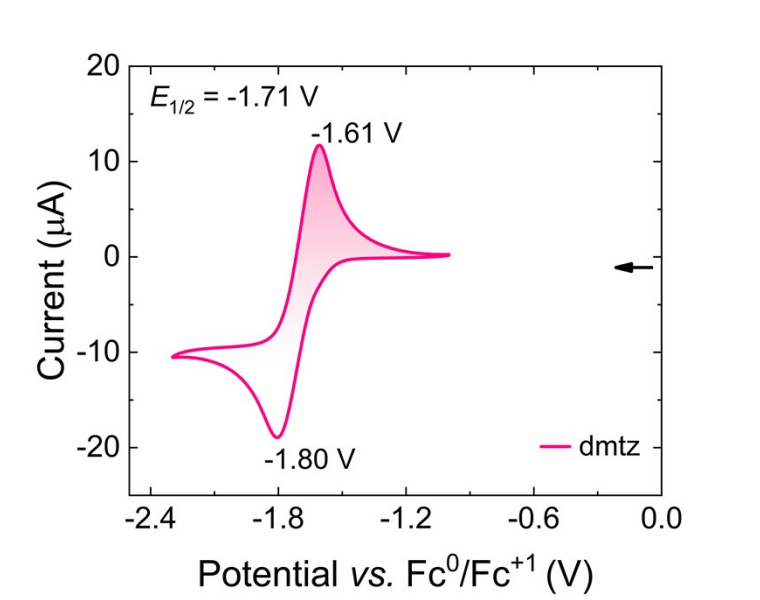

Fig. S1: Cyclic voltammograms of dmtz measured in dichloromethane (DCM) at room temperature with $[Bu_4N][PF_6]$ (0.1 M) as supporting electrolyte, using a scan rate of 0.1 V/s.

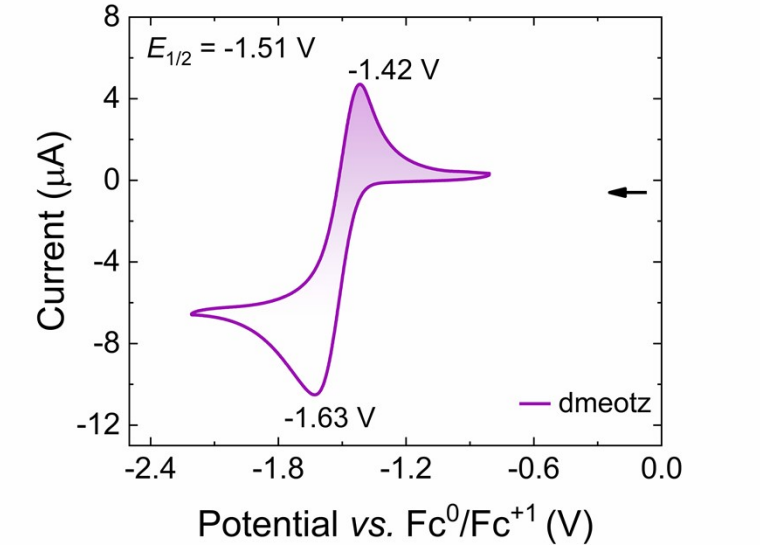

Fig. S2: Cyclic voltammograms of dmeotz measured in dichloromethane (DCM) at room temperature with $[Bu_4N][PF_6]$ (0.1 M) as supporting electrolyte, using a scan rate of 0.1 V/s.

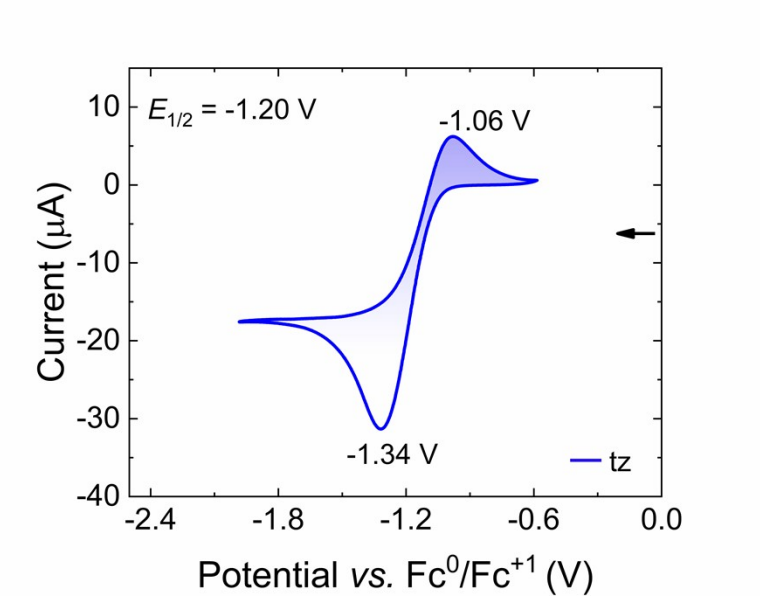

Fig. S3: Cyclic voltammograms of tz measured in dichloromethane (DCM) at room temperature with $[Bu_4N][PF_6]$ (0.1 M) as supporting electrolyte, using a scan rate of 0.1 V/s.

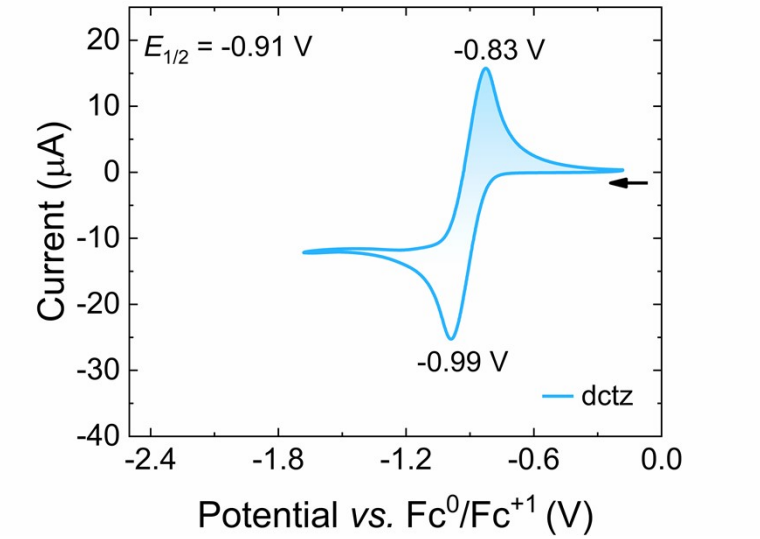

Fig. S4: Cyclic voltammograms of dctz measured in dichloromethane (DCM) at room temperature with $[Bu_4N][PF_6]$ (0.1 M) as supporting electrolyte, using a scan rate of 0.1 V/s.

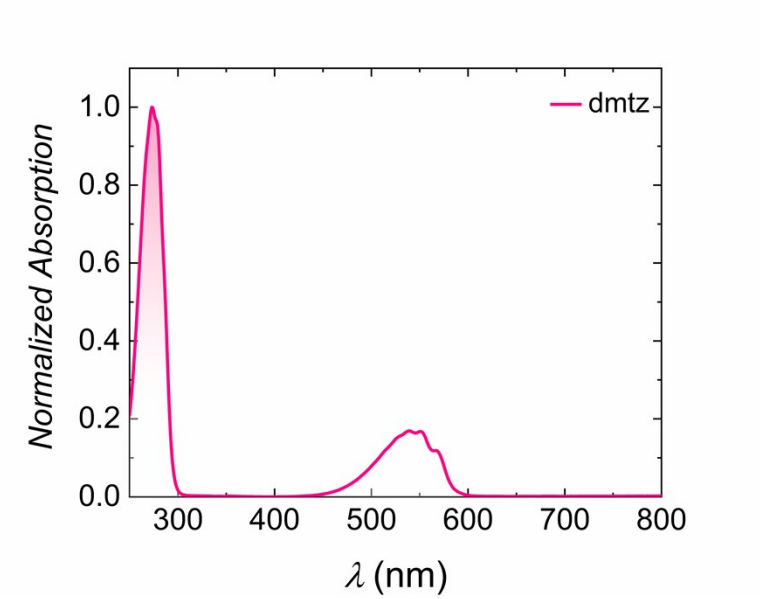

Fig. S5: UV-Vis absorption spectra of dmtz in dichloromethane (DCM) at room temperature.

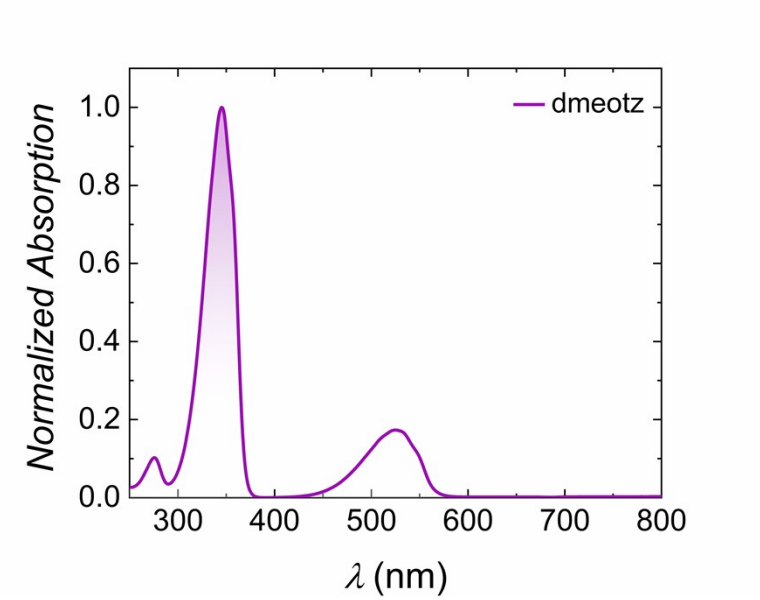

Fig. S6: UV-Vis absorption spectra of dmeotz in dichloromethane (DCM) at room temperature.

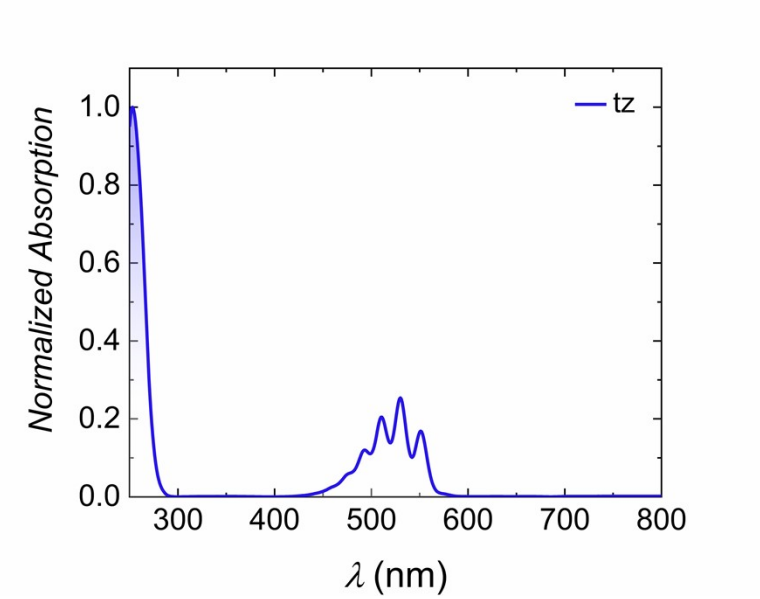

Fig. S7: UV-Vis absorption spectra of tz in dichloromethane (DCM) at room temperature.

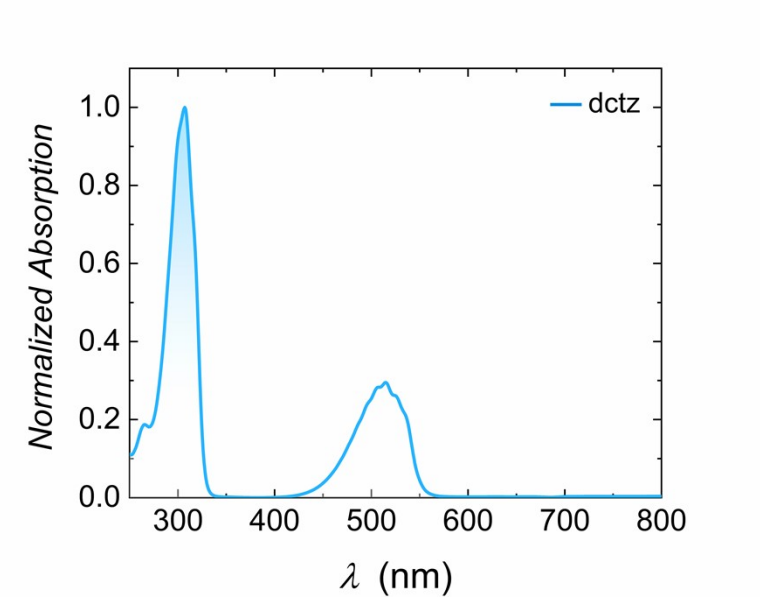

Fig. S8: UV-Vis absorption spectra of dctz in dichloromethane (DCM) at room temperature.

Calculation of the HOMO and LUMO frontier molecular orbitals of all tetrazines from the experimental CV and UV-Vis absorption data:

To further investigate the effect of the substituent on the redox and optoelectronic properties of dmtz, dmeotz, tz and dctz, their frontier molecular orbitals (FMOs) were calculated both *via* experimental and computational means. From the cyclic voltammograms, the LUMO level can be calculated using the following eq. (S1):[14]

$$E_{LUMO}\,(eV) = e((E_{red} - E_{Fc/Fc+}) + 4.8) \qquad (S1)$$

where E_{LUMO} is the energy level (in eV) of the LUMO FMO, e is the number of electrons involved in the redox process (for dmtz, dmeotz, tz and dctz this is 1), E_{red} is the potential at which the corresponding redox process is occurring (in V), after calibration of the ferrocene signal ($E_{Fc/Fc+}$ = +0.48 V *vs.* SCE for DCM solutions using 0.1 M of $[Bu_4N][PF_6]$ as supporting electrolyte). Given that only a quasi-reversible one-electron reduction process is visible in the cyclic voltammograms of these tetrazines, the HOMO energy cannot be calculated from these experiments.

However, the energy gap (E_{gap}), i.e. the smallest possible electronic transition and thus the minimal amount of energy needed to promote an electron to a MO of higher energy, can be obtained *via* UV-Vis absorption spectroscopy. The onset wavelength of the absorption band in the visible region of the spectra can be used to measure the bang gap using the following eq. (S2):

$$E_{gap}\,(J) = \frac{hc}{\lambda} \qquad (S2)$$

where, *h* is Planck's constant (6.626 x 10^{-34} J·s), c is the speed of light in a vacuum (2.998 x 10^8 m/s) and λ is the onset wavelength of absorption. Rearrangement of the unit sets and the constants *h* and *c* we can simplify eq. (2) to: $E_{gap}\,(eV) = 1240/\lambda$.[14]

As such, the HOMO energy can be deduced from the electrochemically obtained LUMO energy and the optically-measured energy gap (E_{gap}) using the following eq. (S3):

$$E_{HOMO}\,(eV) = E_{LUMO} - E_{gap} \qquad (S3)$$

Table S1. Redox potential, onset wavelength, E_{gap} and FMO levels for dmtz, dmeotz, tz and dctz.

	Reduction Potential ($E_{1/2}$) (V *vs.* Fc/Fc$^+$)	λ_{onset} (nm)	[a]E_{gap} (eV)	[b]E_{gap} (eV)	[a]HOMO (eV)	[a]LUMO (ev)	[b]HOMO (eV)	[b]LUMO (ev)
dmtz	-1.71	586	2.12	2.13	-4.73	-2.61	-6.66	-3.29
dmeotz	-1.51	565	2.19	2.39	-5.00	-2.81	-6.69	-3.04
tz	-1.20	568	2.18	2.38	-5.31	-3.13	-6.77	-3.13
dctz	-0.91	550	2.25	2.42	-5.66	-3.41	-7.59	-3.92

[a] The experimentally determined HOMO-LUMO E_{gap}, as well as the HOMO and LUMO levels. [b] The DFT calculated HOMO-LUMO E_{gap}, as well as the HOMO and LUMO levels. Energy gaps were calculated at the CAM-B3LYP/def2-TZVPP level of theory as an energy difference of the ground and first excited state, whereas the energies of HOMOs and LUMOs were extracted from the B3LYP/def2-TZVPP calculations. Thus, the calculated energy gaps present the so-called optical energy gaps.[15] Both the B3LYP and CAM-B3LYP calculations were performed using Gaussian 16.[16]

3. IR Spectroscopy

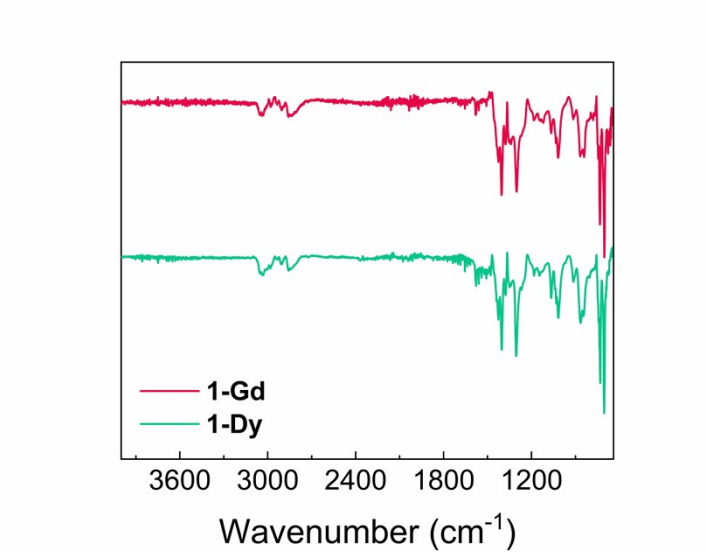

Fig. S9: Solid-state infrared (IR) spectra of complexes **1-Gd** (magenta) and **1-Dy** (teal).

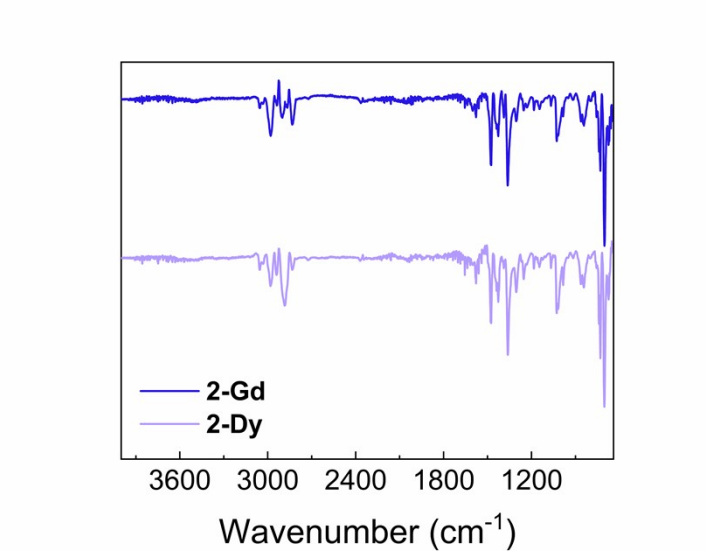

Fig. S10: Solid-state infrared (IR) spectra of complexes **2-Gd** (blue) and **2-Dy** (violet).

4. Single-crystal X-ray data and molecular features

Table S2. Crystallographic data and refinement details for **1-Gd**, **1-Dy**, **2-Gd** and **2-Dy**.

Compound reference	1-Gd	1-Dy	2-Gd	2-Dy
Chemical formula	$C_{80}H_{110}BGd_2N_4O_3$	$C_{80}H_{110}BDy_2N_4O_3$	$C_{72}H_{94}BGd_2N_4O_3$	$C_{72}H_{94}BDy_2N_4O_3$
Formula mass	1501.02	1511.52	1388.82	1399.32
Crystal system	Monoclinic	Monoclinic	Triclinic	Triclinic
a/Å	11.4420(4)	11.4098(4)	14.7079(4)	14.6753(6)
b/Å	14.4505(6)	14.3772(6)	15.7698(4)	15.6865(6)
c/Å	22.8062(8)	22.7954(9)	15.9308(4)	15.9328(6)
α/°	90	90	92.0670(10)	92.173(2)
β/°	100.137(2)	99.705(2)	115.074(2)	114.768(3)
γ/°	90	90	93.0180(10)	93.217(2)
Unit cell volume/Å^3	3712.0(2)	3685.9(2)	3335.18(16)	3317.5(2)
Temperature/K	213(2)	200(2)	200(2)	200(2)
Space group	*P*2/c	*P*2/c	$P\bar{1}$	$P\bar{1}$
No. of formula units/unit cell, *Z*	2	2	2	2
Radiation type	Mo Kα	Mo Kα	Mo Kα	Mo Kα
Absorption coefficient, *μ*/mm^{-1}	1.820	2.060	2.019	2.283
No. of reflections measured	53956	49472	124566	138583
No. of independent reflections	8122	8065	14538	15558
Data / parameters / restraints	8122 / 418 / 225	8065 / 418 / 226	14538 / 919 / 597	15558 / 853 / 355
R_{int}	0.0332	0.0531	0.0273	0.0271
Final R_1 values (all data)	0.0485	0.0689	0.0366	0.0345
Final $wR_2(F^2)$ values (all data)	0.0976	0.1547	0.0744	0.0716
Final R_1 values ($I > 2\sigma(I)$)	0.0363	0.0555	0.0289	0.0287
Final $wR_2(F^2)$ values ($I > 2\sigma(I)$)	0.0880	0.1461	0.0668	0.0659
Goodness of fit on F^2	1.108	1.181	1.084	1.116
Largest diff. peak and hole (eÅ^{-3})	1.127 / -0.858	2.006 / -0.918	1.579 / -1.187	1.697 / -1.175
CCDC number	2373023	2373024	2373025	2373026

Table S3. Selected bond distances (Å) and angles (º) for **1-Gd** and **1-Dy**.

Distance/angle			Distance/angle
1-Gd			
Gd−Gd′	7.055(4)	Gd−O	2.452(3)
Gd−N1	2.429(3)	Gd−N2′	2.495(3)
Gd−Cp^*_{cent}A	2.444(4)	Gd−Cp^*_{cent}B	2.444(4)
Gd−$dmtz_{cent}$	3.527(7)	N1−N2′	1.393(4)
C1−N1	1.322(5)	C1−N2	1.324(5)
O−Gd−Cp^*_{cent}A	100.71(72)	O−Gd−Cp^*_{cent}B	103.13(76)
N1−Gd−Cp^*_{cent}A	100.81(71)	N1−Gd−Cp^*_{cent}B	98.77(80)
N2′−Gd−Cp^*_{cent}A	112.98(69)	N2′−Gd−Cp^*_{cent}B	103.91(78)
Cp^*_{cent}A−Gd−Cp^*_{cent}B	137.41(12)	N1−Gd−N2′	32.84(1)
1-Dy			
Dy−Dy′	7.013(4)	Dy−O	2.433(4)
Dy−N1	2.395 (6)	Dy−N2′	2.472(4)
Dy−Cp^*_{cent}A	2.414(4)	Dy−Cp^*_{cent}B	2.401(3)
Dy−$dmtz_{cent}$	3.506(3)	N1−N2′	1.382(7)
C1−N1	1.332(8)	C1−N2	1.333(7)
O−Dy−Cp^*_{cent}A	100.62(11)	O−Dy−Cp^*_{cent}B	102.88(12)
N1−Dy−Cp^*_{cent}A	101.02(12)	N1−Dy−Cp^*_{cent}B	99.00(14)
N2′−Dy−Cp^*_{cent}A	112.95(14)	N2′−Dy−Cp^*_{cent}B	104.21(11)
Cp^*_{cent}A−Dy−Cp^*_{cent}B	137.48(12)	N1−Dy−N2′	32.95(17)

Cp^*_{cent}A: C7-C11; Cp^*_{cent}B: C17-C21.

Table S4. Selected bond distances (Å) and angles (º) for **2-Gd** and **2-Dy**.

Distance/angle			Distance/angle
2-Gd			
Gd1−Gd2	7.0269(5)	Gd2−O3	2.454(2)
Gd1−N1	2.454(3)	Gd2−N3	2.474(3)
Gd1−N2	2.386(3)	Gd2−N4	2.454(3)
Gd1−Cp^*_{cent}A	2.428(2)	Gd2−Cp^*_{cent}C	2.417(5)
Gd1−Cp^*_{cent}B	2.367(4)	Gd2−Cp^*_{cent}D	2.435(5)
Gd1−$dmeotz_{cent}$	3.486(6)	Gd2−$dmeotz_{cent}$	3.541(3)
N1−N2	1.407(3)	N3−N4	1.374(3)
C1−N1	1.322(5)	C1−N4	1.327(5)
C2−N2	1.313(5)	C2−N3	1.331(5)
Cp^*_{cent}A−Gd1−Cp^*_{cent}B	139.34(2)	Cp^*_{cent}C−Gd2−Cp^*_{cent}D	136.98(2)
N1−Gd1−N2	33.75(9)	N3−Gd2−N4	32.37(9)
N1−Gd1−Cp^*_{cent}A	110.81(6)	N3−Gd2−Cp^*_{cent}C	107.93(6)
N1−Gd1−Cp^*_{cent}B	109.48(3)	N3−Gd2−Cp^*_{cent}D	109.30(7)
N2−Gd1−Cp^*_{cent}A	108.72(2)	N4−Gd2−Cp^*_{cent}C	99.36(8)
N2−Gd1−Cp^*_{cent}B	107.64(1)	N4−Gd2−Cp^*_{cent}D	100.57(2)
2-Dy			
Dy1−Dy2	6.981(6)	Dy2−O3	2.432(2)
Dy1−N1	2.428(3)	Dy2−N3	2.451(3)
Dy1−N2	2.361(3)	Dy2−N4	2.434(3)
Dy1−Cp^*_{cent}A	2.378(3)	Dy2−Cp^*_{cent}C	2.387(6)
Dy1−Cp^*_{cent}B	2.335(4)	Dy2−Cp^*_{cent}D	2.406(5)
Dy1−$dmeotz_{cent}$	3.462(1)	Dy2−$dmeotz_{cent}$	3.521(2)
N1−N2	1.401(3)	N3−N4	1.373(3)
C1−N1	1.326(5)	C1−N4	1.328(5)
C2−N2	1.315(5)	C2−N3	1.334(5)
Cp^*_{cent}A−Dy1−Cp^*_{cent}B	139.60(2)	Cp^*_{cent}C−Dy2−Cp^*_{cent}D	136.72(2)
N1−Dy1−N2	34.00(9)	N3−Dy2−N4	32.63(9)
N1−Dy1−Cp^*_{cent}A	110.56(1)	N3−Dy2−Cp^*_{cent}C	108.18(2)
N1−Dy1−Cp^*_{cent}B	109.26(4)	N3−Dy2−Cp^*_{cent}D	109.74(6)
N2−Dy1−Cp^*_{cent}A	109.05(6)	N4−Dy2−Cp^*_{cent}C	99.69(7)
N2−Dy1−Cp^*_{cent}B	107.56(8)	N4−Dy2−Cp^*_{cent}D	100.99(8)

Cp^*_{cent}A: C9-C13; Cp^*_{cent}B: C19-C23; Cp^*_{cent}C: C29-C33; Cp^*_{cent}D: C39-C43.

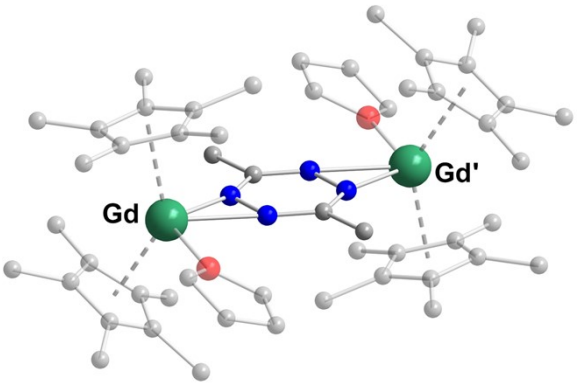

$[(Cp^*_2Gd)_2(dmtz^{\bullet-})(THF)][BPh_4]$

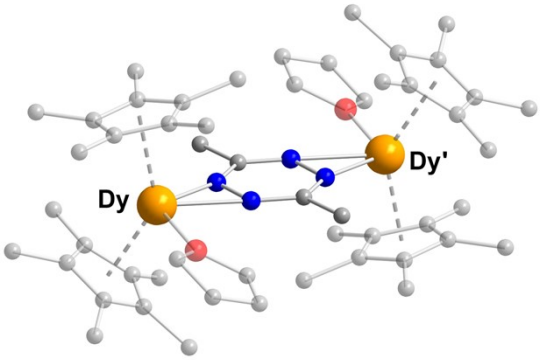

$[(Cp^*_2Dy)_2(dmtz^{\bullet-})(THF)][BPh_4]$

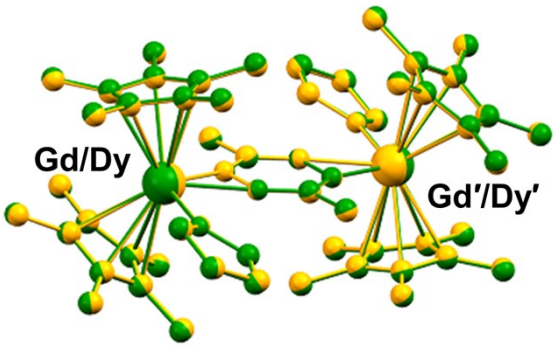

Fig. S11: Molecular structures of **1-Gd** (top) and **1-Dy** (middle), as well as structural overlay (bottom) of **1-Gd** (green) and **1-Dy** (orange), highlighting that both complexes are isostructural. For clarity reasons BPh_4^- moieties, THF solvent molecules and H-atoms have been omitted.

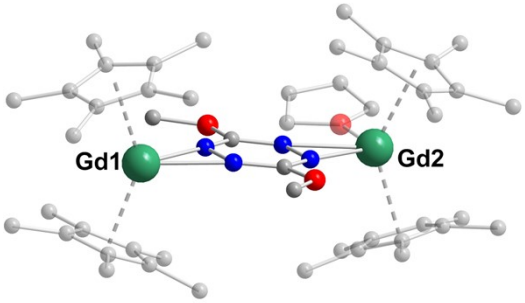

[(Cp*$_2$Gd)$_2$(dmeotz$^{\bullet-}$)(THF)][BPh$_4$]

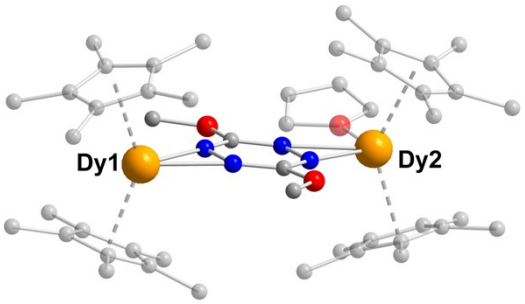

[(Cp*$_2$Dy)$_2$(dmeotz$^{\bullet-}$)(THF)][BPh$_4$]

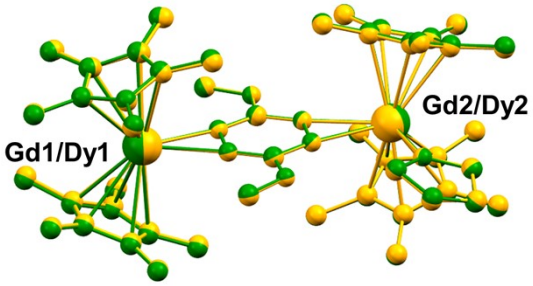

Fig. S12: Molecular structures of **2-Gd** (top) and **2-Dy** (middle), as well as structural overlay (bottom) of **2-Gd** (green) and **2-Dy** (orange), highlighting that both complexes are isostructural. For clarity reasons BPh_4^- moieties, disorder conformers and H-atoms have been omitted.

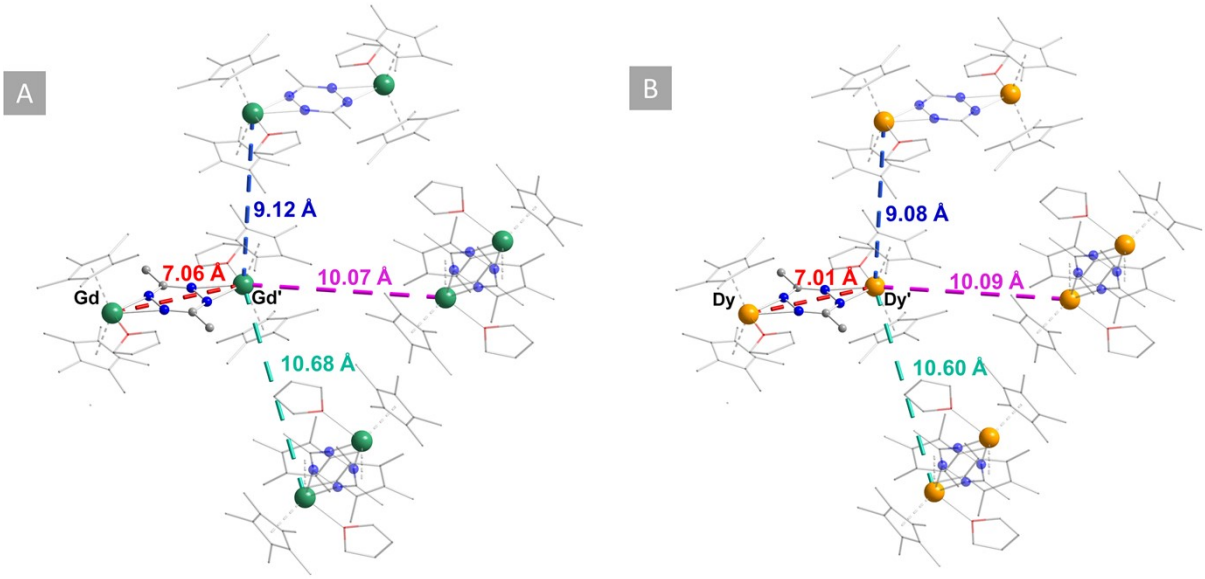

Fig. S13: Intramolecular and intermolecular Ln···Ln distances for **1-Gd** (A) and **1-Dy** (B). For clarity reasons, partial transparency has been employed and BPh_4^-, H-atoms and lattice solvent molecules have been omitted. Each Ln···Ln distance is colour coded.

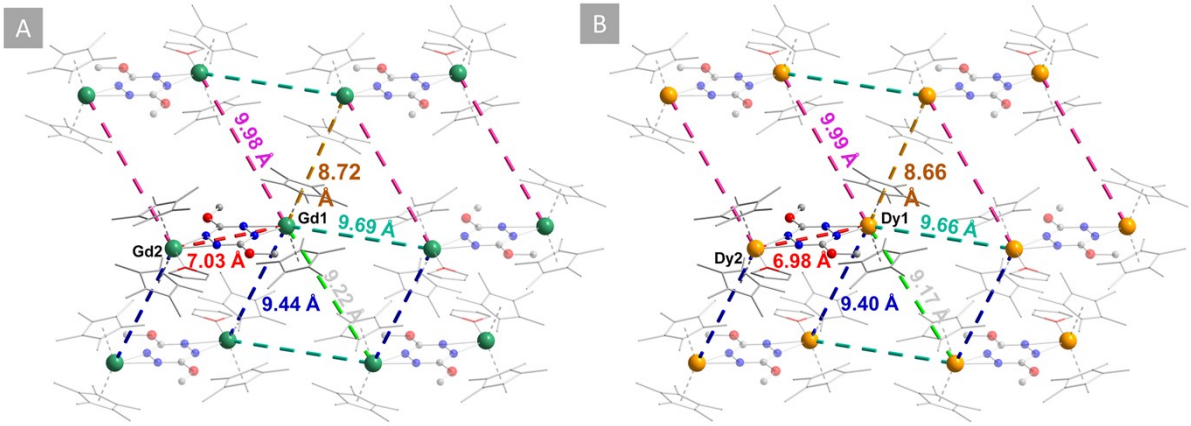

Fig. S14: Intramolecular and intermolecular Ln···Ln distances for **2-Gd** (A) and **2-Dy** (B). For clarity reasons, partial transparency has been employed and BPh_4^-, as well as H-atoms and disorder conformers have been omitted. Each Ln···Ln distance is colour coded.

5. Additional dc magnetic data for complexes 1-Ln and 2-Ln

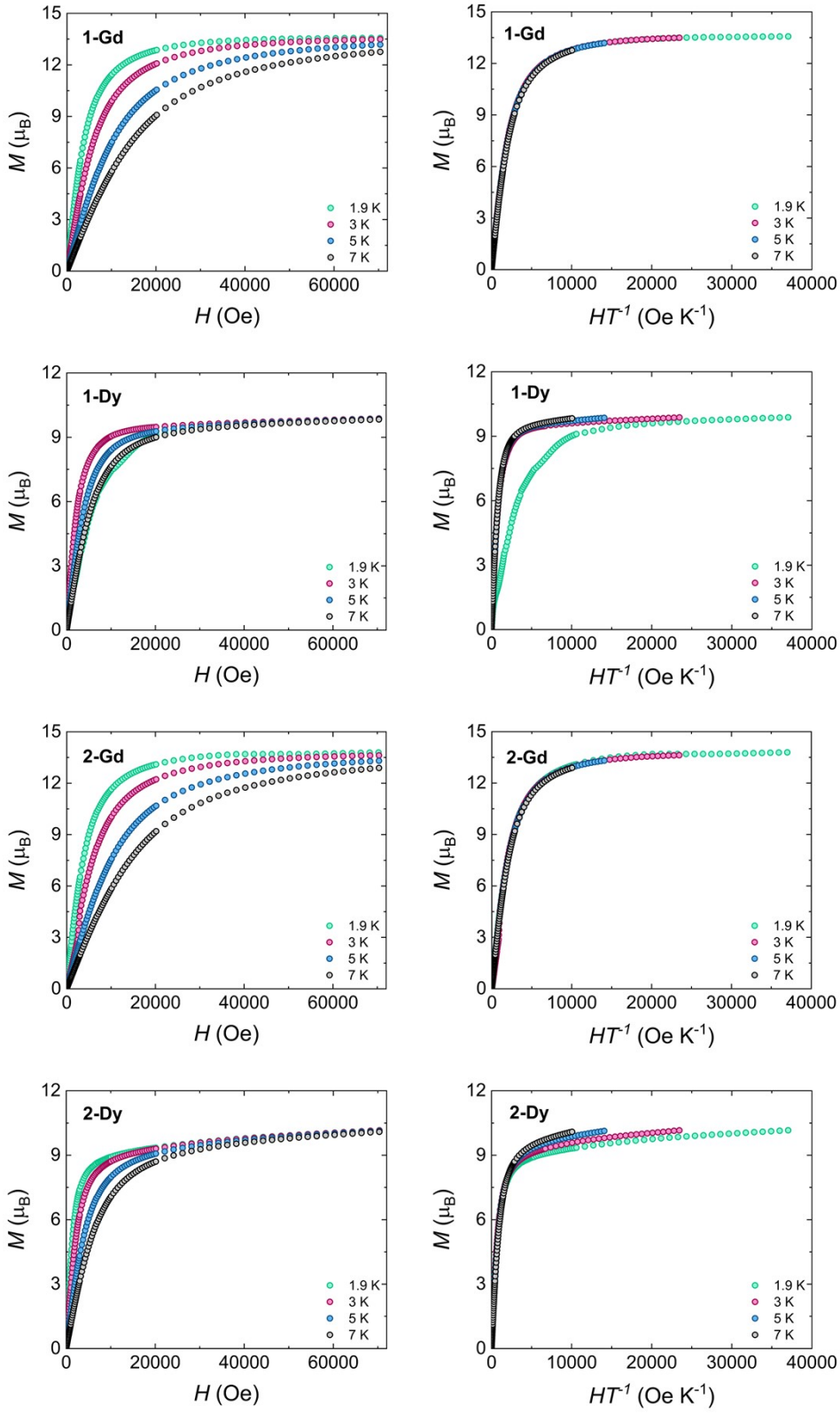

Fig. S15: Field dependence of the magnetization (top) and the reduced magnetization (bottom) for **1-Gd**, **1-Dy**, **2-Gd** and **2-Dy** at the indicated temperatures.

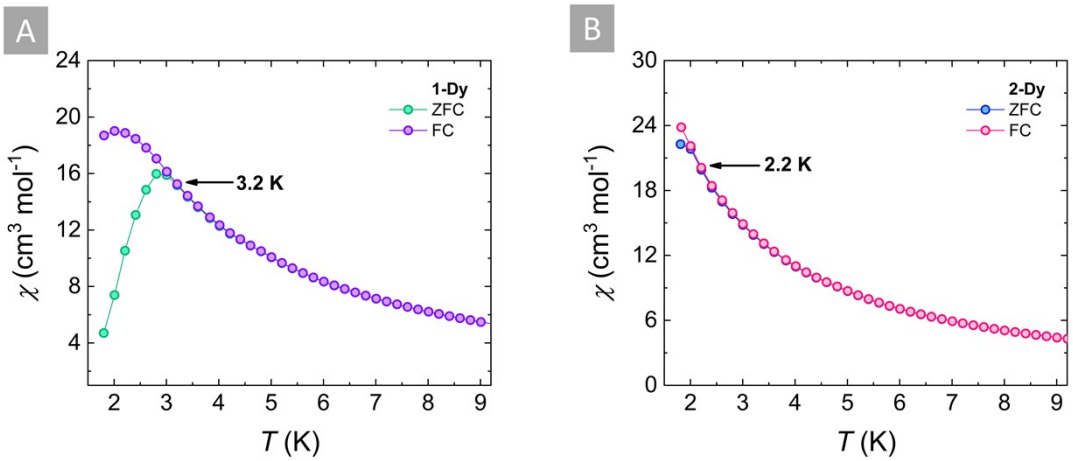

Fig. S16: Zero-field-cooled and field-cooled (ZFC/FC) curves for **1-Dy** (A) and **2-Dy** (B) under an applied static field of 1000 Oe. Data were collected at an average sweep rate of 0.2 K min^{-1}. ZFC and FC susceptibilities bifurcate at 3.2 K for **1-Dy** and 2.2 K for **2-Dy**, as indicated by the respective black arrows.

6. Computational details and discussion

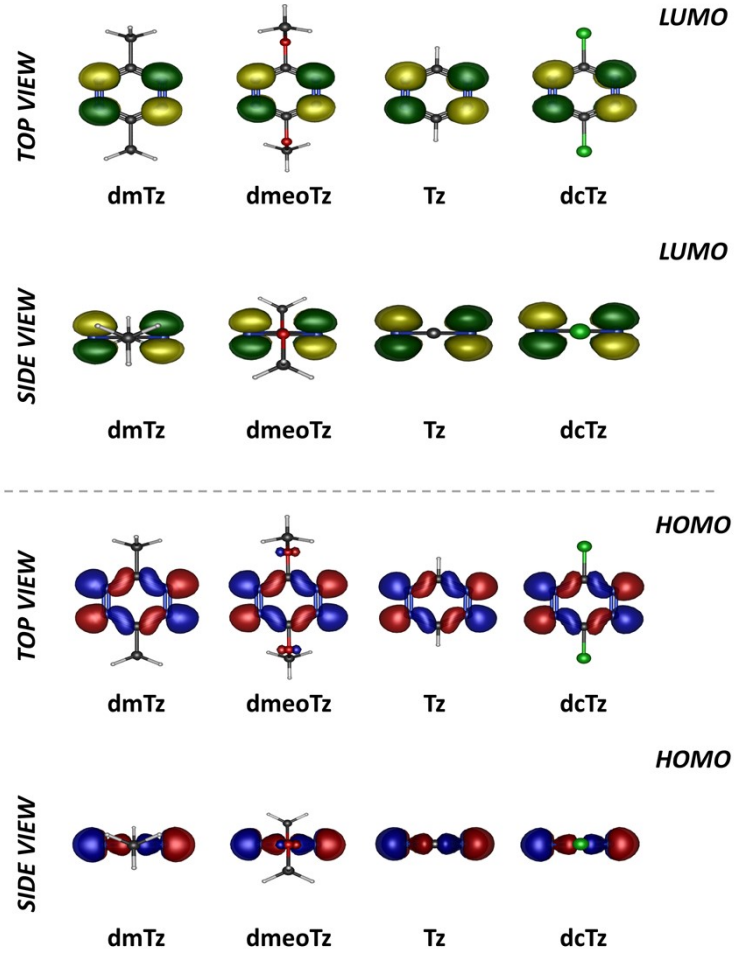

Fig. S17: DFT calculated frontier molecular orbitals for dmtz, dmeotz, tz and dctz, respectively.

The SA-CASSCF[17,18] calculations were performed for each individual Dy^{III} ion present in the radical-bridged complexes **1-Dy** and **2-Dy** utilizing the OpenMolcas quantum chemistry software version 20.11.[19] Before conducting the SA-CASSCF calculations, the positions of the hydrogen atoms were optimized at the density functional theory (DFT) level using the same functional and basis set as described below. In the SA-CASSCF calculations, one of the Dy^{III} ions was substituted with a Y^{III} ion, and the $dmtz^{\bullet-}$ and $dmeotz^{\bullet-}$ ligands were treated either as a neutral ligand (with one less electron) or as a double anion (with one additional electron), rather than as a radical monoanion. In other words, due to the radical nature of the bridging tetrazine ligands they were treated as closed-shell species in the SA-CASSCF calculations and their crystal fields acting on each Dy^{III} ion in **1-Dy** and **2-Dy** were taken into account in an average fashion employing a previously reported methodology.[20] The active space used for the Dy^{III} ions included nine 4*f* electrons and seven 4*f* orbitals. All 21 sextets, 224 quartets, and 490 doublets states of the Dy^{III} ion were solved in the SA-CASSCF calculations. The spin-orbit interaction was taken into account in the subsequent spin-orbit restricted active space interaction (SO-RASSI)[21] calculations by mixing all 21 sextet states, the lowest 128 quartets, and the lowest 130 doublets. In all *ab initio* calculations, scalar relativistic effects were considered by employing the exact two-component (X2C) transformation.[22–24] Additionally, the Cholesky decomposition of two-electron integrals, with a threshold value of 10^{-8} (in atomic units), was utilized to accelerate the computations. Roos' relativistically contracted atomic natural orbital (ANO-RCC) basis sets of a polarized valence triple-ζ (TZVP) quality were employed for the Dy^{III} ions, while polarized valence double-ζ (VDZP) quality basis sets were utilized for all remaining atoms.[25,26] The *ab initio* crystal field parameters of the Dy^{III} ions were extracted from the SA-CASSCF calculations, which were performed for the complexes incorporating the bridging radical ligands as closed-shell species, using the SINGLE_ANISO[27–29] module. The averaged crystal field parameters were then derived for each Dy^{III} center from the *ab initio* crystal field parameters using the previously reported approach.[20] Simulation of low-lying exchange energy levels of **1-Dy** and **2-Dy** were carried out in a qualitive manner using the PHI[30] software (version 3.1.6) and same Hamiltonian as described previously.[31]

The effect of substitution at the 3- and 6-positions of the tetrazine rings on the exchange interaction was investigated by conducting broken symmetry density functional theory (BS-DFT) calculations for nine distinct hypothetical cationic gadolinium complexes, namely **1-GdMe^{THF}**, **1-GdMe**, **2-^{cis}GdMeO^{THF}**, **2-^{cis}GdMeO**, **2-^{trans}GdMeO**, **3-GdCl^{THF}**, **3-GdCl,** **4-GdOH^{THF}** and **5-GdNH$_2$^{THF}** (Fig. S18).

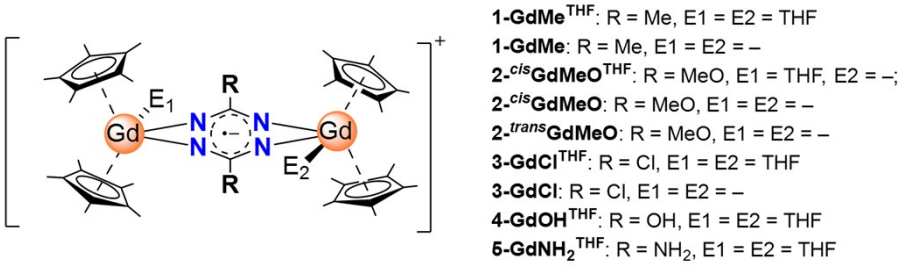

Fig. S18: Visualization of structures of the cationic gadolinium complexes **1-GdMe^{THF}**, **1-GdMe**, **2-^{cis}GdMeO^{THF}**, **2-^{cis}GdMeO**, **2-^{trans}GdMeO**, **3-GdCl^{THF}**, **3-GdCl, 4-GdOH^{THF}**, and **5-GdNH$_2$^{THF}**.

The initial geometries of all complexes were extracted from the crystal structures of **1-Gd** and **2-Gd**, which were also included in the BS-DFT calculations. Full geometry optimizations without symmetry constraints were performed for the intermediate spin state (S=13/2, αβα = Gd(↑)-Rad(↓)-Gd(↑)) of **1-GdMe^{THF}**, **1-GdMe**, **2-^{cis}GdMeO^{THF}**, **2-^{cis}GdMeO**, **2-^{trans}GdMeO**, **3-GdCl^{THF}**, **3-GdCl**, **4-GdOH^{THF}**, and **5-GdNH$_2$^{THF}**, whereas for **1-Gd** and **2-Gd** only the positions

of the hydrogen atoms were optimized in a gas-phase, using Gaussian 16.[16] The nature of the converged minima on the potential energy hypersurface was confirmed by frequency analyses. The geometry optimizations and frequency calculations were performed by employing the B3LYP exchange-correlation functional in conjunction with the Cundari-Stevens[32] (CSDZ, for Gd) and def2-TZVPP[33–36] (for all other elements) basis sets. The D3 empirical dispersion correction along with the damping function was applied to account for dispersion forces.[37,38] All optimized structures and their selected geometrical parameters are given in Tables S5–S10. As evident by Tables S5–S10, the optimized geometries of **1-GdMe^{THF}** and **2-^{cis}GdMeO^{THF}** are in reasonable agreement with the crystal structures of **1-Gd** and **2-Gd.**

Table S5. Selected bond lengths (Å) and angles (°) for **1-Gd** (crystal structure) and **1-GdMe^{THF}** (optimized in the gas-phase). Exp.–Opt. is the difference between the experimental and calculated data obtained from Gaussian (G) or ADF (A) calculation (see below), whereas Opt.(G)–Opt.(A) is the difference between the optimized geometries obtained from Gaussian and ADF calculations.

Bond /Angle	1-Gd	1-GdMe^{THF} (G)	Exp.–Opt.(G)	1-GdMe^{THF} (A)	Exp.–Opt.(A)	Opt.(G)–Opt.(A)
Gd–Gd′	7.055	6.994	0.061	7.196	-0.141	-0.202
Gd–N1	2.429	2.429	0.000	2.488	-0.059	-0.059
Gd–N2	2.495	2.391	0.104	2.576	-0.081	-0.185
Gd–O	2.452	2.371	0.081	2.534	-0.082	-0.163
Gd′–N1′	2.429	2.429	0.000	2.487	-0.058	-0.058
Gd′–N2′	2.495	2.494	0.001	2.577	-0.082	-0.083
Gd′–O′	2.452	2.397	0.055	2.534	-0.082	-0.137
Gd–Cp*$_{cent}$A	2.444	2.507	-0.063	2.494	-0.050	0.013
Gd–Cp*$_{cent}$B	2.444	2.453	-0.009	2.497	-0.053	-0.044
Gd′–Cp*$_{cent}$A′	2.444	2.468	-0.024	2.496	-0.052	-0.028
Gd′–Cp*$_{cent}$B′	2.444	2.440	0.004	2.495	-0.051	-0.055
C1–N1	1.322	1.305	0.017	1.324	-0.002	-0.019
C1′–N2	1.324	1.325	-0.001	1.384	-0.060	-0.059
N1–N2	1.393	1.341	0.052	1.382	0.011	-0.041
Gd–dmtz$_{cent}$	3.528	3.468	0.060	3.598	-0.070	-0.130
Gd′–dmtz$_{cent}$	3.528	3.528	0.000	3.598	-0.070	-0.070
N1–Gd–N2	32.95	32.30	0.650	31.60	1.35	0.70
N1′–Gd′–N2′	32.95	32.84	0.110	31.60	1.35	1.24
O–Gd–N1	117.39	121.85	-4.460	115.46	1.93	6.39
O–Gd–N2	84.81	89.83	-5.020	84.17	0.64	5.66
O′–Gd′–N1′	117.39	117.74	-0.350	115.32	2.07	2.42
O′–Gd′–N2′	84.81	85.17	-0.360	84.04	0.77	1.13
O–Gd–Cp*$_{cent}$A	100.71	101.20	-0.490	99.91	0.80	1.29
O′–Gd′–Cp*$_{cent}$A′	100.71	101.62	-0.910	99.92	0.79	1.70
N1–Gd–Cp*$_{cent}$A	100.81	99.94	0.870	102.73	-1.92	-2.79
N1′–Gd′–Cp*$_{cent}$A′	100.81	100.40	0.410	102.67	-1.86	-2.27
N2–Gd–Cp*$_{cent}$A	112.98	113.33	-0.350	114.45	-1.47	-1.12
N2′–Gd′–Cp*$_{cent}$A′	112.98	113.23	-0.250	114.40	-1.42	-1.17
O–Gd–Cp*$_{cent}$B	103.13	104.88	-1.750	103.15	-0.02	1.73
O′–Gd′–Cp*$_{cent}$B′	103.13	104.54	-1.410	103.25	-0.12	1.29

N1−Gd−Cp*$_{cent}$B	98.77	98.89	-0.120	99.09	-0.32	-0.20
N1′−Gd′−Cp*$_{cent}$B′	98.77	98.43	0.340	99.25	-0.48	-0.82
N2−Gd−Cp*$_{cent}$B	103.91	105.68	-1.770	103.35	0.56	2.33
N2′−Gd′−Cp*$_{cent}$B′	103.91	104.33	-0.420	103.52	0.39	0.81
Cp*$_{cent}$A−Gd−Cp*$_{cent}$B	137.41	132.59	4.820	137.27	0.14	-4.68
Cp*$_{cent}$A′−Gd′−Cp*$_{cent}$B′	137.41	135.48	1.930	137.15	0.26	-1.67
O−Gd−dmtz$_{cent}$	102.29	106.69	-4.400	101.24	1.05	5.45
O′−Gd′−dmtz$_{cent}$	102.29	102.74	-0.450	101.15	1.14	1.59

Cp*$_{cent}$A: C7-C11; Cp*$_{cent}$B: C17-C21, Cp*$_{cent}$A′: C7′-C11′; Cp*$_{cent}$B′: C17′-C21′

Table S6. Selected bond lengths (Å) and angles (°) for **2-Gd** (crystal structure) and **2-^{cis}GdMeO^{THF}** (optimized in the gas-phase). Exp.–Opt. is the difference between the experimental and calculated data obtained from Gaussian (G) or ADF (A) calculation (see below), whereas Opt.(G)–Opt.(A) is the difference between the optimized geometries obtained from Gaussian and ADF calculations.

Bond /Angle	2-Gd	2-^{cis}GdMeO^{THF} (G)	Exp.–Opt.(G)	2-^{cis}GdMeO^{THF} (A)	Exp.–Opt.(A)	Opt.(G)–Opt.(A)
Gd1−Gd2	7.027	7.085	-0.058	7.162	-0.135	-0.077
Gd1−N1	2.454	2.448	0.006	2.479	-0.025	-0.031
Gd1−N2	2.386	2.449	-0.063	2.479	-0.093	-0.030
Gd1−Cp*$_{cent}$A	2.428	2.423	0.005	2.451	-0.023	-0.028
Gd1−Cp*$_{cent}$B	2.367	2.424	-0.057	2.447	-0.080	-0.023
Gd1−dmeotz$_{cent}$	3.486	3.513	-0.027	3.549	-0.063	-0.036
N1−N2	1.407	1.387	0.020	1.391	0.016	-0.004
C1−N1	1.322	1.318	0.004	1.322	0.000	-0.004
C2−N2	1.313	1.318	-0.005	1.322	-0.009	-0.004
Gd2−O3	2.454	2.482	-0.028	2.513	-0.059	-0.031
Gd2−N3	2.474	2.580	-0.106	2.597	-0.123	-0.017
Gd2−N4	2.454	2.435	0.019	2.485	-0.031	-0.050
Gd2−Cp*$_{cent}$C	2.417	2.456	-0.039	2.492	-0.075	-0.036
Gd2−Cp*$_{cent}$D	2.435	2.463	-0.028	2.485	-0.050	-0.022
Gd2−dmeotz$_{cent}$	3.541	3.577	-0.036	3.618	-0.077	-0.041
N3−N4	1.374	1.365	0.009	1.369	0.005	-0.004
C1−N4	1.327	1.328	-0.001	1.330	-0.003	-0.002
C2−N3	1.331	1.328	0.003	1.332	-0.001	-0.004
Cp*$_{cent}$A−Gd1−Cp*$_{cent}$B	139.60	149.13	-9.53	141.37	-1.77	7.76
N1−Gd1−N2	34.00	32.91	1.09	32.59	1.41	0.32
N1−Gd1−Cp*$_{cent}$A	110.56	104.48	6.08	108.27	2.29	-3.79
N1−Gd1−Cp*$_{cent}$B	109.26	105.35	3.91	108.6	0.66	-3.25
N2−Gd1−Cp*$_{cent}$A	109.05	103.06	5.99	107.39	1.66	-4.33
N2−Gd1−Cp*$_{cent}$B	107.56	106.25	1.31	109.78	-2.22	-3.53
Cp*$_{cent}$C−Gd2−Cp*$_{cent}$D	136.72	142.73	-6.01	154.89	-18.17	-12.16

N3−Gd2−N4	32.63	31.42	1.21	31.14	1.49	0.28
N3−Gd2−Cp*$_{cent}$C	108.18	109.87	-1.69	108.64	-0.46	1.23
N3−Gd2−Cp*$_{cent}$D	109.74	99.59	10.15	96.35	13.39	3.24
N4−Gd2−Cp*$_{cent}$C	99.69	97.75	1.94	100.25	-0.56	-2.50
N4−Gd2−Cp*$_{cent}$D	100.99	95.72	5.27	99.46	1.53	-3.74
O3−Gd2−N3	83.49	82.41	1.08	83.19	0.30	-0.78
O3−Gd2−N4	115.84	113.62	2.22	114.34	1.50	-0.72
O3−Gd2−Cp*$_{cent}$C	103.98	103.76	0.22	102.59	1.39	1.17
O3−Gd2−Cp*$_{cent}$D	100.98	102.28	-1.30	102.03	-1.05	0.25

Cp*$_{cent}$A: C9-C13; Cp*$_{cent}$B: C19-C23; Cp*$_{cent}$C: C29-C33; Cp*$_{cent}$D: C39-C43.

Table S7. Selected bond lengths (Å) and angles (°) for **1-GdMe** (optimized in the gas-phase). Opt.(G)–Opt.(A) is the difference between the optimized geometries obtained from Gaussian and ADF calculations (see below).

Bond /Angle	1-GdMe (G)	1-GdMe (A)	Opt.(G)–Opt.(A)
Gd1−Gd2	7.056	7.087	0.031
Gd1−N1	2.467	2.48	0.013
Gd1−N2	2.458	2.477	0.019
Gd1−Cp*$_{cent}$A	2.416	2.437	0.021
Gd1−Cp*$_{cent}$B	2.414	2.435	0.021
Gd1−dmtz$_{cent}$	3.528	3.544	0.016
N1−N2	1.380	1.384	0.004
C1−N1	1.326	1.33	0.004
C2−N2	1.322	1.325	0.003
Gd2−N3	2.467	2.48	0.013
Gd2−N4	2.458	2.477	0.019
Gd2−Cp*$_{cent}$C	2.414	2.435	0.021
Gd2−Cp*$_{cent}$D	2.416	2.437	0.021
Gd2−dmeotz$_{cent}$	3.528	3.544	0.016
N3−N4	1.380	1.384	0.004
C1−N4	1.322	1.325	0.003
C2−N3	1.326	1.33	0.004
Cp*$_{cent}$A−Gd1−Cp*$_{cent}$B	149.26	143.29	-5.97
N1−Gd1−N2	32.54	32.43	-0.11
N1−Gd1−Cp*$_{cent}$A	104.70	108.59	3.89
N1−Gd1−Cp*$_{cent}$B	103.35	107.46	4.11
N2−Gd1−Cp*$_{cent}$A	105.91	107.78	1.87
N2−Gd1−Cp*$_{cent}$B	104.48	106.24	1.76
Cp*$_{cent}$C−Gd2−Cp*$_{cent}$D	149.26	143.29	-5.97
N3−Gd2−N4	32.54	32.43	-0.11

N3−Gd2−Cp*$_{cent}$C	103.35	107.46	4.11
N3−Gd2−Cp*$_{cent}$D	104.70	108.59	3.89
N4−Gd2−Cp*$_{cent}$C	104.48	106.25	1.77
N4−Gd2−Cp*$_{cent}$D	105.91	107.78	1.87

Table S8. Selected bond lengths (Å) and angles (°) for **2-^{cis}GdMeO** (optimized in the gas-phase) and **2-^{trans}GdMeO** (optimized in the gas-phase). Opt.(G)–Opt.(A) is the difference between the optimized geometries obtained from Gaussian and ADF calculations (see below).

Bond /Angle	2-^{cis}GdMeO (G)	2-^{cis}GdMeO (A)	Opt.(G)–Opt.(A)	2-^{trans}GdMeO (G)	2-^{trans}GdMeO (A)	Opt.(G)–Opt.(A)
Gd1−Gd2	7.040	7.104	-0.064	7.043	7.111	-0.068
Gd1−N1	2.451	2.479	-0.028	2.409	2.457	-0.048
Gd1−N2	2.451	2.479	-0.028	2.498	2.515	-0.017
Gd1−Cp*$_{cent}$A	2.422	2.448	-0.026	2.408	2.439	-0.031
Gd1−Cp*$_{cent}$B	2.424	2.446	-0.022	2.410	2.441	-0.031
Gd1−dmeotz$_{cent}$	3.519	3.549	-0.030	3.522	3.558	-0.036
N1−N2	1.387	1.391	-0.004	1.376	1.379	-0.003
C1−N1	1.318	1.322	-0.004	1.325	1.329	-0.004
C2−N2	1.319	1.322	-0.003	1.320	1.324	-0.004
Gd2−N3	2.459	2.483	-0.024	2.408	1.329	1.079
Gd2−N4	2.440	2.481	-0.041	2.498	1.324	1.174
Gd2−Cp*$_{cent}$C	2.404	2.437	-0.033	2.408	2.437	-0.029
Gd2−Cp*$_{cent}$D	2.406	2.435	-0.029	2.411	2.441	-0.03
Gd2−dmeotz$_{cent}$	3.521	3.556	-0.035	3.521	3.557	-0.036
N3−N4	1.367	1.370	-0.003	1.376	1.379	-0.003
C1−N4	1.327	1.331	-0.004	1.320	1.324	-0.004
C2−N3	1.327	1.331	-0.004	1.325	1.329	-0.004
Cp*$_{cent}$A−Gd1−Cp*$_{cent}$B	149.84	141.84	8.00	149.77	142.65	7.12
N1−Gd1−N2	32.87	32.58	0.29	32.50	32.19	0.31
N1−Gd1−Cp*$_{cent}$A	103.83	107.30	-3.47	102.58	107.23	-4.65
N1−Gd1−Cp*$_{cent}$B	104.99	109.36	-4.37	101.66	107.49	-5.83
N2−Gd1−Cp*$_{cent}$A	103.90	108.49	-4.59	104.45	108.16	-3.71
N2−Gd1−Cp*$_{cent}$B	103.90	107.99	-4.09	105.71	108.49	-2.78
Cp*$_{cent}$C−Gd2−Cp*$_{cent}$D	151.48	143.51	7.97	149.81	142.60	7.21
N3−Gd2−N4	32.40	32.04	0.36	32.51	32.18	0.33
N3−Gd2−Cp*$_{cent}$C	103.39	106.55	-3.16	102.73	107.49	-4.76
N3−Gd2−Cp*$_{cent}$D	104.82	108.66	-3.84	101.45	107.05	-5.6
N4−Gd2−Cp*$_{cent}$C	103.98	107.84	-3.86	104.56	108.74	-4.18
N4−Gd2−Cp*$_{cent}$D	102.03	106.99	-4.96	105.53	108.08	-2.55

Cp*$_{cent}$A: C9-C13; Cp*$_{cent}$B: C19-C23; Cp*$_{cent}$C: C29-C33; Cp*$_{cent}$D: C39-C43.

Table S9. Selected bond lengths (Å) and angles (°) for **3-GdCl^{THF}** (optimized in the gas-phase) and **3-GdCl** (optimized in the gas-phase). Opt.(G)–Opt.(A) is the difference between the optimized geometries obtained from Gaussian and ADF calculations (see below).

Bond /Angle	3-GdCl^{THF} (G)	3-GdCl^{THF} (A)	Opt.(G)–Opt.(A)	3-GdCl (G)	3-GdCl (A)	Opt.(G)– Opt.(A)
Gd1−Gd2	7.300	7.292	0.008	7.137	7.149	-0.012
Gd1−N1	2.499	2.513	-0.014	2.491	2.499	-0.008
Gd1−N2	2.649	2.624	0.025	2.496	2.502	-0.006
Gd1−Cp*$_{cent}$A	2.465	2.482	-0.017	2.404	2.431	-0.027
Gd1−Cp*$_{cent}$B	2.469	2.490	-0.021	2.406	2.431	-0.025
Gd1−dCltz$_{cent}$	3.650	3.646	0.004	3.568	3.574	-0.006
N1−N2	1.383	1.386	-0.003	1.383	1.387	-0.004
C1−N1	1.316	1.319	-0.003	1.316	1.32	-0.004
C2−N2	1.317	1.322	-0.005	1.317	1.319	-0.002
Gd1−O4	2.511	2.523	-0.012	–	–	–
Gd2−O3	2.511	2.523	-0.012	–	–	–
Gd2−N3	2.499	2.513	-0.014	2.491	2.499	-0.008
Gd2−N4	2.649	2.624	0.025	2.496	2.502	-0.006
Gd2−Cp*$_{cent}$C	2.469	2.490	-0.021	2.406	2.431	-0.025
Gd2−Cp*$_{cent}$D	2.465	2.482	-0.017	2.404	2.431	-0.027
Gd2−dCltz$_{cent}$	3.650	3.646	0.004	3.568	3.574	-0.006
N3−N4	1.383	1.386	-0.003	1.383	1.387	-0.004
C1−N4	1.317	1.322	-0.005	1.316	1.319	-0.003
C2−N3	1.316	1.319	-0.003	1.316	1.32	-0.004
Cp*$_{cent}$A−Gd1−Cp*$_{cent}$B	142.13	138.42	3.71	149.94	144.37	5.57
N1−Gd1−N2	31.00	31.21	-0.21	32.20	32.2	0.00
N1−Gd1−Cp*$_{cent}$A	99.27	101.17	-1.90	105.39	107.87	-2.48
N1−Gd1−Cp*$_{cent}$B	96.56	98.87	-2.31	103.17	106.42	-3.25
N2−Gd1−Cp*$_{cent}$A	109.59	110.41	-0.82	105.56	107.93	-2.37
N2−Gd1−Cp*$_{cent}$B	101.63	105.59	-3.96	103.56	106.16	-2.60
O4−Gd1−N1	113.81	115.83	-2.02	–	–	–
O4−Gd1−N2	82.99	94.68	-11.69	–	–	–
O4−Gd1−Cp*$_{cent}$A	100.84	100.25	0.59	–	–	–
O4−Gd1−Cp*$_{cent}$B	103.79	103.15	0.64	–	–	–
Cp*$_{cent}$C−Gd2−Cp*$_{cent}$D	142.13	138.42	3.71	149.94	144.37	5.57
N3−Gd2−N4	31.00	31.21	-0.21	32.20	32.20	0.00
N3−Gd2−Cp*$_{cent}$C	96.56	98.87	-2.31	103.17	106.42	-3.25
N3−Gd2−Cp*$_{cent}$D	99.27	101.17	-1.90	105.39	107.87	-2.48
N4−Gd2−Cp*$_{cent}$C	101.63	105.59	-3.96	103.56	106.16	-2.60
N4−Gd2−Cp*$_{cent}$D	109.59	110.41	-0.82	105.56	107.93	-2.37
O3−Gd2−N3	113.81	115.83	-2.02	–	–	–

O3−Gd2−N4	82.99	84.68	-1.69	–	–	–
O3−Gd2−Cp*$_{cent}$C	103.79	103.15	0.64	–	–	–
O3−Gd2−Cp*$_{cent}$D	100.84	100.25	0.59	–	–	–

Table S10. Selected bond lengths (Å) and angles (°) for **4-GdOH^{THF}** (optimized in the gas-phase) and **5-GdNH$_2$^{THF}** (optimized in the gas-phase). Opt.(G)–Opt.(A) is the difference between the optimized geometries obtained from Gaussian and ADF calculations (see below).

Bond /Angle	4-GdOH^{THF} (G)	4-GdOH^{THF} (A)	Opt.(G)– Opt.(A)	5-GdNH$_2$^{THF} (G)	5-GdNH$_2$^{THF} (A)	Opt.(G)– Opt.(A)
Gd1−Gd2	7.055	7.248	-0.193	7.055	7.193	-0.138
Gd1−N1	2.429	2.487	-0.058	2.429	2.476	-0.047
Gd1−N2	2.495	2.611	-0.116	2.495	2.568	-0.073
Gd1−Cp*$_{cent}$A	2.444	2.487	-0.043	2.444	2.496	-0.052
Gd1−Cp*$_{cent}$B	2.430	2.479	-0.049	2.430	2.492	-0.062
Gd1−dohtz$_{cent}$ / dnh2tz$_{cent}$	3.528	3.624	-0.096	3.528	3.597	-0.069
N1−N2	1.393	1.378	0.015	1.393	1.374	0.019
C1−N1	1.322	1.321	0.001	1.322	1.330	-0.008
C2−N2	1.324	1.326	-0.002	1.325	1.335	-0.01
Gd1−O4	2.452	2.549	-0.097	2.452	2.541	-0.089
Gd2−O3	2.452	2.549	-0.097	2.452	2.541	-0.089
Gd2−N3	2.429	2.487	-0.058	2.429	2.476	-0.047
Gd2−N4	2.495	2.611	-0.116	2.495	2.568	-0.073
Gd2−Cp*$_{cent}$C	2.430	2.479	-0.049	2.430	2.492	-0.062
Gd2−Cp*$_{cent}$D	2.444	2.487	-0.043	2.444	2.496	-0.052
Gd2−dohtz$_{cent}$ / dnh2tz$_{cent}$	3.528	3.624	-0.096	3.528	3.597	-0.069
N3−N4	1.393	1.378	0.015	1.393	1.374	0.019
C1−N4	1.322	1.321	0.001	1.322	1.335	-0.013
C2−N3	1.324	1.326	-0.002	1.325	1.330	-0.005
Cp*$_{cent}$A−Gd1−Cp*$_{cent}$B	137.41	137.94	-0.53	137.41	154.26	-16.85
N1−Gd1−N2	32.84	31.25	1.59	32.83	31.56	1.27
N1−Gd1−Cp*$_{cent}$A	100.82	99.69	1.13	100.82	102.44	-1.62
N1−Gd1−Cp*$_{cent}$B	98.77	102.21	-3.44	98.77	99.58	-0.81
N2−Gd1−Cp*$_{cent}$A	112.99	104.87	8.12	112.99	113.10	-0.11
N2−Gd1−Cp*$_{cent}$B	103.91	112.47	-8.56	103.90	105.06	-1.16
O4−Gd1−N1	117.40	112.45	4.95	117.39	114.75	2.64
O4−Gd1−N2	84.81	81.39	3.42	84.81	83.08	1.73
O4−Gd1−Cp*$_{cent}$A	100.72	103.93	-3.21	100.72	100.24	0.48
O4−Gd1−Cp*$_{cent}$B	103.14	100.2	2.94	103.14	103.65	-0.51
Cp*$_{cent}$C−Gd2−Cp*$_{cent}$D	137.41	137.94	-0.53	137.41	136.87	0.54
N3−Gd2−N4	32.84	31.25	1.59	32.83	31.56	1.27
N3−Gd2−Cp*$_{cent}$C	98.77	99.69	-0.92	98.77	99.58	-0.81

N3−Gd2−Cp*$_{cent}$D	100.82	102.21	-1.39	100.82	102.44	-1.62
N4−Gd2−Cp*$_{cent}$C	103.91	104.87	-0.96	103.90	105.06	-1.16
N4−Gd2−Cp*$_{cent}$D	112.99	112.49	0.50	112.99	113.10	-0.11
O3−Gd2−N3	117.40	112.45	4.95	117.39	114.45	2.94
O3−Gd2−N4	84.81	81.39	3.42	84.81	83.08	1.73
O3−Gd2−Cp*$_{cent}$C	103.14	103.93	-0.79	103.14	103.65	-0.51
O3−Gd2−Cp*$_{cent}$D	100.72	100.20	0.52	100.72	100.24	0.48

To determine the Gd–Rad ($J_{Gd\text{-}Rad}$) and Gd-Gd ($J_{Gd\text{-}Gd}$) exchange coupling constants, the scalar relativistic single-point BS-DFT calculations were conducted with ORCA (version 5.0.3)[39] for the crystal structures (**1-Gd** and **2-Gd**), as well as for the optimized complexes (**1-GdMe^{THF}**, **1-GdMe**, **2-*cis*GdMeO^{THF}**, **2-*cis*GdMeO**, **2-*trans*GdMeO**, **3-GdCl^{THF}**, **3-GdCl**, **4-GdOH^{THF}** and **5-GdNH$_2$^{THF}**). In the calculations, the long-range corrected exchange correlation functional, namely CAM-B3LYP, was used in conjunction with the SARC-ZORA-def2-TZVPP basis sets for Gd and the ZORA-def2-TZVPP basis sets for all other atoms.[33,40,41] Scalar relativistic effects were addressed using the zeroth-order regular approximation (ZORA).[42] According to the standard procedure, the BS states can be constructed as the energy expectation values of Ising states that diagonalize the Heisenberg–Dirac–van Vleck (HDvV) Hamiltonian.[43] Therefore, the following HDvV Hamiltonian:

$$\hat{H}_{HDvV} = -2J_{Gd1-Rad}(\hat{S}_{Gd1}\hat{S}_{Rad}) - 2J_{Gd2-Rad}(\hat{S}_{Gd2}\hat{S}_{Rad}) - 2J_{Gd1-Gd2}(\hat{S}_{Gd1}\hat{S}_{Gd2}) \quad \text{(S4)}$$

was used to evaluate the exchange interactions. In equation S4, $J_{Gd\text{-}Rad}$ and $J_{Gd\text{-}Gd}$ are the exchange interactions coupling constants and $\hat{S}_{Rad}$, $\hat{S}_{Gd1}$, $\hat{S}_{Gd2}$ are effective spin operators acting on the projection of the local spin at the radical and metal sites. For further simplification of the equations, it was assumed that $J_{Gd1\text{-}Rad}$ equals to $J_{Gd2\text{-}Rad}$, due to the (pseudo) inversion center of the investigated complexes. To extract the final values for the $J_{Gd\text{-}Rad}$ and $J_{Gd\text{-}Gd}$ coupling constants, the energies of the three different BS states – ααα, αβα, and ααβ – were calculated, and the exchange coupling constants were obtained from the energy differences of the BS states as:

$$J_{Gd-Rad} = \frac{E_{IS} - E_{HS}}{14} \quad \text{(S5)}$$

$$J_{Gd-Gd} = \frac{2E_{LS} - E_{IS} - E_{HS}}{98} \quad \text{(S6)}$$

Table S11 lists the calculated exchange coupling constants, and it is evident from the calculated data that the exchange coupling constants of the optimized structures of **1-GdMe^{THF}** and **2-*cis*GdMeO^{THF}** match well with the ones obtained for the crystal structures **1-Gd** and **2-Gd**. The results verify that minor geometrical changes around the coordination environment of the metal centers during optimization do not substantially impact the values of the exchange coupling constants. Importantly, the calculated values of **1-Gd** and **2-Gd** are also in reasonable agreement with the experimental values although they are slightly higher. For all complexes, the calculated $J_{Gd\text{-}Gd}$ values are within the error limits of BS-DFT approach, and no reliable conclusions can be drawn from them.

Table S11. Energies of the three BS states and exchange coupling constants $J_{Gd\text{-}Rad}$ and $J_{Gd\text{-}Gd}$ for the crystal structures and nine hypothetical complexes.

	E_{HS} (hartree)	E_{IS} (hartree)	E_{LS} (hartree)	$J_{Gd\text{-}Rad}$ (cm^{-1})	$J_{Gd\text{-}Gd}$ (cm^{-1})
1-Gd	-25448.45515884	-25448.45591544	-25448.45554425	-11.86	-0.03
2-Gd	-25366.50647563	-25366.50732690	-25366.50696102	-13.35	-0.27
1-GdMe^{THF}	-25448.43880306	-25448.43961226	-25448.43921506	-12.69	-0.03
1-GdMe	-24983.28889603	-24983.28979368	-24983.28935317	-14.07	-0.04
2-^{cis}GdMeO^{THF}	-25366.54572892	-25366.54649161	-25366.5461419	-11.96	-0.14
2-^{cis}GdMeO	-25133.90674562	-25133.90762840	-25133.90716395	-13.84	0.10
2-^{trans}GdMeO	-25133.90796180	-25133.90889148	-25133.90843234	-14.57	-0.03
3-GdCl^{THF}	-26293.65184203	-26293.65236031	-26293.65210533	-8.12	-0.02
3-GdCl	-25828.38022252	-25828.38097954	-25828.38060863	-11.87	-0.03
4-GdOH^{THF}	-25520.45123314	-25520.45198570	-25520.45161498	-11.80	-0.02
5-GdNH$_2$^{THF}	-25480.62510876	-25480.62586960	-25480.62549396	-11.93	-0.02

To gain further insight into the influence of the bridging tetrazine ligands on the magnetic properties of **1-Dy** and **2-Dy**, the geometries of free radicals **$R_2tz^{\bullet-}$** were optimized at the B3LYP-D3/def2-TZVPP level of theory using Gaussian 16[16] and their spin populations were calculated with Mulliken (MPA) and Atoms in molecules (AIM) populations analyses. For the comparison purpose the same calculations were also carried out for $R_2bpym^{\bullet-}$. AIMAll package was used for the AIM analyses.[44,45] Figure S19 show the investigated radicals and the results of analyses are given in Tables S12 and S13.

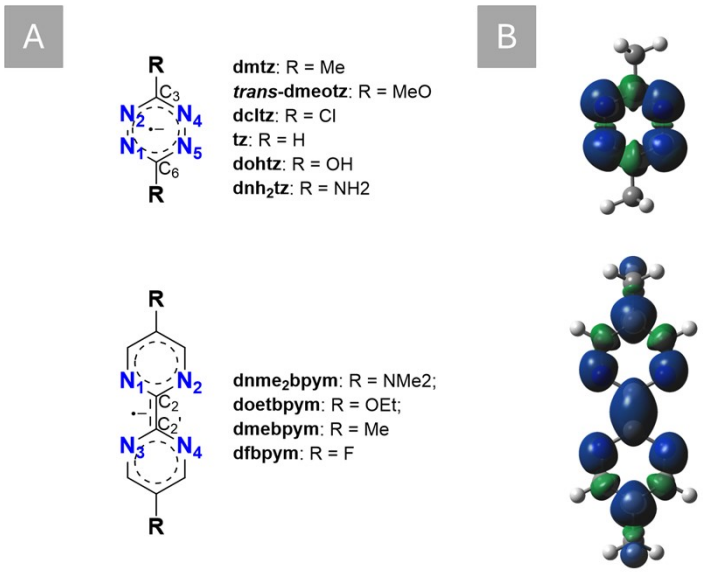

Fig. S19: (A) Structures of the tetrazine radical with R substituents at the 3- and 6-positions (top) and the 2,2′-bipyrimidine radical with R substituents at the 5- and 5′-positions (bottom). (B) Spin density distribution for the gas-phase optimized structures of $dmtz^{\bullet-}$ (top) and 5,5'-Me_2-$bpym^{\bullet-}$ (bottom; blue = α spin density, green = β spin density).

Table S12. Calculated AIM and MPA spin populations for tetrazine radicals along with their point group symmetries utilized in the calculations.

Compound	Point group		N_1	N_2	N_3	N_4	Sum of N	C_3	C_6
tz	D_{2h}	AIM	0.2815	0.2815	0.2815	0.2815	1.1259	-0.0630	-0.0630
		MPA	0.3007	0.3007	0.3007	0.3007	1.2028	-0.1014	-0.1014
dcltz	D_{2h}	AIM	0.2826	0.2826	0.2826	0.2826	1.1303	-0.0576	-0.0576
		MPA	0.2942	0.2942	0.2942	0.2942	1.1767	-0.0825	-0.0825
dmtz	C_{2h}	AIM	0.3408	0.2004	0.3408	0.2004	1.0823	-0.0419	-0.0419
		MPA	0.3711	0.1951	0.3711	0.1951	1.1323	-0.0656	-0.0656
dmeotz	C_{2h}	AIM	0.2588	0.3000	0.2588	0.3000	1.1176	-0.0500	-0.0500
		MPA	0.2631	0.3221	0.2631	0.3221	1.1702	-0.0742	-0.0742
dohtz	C_{2h}	AIM	0.2760	0.2851	0.2760	0.2851	1.1222	-0.0494	-0.0494
		MPA	0.2883	0.2989	0.2883	0.2989	1.1744	-0.0760	-0.0760
dnh$_2$tz	C_{2h}	AIM	0.2780	0.2780	0.2780	0.2780	1.1122	-0.0475	-0.0475
		MPA	0.2915	0.2915	0.2915	0.2915	1.1660	-0.0750	-0.0750

Table S13. Calculated AIM and MPA spin populations for 2,2′-bipyrimidine radicals along with their point group symmetries utilized in calculations.

Compound	Point group		N_1	N_2	N_3	N_4	Sum of N	C_2	$C_{2'}$
dnme2	C_{2h}	AIM	0.0980	0.0980	0.0980	0.0980	0.3918	-0.0115	-0.0115
		MPA	0.1012	0.1012	0.1012	0.1012	0.4049	-0.0152	-0.0152
doetbpym	C_{2h}	AIM	0.0838	0.1337	0.0838	0.1337	0.4349	0.1482	0.1482
		MPA	0.0781	0.1380	0.0781	0.1380	0.4321	0.1488	0.1488
dmebpym	C_{2h}	AIM	0.0960	0.0960	0.0960	0.0960	0.3840	0.1527	0.1527
		MPA	0.0913	0.0913	0.0913	0.0913	0.3650	0.1543	0.1543
dfbpym	D_{2h}	AIM	0.1091	0.1091	0.1091	0.1091	0.4365	0.1536	0.1536
		MPA	0.1083	0.1083	0.1083	0.1083	0.4331	0.1548	0.1548

The fragment orbital analysis for **1-GdMe^{THF}**, **1-GdMe**, **2-*cis*GdMeO^{THF}**, **2-*cis*GdMeO**, **3-GdCl^{THF}** and **3-GdCl** was conducted using the Amsterdam Density Functional (ADF) code[46,47] within the Amsterdam Modelling Suite (AMS) driver program.[48] Before orbital analysis, the geometries of **1-GdMe^{THF}**, **1-GdMe**, **2-*cis*GdMeO^{THF}**, **2-*cis*GdMeO**, **3-GdCl^{THF}** and **3-GdCl** obtained from the Gaussian 16 calculations were re-optimized with ADF. The B3LYP exchange-correlation functional (XC) and Grimme DFT-D3 dispersion-correction with Becke-Johnson damping (BJ) were used in the calculations.[37,38,49] The zeroth-order regular approximation (ZORA) was used to account for scalar relativistic effects.[50–52] Doubly polarized triple-zeta-quality Slater type basis set (TZ2P) designed for ZORA calculations was utilized for all atoms.[53] The geometry optimizations were performed with the frozen core approximation. The 1*s* orbitals for carbon, nitrogen and oxygen atoms and orbitals up to 5*p* for Gd were treated as frozen core. The ADF optimized geometries were in good agreement with their gaussian optimized geometries (see Tables S5-10). The orbital interaction analysis was performed as single point calculations at the same level of theory, but without the frozen core approximation

for all investigated complexes. In orbital interaction analysis **1-GdMe^{THF}** and **3-GdCl^{THF}** were divided into the nine fragments named as “Gd1”, “Gd2”, “tz”, “Cp1A”, “Cp1B”, “Cp2A”, “Cp2B”, “THF1”, and “THF2”, **2-*cis*GdMeO^{THF}** was divided into eight fragments named as “Gd1”, “Gd2”, “tz”, “Cp1A”, “Cp1B”, “Cp2A”, “Cp2B”, and “THF2”, while **1-GdMe**, **2-*cis*GdMeO**, and **3-GdCl** were divided into the seven fragments named as “Gd1”, “Gd2”, “tz”, “Cp1A”, “Cp1B”, “Cp2A”, “Cp2B”. The qualitative molecular orbital diagrams obtained for **1-GdMe^{THF}**, **1-GdMe**, **2-*cis*GdMeO^{THF}**, **2-*cis*GdMeO**, **3-GdCl^{THF}**, and **3-GdCl** are presented in Figures S20–25.

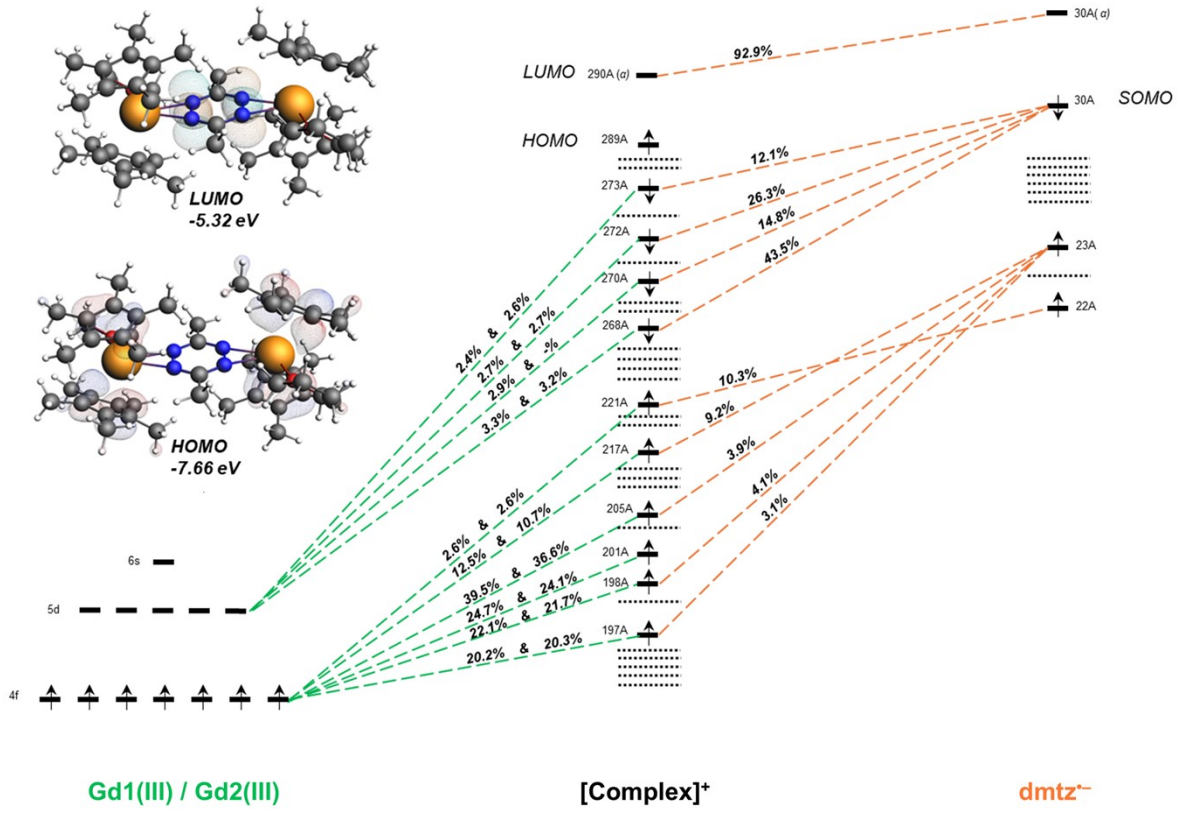

Fig. S20: Qualitative molecular orbital diagram of **1-GdMe^{THF}** representing the contribution (%) of the orbitals of the Gd^{III} ions and the dmtz$^{\bullet-}$ ligand to the respective metal-ligand molecular orbitals. Only contributions larger than 2.5 % are shown, and all other fragments, expect the Gd^{III} ions and the dmtz$^{\bullet-}$, are omitted from the diagram. The energy axis is not drawn in scale, while the dotted lines represent the orbitals omitted from the Figure. Due to the spin unrestricted formalism was used in the analysis, *α* and *β* spins/orbitals are presented separately.

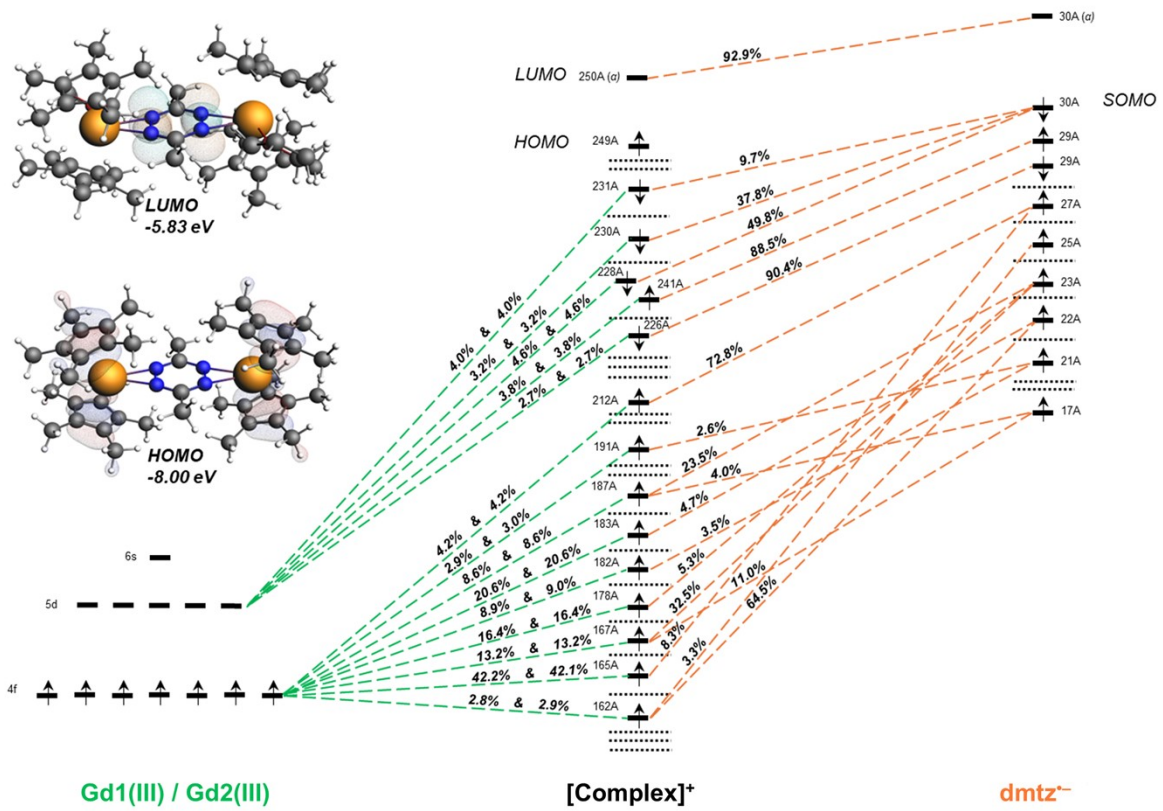

Fig. S21: Qualitative molecular orbital diagram of **1-GdMe** representing the contribution (%) of the orbitals of the Gd^{III} ions and the $dmtz^{\bullet-}$ ligand to the respective metal-ligand molecular orbitals. Only contributions larger than 2.5 % are shown, and all other fragments, expect the Gd^{III} ions and the $dmtz^{\bullet-}$, are omitted from the diagram. The energy axis is not drawn in scale, while the dotted lines represent the orbitals omitted from the Figure. Due to the spin unrestricted formalism was used in the analysis, *α* and *β* spins/orbitals are presented separately.

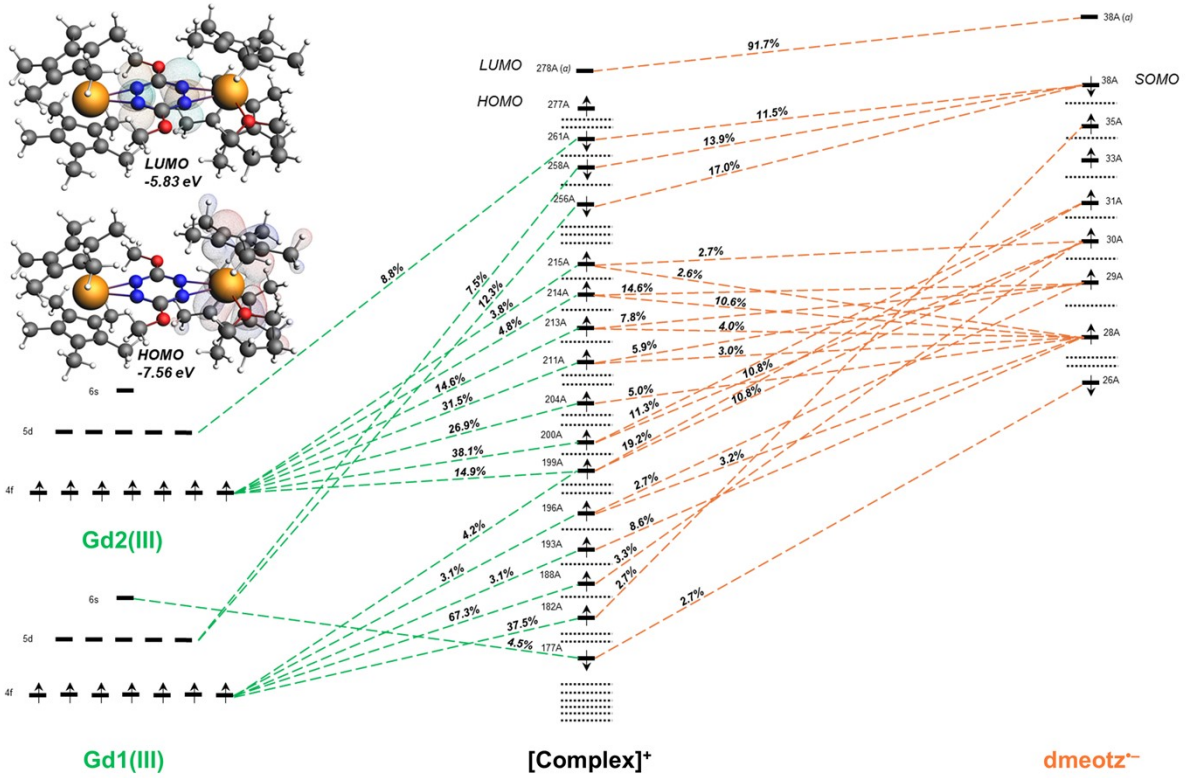

Fig. S22: Qualitative molecular orbital diagram of **2-*cis*GdMeO^{THF}** representing the contribution (%) of the orbitals of the Gd^{III} ions and the $dmeotz^{\bullet-}$ ligand to the respective metal-ligand molecular orbitals. Only contributions larger than 2.5 % are shown, and all other fragments, expect the Gd^{III} ions and the $dmeotz^{\bullet-}$, are omitted from the diagram. The energy axis is not drawn in scale, while the dotted lines represent the orbitals omitted from Figure. Due to the spin unrestricted formalism was used in the analysis, *α* and *β* spins/orbitals are presented separately.

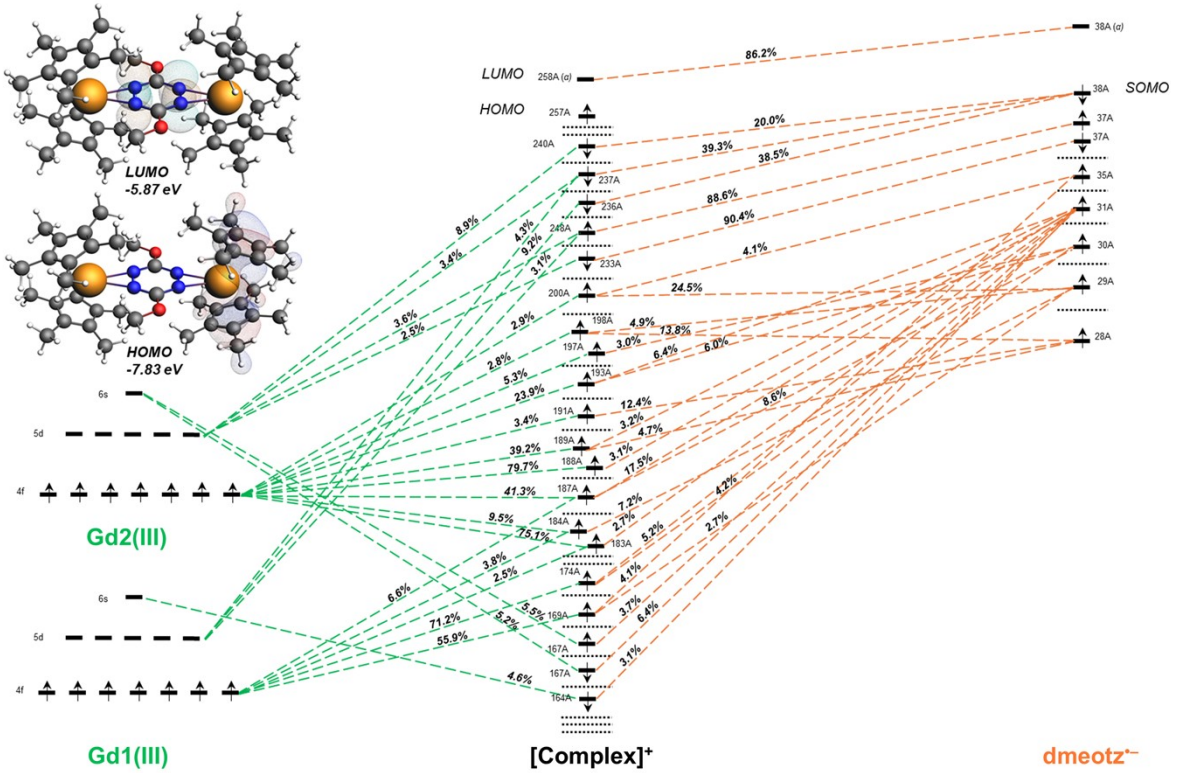

Fig. S23: Qualitative molecular orbital diagram of **2-*cis*GdMeO** representing the contribution (%) of the orbitals of the Gd^{III} ions and the $dmeotz^{\bullet-}$ ligand to the respective metal-ligand molecular orbitals. Only contributions larger than 2.5 % are shown, and all other fragments, expect the Gd^{III} ions and the $dmeotz^{\bullet-}$, are omitted from the diagram. The energy axis is not drawn in scale, while the dotted lines represent the orbitals omitted from Figure. Due to the spin unrestricted formalism was used in the analysis, *α* and *β* spins/orbitals are presented separately.

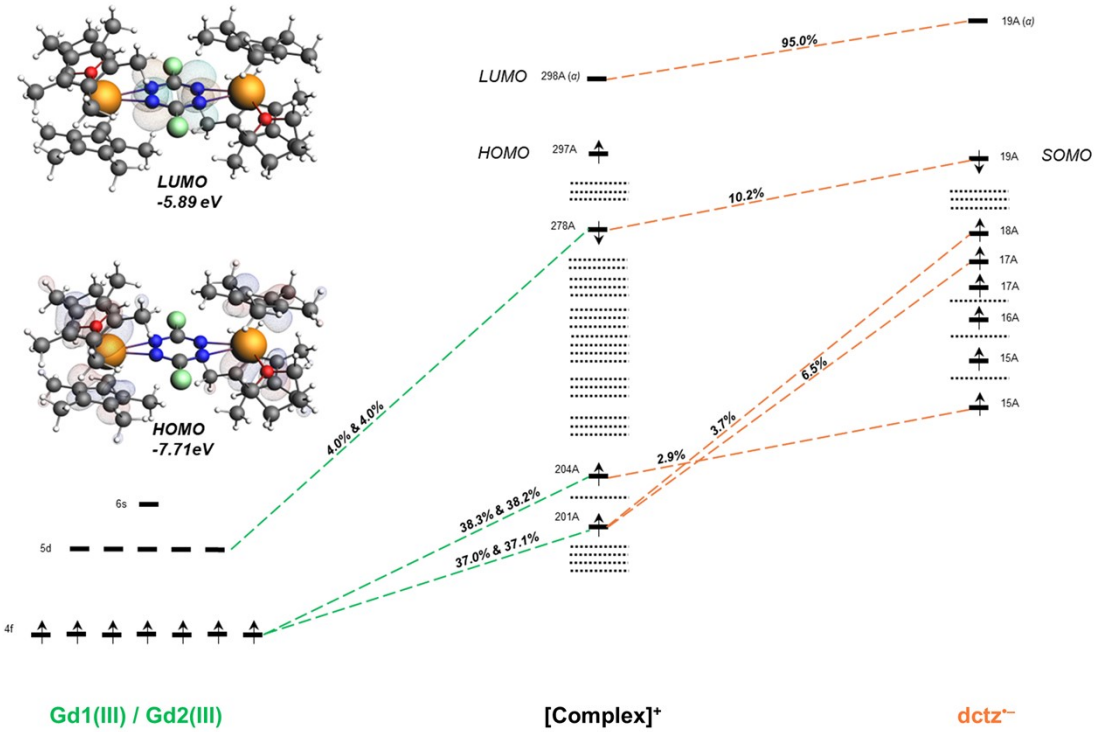

Fig. S24: Qualitative molecular orbital diagram of **3-GdCl^{THF}** representing the contribution (%) of the orbitals of the Gd^{III} ions and the dctz$^{\bullet-}$ ligand to the respective metal-ligand molecular orbitals. Only contributions larger than 2.5 % are shown, and all other fragments, expect the Gd^{III} ions and the dctz$^{\bullet-}$, are omitted from the diagram. The energy axis is not drawn in scale, while the dotted lines represent the orbitals omitted from Figure. Due to the spin unrestricted formalism was used in the analysis, *α* and *β* spins/orbitals are presented separately.

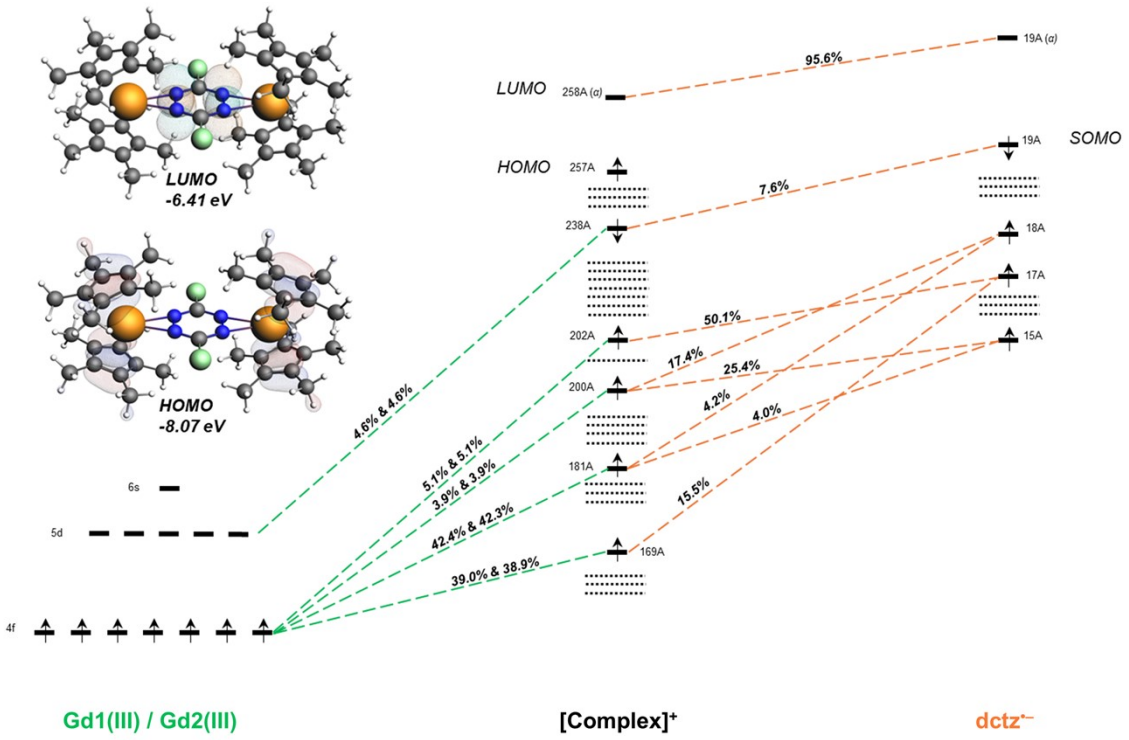

Fig. S25: Qualitative molecular orbital diagram of **3-GdCl** representing the contribution (%) of the orbitals of the Gd^{III} ions and the $dctz^{\bullet-}$ ligand to the respective metal-ligand molecular orbitals. Only contributions larger than 2.5 % are shown, and all other fragments, expect the Gd^{III} ions and the $dctz^{\bullet-}$, are omitted from the diagram. The energy axis is not drawn in scale, while the dotted lines represent the orbitals omitted from Figure. Due to the spin unrestricted formalism was used in the analysis, *α* and *β* spins/orbitals are presented separately.

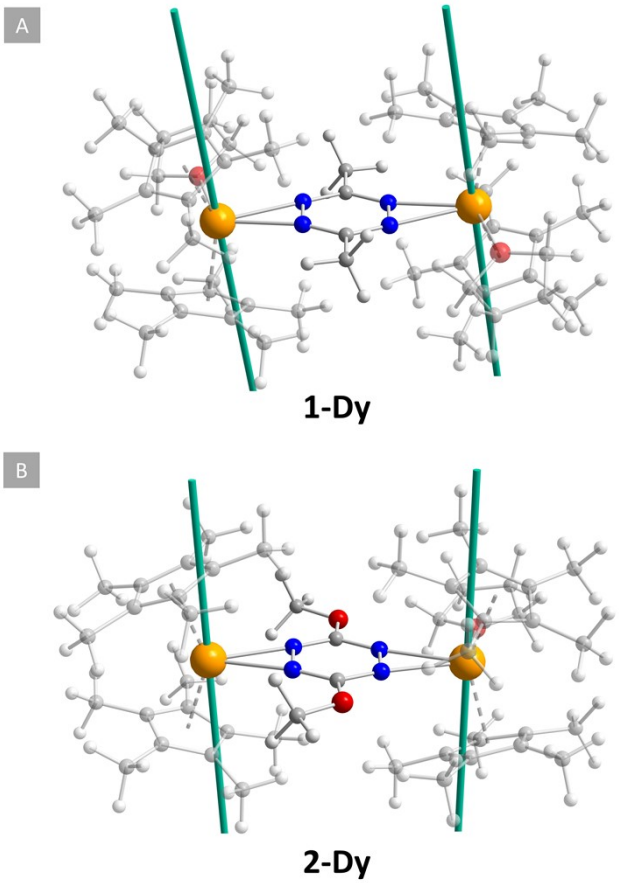

Fig. S26: Orientations of the main magnetic axes of the ground Kramers' doublets for **1-Dy** (A) and **2-Dy** (B).

Table S14. Energies and ***g*** tensors for the eight lowest local KDs of Dy^{III} ions in **1-Dy** arising from the crystal splitting of the $^6H_{15/2}$ ground multiplet as well as the angle θ between the magnetic axes of the given excited and ground KDs.

KD	*E* (cm^{-1})	g_x	g_y	g_z	θ (°)
1	0	0.017	0.030	19.718	-
2	160	0.251	0.420	17.082	1.7
3	241	3.050	8.886	9.974	136.6
4	276	2.916	4.474	7.846	101.5
5	339	2.234	4.155	8.860	128.0
6	357	2.148	6.944	11.185	82.2
7	409	0.161	1.344	16.240	92.0
8	442	0.545	2.603	17.088	75.3

Table S15. Energies and ***g*** tensors for the eight lowest local KDs of Dy1 and Dy2 ions in **2-Dy** arising from the crystal splitting of the $^6H_{15/2}$ ground multiplet as well as the angle θ between the magnetic axes of the given excited and ground KDs.

	Dy1 ion					Dy2 ion with coordinated THF				
KD	***E*** **(cm^{-1})**	**g_x**	**g_y**	**g_z**	**θ (°)**	***E*** **(cm^{-1})**	**g_x**	**g_y**	**g_z**	**θ (°)**
1	0	0.013	0.023	19.761	-	0	0.012	0.023	19.745	-
2	240	0.324	0.547	16.692	2.9	171	0.096	0.176	17.085	179.1
3	382	3.385	5.769	12.531	83.9	278	2.320	4.617	12.727	169.4
4	445	2.478	5.798	6.969	98.3	322	2.579	6.766	7.542	126.9
5	535	2.996	5.360	9.914	87.1	364	1.260	3.386	14.840	91.1
6	609	1.468	1.855	13.704	88.4	400	1.759	2.042	12.316	92.2
7	718	0.058	0.065	17.073	89.1	457	0.498	0.837	18.839	87.4
8	1018	0.003	0.005	19.959	90.1	510	0.050	0.367	19.450	88.9

Table S16. Percentage composition of the SO-RASSI wave functions for each M_J state of the ground multiplet (J = 15/2) of Dy ion in **1-Dy**.

M_J	KD1		KD2		KD3		KD4		KD5		KD6		KD7		KD8	
-15/2	0.0	84.4	0.0	12.8	0.0	1.7	0.0	0.6	0.0	0.4	0.0	0.0	0.0	0.1	0.0	0.0
-13/2	0.0	8.4	0.0	58.1	1.6	15.4	2.5	6.8	0.5	2.5	0.8	2.2	0.4	0.3	0.0	0.4
-11/2	0.0	5.0	0.0	23.7	1.1	15.1	9.6	14.5	3.0	14.9	4.1	4.4	0.5	0.0	0.5	3.4
-9/2	0.0	1.9	0.0	3.8	3.4	35.8	13.5	2.6	4.9	11.0	1.4	9.6	0.4	5.1	0.4	6.1
-7/2	0.0	0.2	0.0	0.4	6.8	0.8	39.6	1.2	2.7	16.2	2.5	12.5	4.8	5.0	4.4	2.9
-5/2	0.0	0.1	0.0	0.2	0.5	9.0	0.3	2.5	3.0	29.9	3.5	20.4	0.1	20.3	9.1	1.0
-3/2	0.0	0.0	0.1	0.7	3.4	0.9	3.3	0.1	0.7	4.5	20.7	8.6	13.7	15.2	26.3	2.0
-1/2	0.0	0.0	0.1	0.0	0.5	4.0	2.6	0.4	4.7	0.8	3.5	5.8	13.1	21.0	39.0	4.5
1/2	0.0	0.0	0.0	0.1	4.0	0.5	0.4	2.6	0.8	4.7	5.8	3.5	21.0	13.1	4.5	39.0
3/2	0.0	0.0	0.7	0.1	0.9	3.4	0.1	3.3	4.5	0.7	8.6	20.7	15.2	13.7	2.0	26.3
5/2	0.1	0.0	0.2	0.0	9.0	0.5	2.5	0.3	29.9	3.0	20.4	3.5	20.3	0.1	1.0	9.1
7/2	0.2	0.0	0.4	0.0	0.8	6.8	1.2	39.6	16.2	2.7	12.5	2.5	5.0	4.8	2.9	4.4
9/2	1.9	0.0	3.8	0.0	35.8	3.4	2.6	13.5	11.0	4.9	9.6	1.4	5.1	0.4	6.1	0.4
11/2	5.0	0.0	23.7	0.0	15.1	1.1	14.5	9.6	14.9	3.0	4.4	4.1	0.0	0.5	3.4	0.5
13/2	8.4	0.0	58.1	0.0	15.4	1.6	6.8	2.5	2.5	0.5	2.2	0.8	0.3	0.4	0.4	0.0
15/2	84.4	0.0	12.8	0.0	1.7	0.0	0.6	0.0	0.4	0.0	0.0	0.0	0.1	0.0	0.0	0.0

Table S17. Percentage composition of the SO-RASSI wave functions for each M_J state of the ground multiplet (J = 15/2) of Dy1 in **2-Dy**.

M_J	KD1		KD2		KD3		KD4		KD5		KD6		KD7		KD8	
-15/2	0.0	95.6	0.0	0.1	2.0	0.0	0.0	2.0	0.0	0.1	0.1	0.0	0.0	0.0	0.0	0.0
-13/2	0.0	0.1	6.7	83.7	0.1	2.1	2.2	0.0	3.7	0.3	0.3	0.3	0.3	0.0	0.1	0.0
-11/2	0.0	4.2	0.0	0.0	32.0	0.0	0.6	50.9	0.1	5.9	2.5	2.1	0.0	1.3	0.0	0.4
-9/2	0.0	0.0	0.6	7.4	0.3	2.8	9.3	0.1	51.2	4.2	8.9	7.4	5.8	0.3	1.6	0.0
-7/2	0.0	0.1	0.1	0.0	18.7	0.1	0.2	0.2	1.6	8.8	20.5	22.1	0.4	21.6	0.0	5.8
-5/2	0.0	0.0	0.1	0.6	0.3	10.4	14.0	0.1	4.3	0.8	7.3	7.4	37.5	1.1	16.1	0.0
-3/2	0.0	0.0	0.2	0.0	15.5	0.2	0.3	7.8	1.0	13.4	1.5	0.8	0.7	26.8	0.1	31.6
-1/2	0.0	0.0	0.0	0.4	0.3	15.2	11.9	0.3	4.2	0.4	10.1	8.8	4.1	0.1	44.1	0.1
1/2	0.0	0.0	0.4	0.0	15.2	0.3	0.3	11.9	0.4	4.2	8.8	10.1	0.1	4.1	0.1	44.1
3/2	0.0	0.0	0.0	0.2	0.2	15.5	7.8	0.3	13.4	1.0	0.8	1.5	26.8	0.7	31.6	0.1
5/2	0.0	0.0	0.6	0.1	10.4	0.3	0.1	14.0	0.8	4.3	7.4	7.3	1.1	37.5	0.0	16.1
7/2	0.1	0.0	0.0	0.1	0.1	18.7	0.2	0.2	8.8	1.6	22.1	20.5	21.6	0.4	5.8	0.0
9/2	0.0	0.0	7.4	0.6	2.8	0.3	0.1	9.3	4.2	51.2	7.4	8.9	0.3	5.8	0.0	1.6
11/2	4.2	0.0	0.0	0.0	0.0	32.0	50.9	0.6	5.9	0.1	2.1	2.5	1.3	0.0	0.4	0.0
13/2	0.1	0.0	83.7	6.7	2.1	0.1	0.0	2.2	0.3	3.7	0.3	0.3	0.0	0.3	0.0	0.1
15/2	95.6	0.0	0.1	0.0	0.0	2.0	2.0	0.0	0.1	0.0	0.0	0.1	0.0	0.0	0.0	0.0

Table S18. Percentage composition of the SO-RASSI wave functions for each M_J state of the ground multiplet (J = 15/2) of Dy2 in **2-Dy**.

M_J	KD1		KD2		KD3		KD4		KD5		KD6		KD7		KD8	
-15/2	0.0	95.2	0.0	0.1	0.5	3.1	0.5	0.0	0.0	0.1	0.0	0.4	0.0	0.0	0.0	0.0
-13/2	0.0	0.1	1.1	95.1	0.2	0.2	0.0	1.9	0.3	0.0	0.8	0.0	0.1	0.0	0.0	0.2
-11/2	0.0	4.7	0.0	0.1	10.9	62.2	9.1	0.6	0.2	0.4	0.0	9.7	0.0	1.3	0.7	0.0
-9/2	0.0	0.0	0.0	3.0	2.0	0.8	1.5	55.8	5.0	1.8	17.3	0.1	8.2	0.5	0.0	4.0
-7/2	0.0	0.0	0.0	0.0	2.1	12.0	2.4	0.1	1.6	15.5	0.0	41.2	0.3	15.8	8.7	0.0
-5/2	0.0	0.0	0.0	0.1	2.2	0.6	0.5	19.9	6.4	1.7	17.9	0.0	30.8	1.6	0.1	18.3
-3/2	0.0	0.0	0.1	0.0	0.2	1.3	6.0	0.2	1.9	31.9	0.2	3.8	0.4	22.5	31.4	0.0
-1/2	0.0	0.0	0.0	0.3	1.3	0.5	0.3	1.1	30.6	2.5	8.4	0.1	18.0	0.3	0.1	36.4
1/2	0.0	0.0	0.3	0.0	0.5	1.3	1.1	0.3	2.5	30.6	0.1	8.4	0.3	18.0	36.4	0.1
3/2	0.0	0.0	0.0	0.1	1.3	0.2	0.2	6.0	31.9	1.9	3.8	0.2	22.5	0.4	0.0	31.4
5/2	0.0	0.0	0.1	0.0	0.6	2.2	19.9	0.5	1.7	6.4	0.0	17.9	1.6	30.8	18.3	0.1
7/2	0.0	0.0	0.0	0.0	12.0	2.1	0.1	2.4	15.5	1.6	41.2	0.0	15.8	0.3	0.0	8.7
9/2	0.0	0.0	3.0	0.0	0.8	2.0	55.8	1.5	1.8	5.0	0.1	17.3	0.5	8.2	4.0	0.0
11/2	4.7	0.0	0.1	0.0	62.2	10.9	0.6	9.1	0.4	0.2	9.7	0.0	1.3	0.0	0.0	0.7
13/2	0.1	0.0	95.1	1.1	0.2	0.2	1.9	0.0	0.0	0.3	0.0	0.8	0.0	0.1	0.2	0.0
15/2	95.2	0.0	0.1	0.0	3.1	0.5	0.0	0.5	0.1	0.0	0.4	0.0	0.0	0.0	0.0	0.0

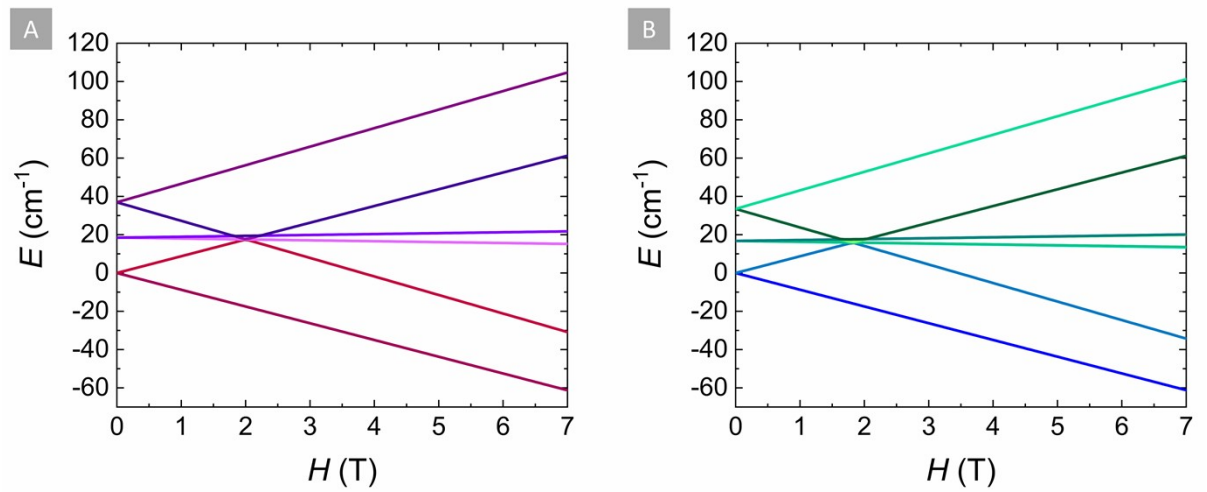

Fig. S27: The splitting of the low-lying exchange states of **1-Dy** (A) and **2-Dy** (B) under an external magnetic field of 1000 Oe, which was applied along the main magnetic axes shown in Figure S26. The first exchange doublet and the third exchange doublet are two-fold degenerate and correspond to two ferrimagnet (↑↓↑ and ↓↑↓; spins ordered as metal-radical-metal) and ferromagnet states (↑↑↑ and ↓↓↓), respectively, whereas the second exchange doublet is four-fold degenerate with the spin configurations of ↑↓↓, ↓↑↑, ↑↑↓, and ↓↓↑.

Table S19. Calculated *ab initio* average crystal-field parameters (cm^{-1}) given in the Iwahara–Chibotaru notation for Dy ions in **1-Dy** and for Dy1 and Dy2 ions in **2-Dy** derived from the crystal field parameters of double anion and neutral.

		Dy ions in 1-Dy			*Dy1 ion in 2-Dy*			*Dy2 ion in 2-Dy*		
k	***q***	***Re(B_{kq})***	***Im(B_{kq})***	***$\|B_{kq}\|$***	***Re(B_{kq})***	***Im(B_{kq})***	***$\|B_{kq}\|$***	***Re(B_{kq})***	***Im(B_{kq})***	***$\|B_{kq}\|$***
2	-2	-27.95	-5.50	28.48	212.87	14.03	213.33	-22.54	-48.93	53.87
2	-1	-0.36	51.56	51.56	-4.37	0.03	4.37	-3.55	-2.35	4.26
2	0	-210.07	0.00	210.07	-426.50	0.00	426.50	-252.56	0.00	252.56
2	1	0.36	51.56	51.56	4.37	0.03	4.37	3.55	-2.35	4.26
2	2	-27.95	5.50	28.48	212.87	-14.03	213.33	-22.54	48.93	53.87
4	-4	-5.51	3.39	6.47	14.29	-3.28	14.66	-8.58	-2.36	8.90
4	-3	-1.18	2.62	2.88	1.35	-1.38	1.93	-1.65	-1.73	2.39
4	-2	13.04	-12.19	17.85	-14.06	-2.16	14.23	2.15	-7.70	8.00
4	-1	-1.01	20.88	20.90	-0.64	-2.36	2.44	1.64	-3.44	3.81
4	0	-25.62	0.00	25.62	-40.52	0.00	40.52	-45.13	0.00	45.13
4	1	1.01	20.88	20.90	0.64	-2.36	2.44	-1.64	-3.44	3.81
4	2	13.04	12.19	17.85	-14.06	2.16	14.23	2.15	7.70	8.00
4	3	1.18	2.62	2.88	-1.35	-1.38	1.93	1.65	-1.73	2.39
4	4	-5.51	-3.39	6.47	14.29	3.28	14.66	-8.58	2.36	8.90
6	-6	-5.39	14.30	15.28	17.60	-1.77	17.69	-15.16	8.28	17.27
6	-5	10.26	4.16	11.07	-0.43	-0.66	0.79	0.66	-0.55	0.85
6	-4	0.24	7.10	7.10	-0.76	-0.78	1.09	-2.33	3.13	3.90
6	-3	-10.67	-8.56	13.68	-0.69	2.10	2.21	1.00	0.70	1.22
6	-2	10.97	-9.70	14.64	25.83	-5.89	26.49	22.95	-14.68	27.24
6	-1	-9.97	-9.75	13.95	1.93	-1.68	2.55	0.41	0.80	0.90
6	0	-14.42	0.00	14.42	-8.75	0.00	8.75	-0.97	0.00	0.97
6	1	9.97	-9.75	13.95	-1.93	-1.68	2.55	-0.41	0.80	0.90

6	2	10.97	9.70	14.64	25.83	5.89	26.49	22.95	14.68	27.24
6	3	10.67	-8.56	13.68	0.69	2.10	2.21	-1.00	0.70	1.22
6	4	0.24	-7.10	7.10	-0.76	0.78	1.09	-2.33	-3.13	3.90
6	5	-10.26	4.16	11.07	0.43	-0.66	0.79	-0.66	-0.55	0.85
6	6	-5.39	-14.30	15.28	17.60	1.77	17.69	-15.16	-8.28	17.27
8	-8	-0.01	-0.04	0.04	0.06	0.01	0.06	0.03	-0.02	0.03
8	-7	-0.02	0.00	0.02	0.00	0.00	0.00	0.00	0.00	0.00
8	-6	0.00	0.02	0.02	-0.05	0.00	0.05	0.00	0.00	0.01
8	-5	-0.04	0.00	0.04	0.01	0.00	0.01	-0.01	0.00	0.01
8	-4	0.04	-0.15	0.16	-0.15	0.04	0.15	0.04	-0.02	0.05
8	-3	0.13	0.08	0.15	-0.02	-0.02	0.03	-0.02	-0.01	0.02
8	-2	-0.10	0.07	0.12	-0.68	0.11	0.69	-0.28	0.27	0.39
8	-1	0.20	0.16	0.26	-0.09	0.05	0.10	-0.01	0.01	0.01
8	0	0.11	0.00	0.11	0.89	0.00	0.89	0.06	0.00	0.06
8	1	-0.20	0.16	0.26	0.09	0.05	0.10	0.01	0.01	0.01
8	2	-0.10	-0.07	0.12	-0.68	-0.11	0.69	-0.28	-0.27	0.39
8	3	-0.13	0.08	0.15	0.02	-0.02	0.03	0.02	-0.01	0.02
8	4	0.04	0.15	0.16	-0.15	-0.04	0.15	0.04	0.02	0.05
8	5	0.04	0.00	0.04	-0.01	0.00	0.01	0.01	0.00	0.01
8	6	0.00	-0.02	0.02	-0.05	0.00	0.05	0.00	0.00	0.01
8	7	0.02	0.00	0.02	0.00	0.00	0.00	0.00	0.00	0.00
8	8	-0.01	0.04	0.04	0.06	-0.01	0.06	0.03	0.02	0.03
10	-10	0.00	-0.01	0.01	0.01	0.00	0.01	0.01	0.00	0.01
10	-9	0.00	0.00	0.01	0.00	0.00	0.00	0.00	0.00	0.00
10	-8	0.00	0.01	0.01	0.01	-0.01	0.01	-0.01	0.01	0.02
10	-7	0.01	-0.01	0.01	0.00	0.00	0.00	0.00	0.00	0.00
10	-6	0.00	-0.01	0.01	-0.01	0.00	0.01	0.01	0.00	0.01
10	-5	-0.02	0.00	0.02	0.00	0.00	0.00	0.00	0.00	0.00
10	-4	0.00	-0.01	0.01	-0.01	0.00	0.01	0.00	0.00	0.01
10	-3	0.01	0.02	0.02	0.00	0.00	0.00	0.00	0.00	0.00
10	-2	0.00	0.00	0.00	-0.03	0.01	0.03	-0.04	0.02	0.05
10	-1	0.01	-0.01	0.02	0.00	0.00	0.00	-0.01	0.00	0.01
10	0	0.06	0.00	0.06	-0.02	0.00	0.02	0.01	0.00	0.01
10	1	-0.01	-0.01	0.02	0.00	0.00	0.00	0.01	0.00	0.01
10	2	0.00	0.00	0.00	-0.03	-0.01	0.03	-0.04	-0.02	0.05
10	3	-0.01	0.02	0.02	0.00	0.00	0.00	0.00	0.00	0.00
10	4	0.00	0.01	0.01	-0.01	0.00	0.01	0.00	0.00	0.01
10	5	0.02	0.00	0.02	0.00	0.00	0.00	0.00	0.00	0.00
10	6	0.00	0.01	0.01	-0.01	0.00	0.01	0.01	0.00	0.01
10	7	-0.01	-0.01	0.01	0.00	0.00	0.00	0.00	0.00	0.00
10	8	0.00	-0.01	0.01	0.01	0.01	0.01	-0.01	-0.01	0.02
10	9	0.00	0.00	0.01	0.00	0.00	0.00	0.00	0.00	0.00
10	10	0.00	0.01	0.01	0.01	0.00	0.01	0.01	0.00	0.01
12	-12	0.00	0.00	0.00	0.00	0.00	0.00	0.00	0.00	0.00
12	-11	0.00	0.00	0.00	0.00	0.00	0.00	0.00	0.00	0.00
12	-10	0.00	0.00	0.00	0.00	0.00	0.00	0.00	0.00	0.00
12	-9	0.00	0.00	0.00	0.00	0.00	0.00	0.00	0.00	0.00
12	-8	0.00	0.00	0.00	0.00	0.00	0.00	0.00	0.00	0.00

12	-7	0.00	0.00	0.00	0.00	0.00	0.00	0.00	0.00	0.00
12	-6	0.00	0.00	0.00	0.00	0.00	0.00	0.00	0.00	0.00
12	-5	0.00	0.00	0.00	0.00	0.00	0.00	0.00	0.00	0.00
12	-4	0.00	0.00	0.00	0.00	0.00	0.00	0.00	0.00	0.00
12	-3	0.00	0.00	0.00	0.00	0.00	0.00	0.00	0.00	0.00
12	-2	0.00	0.00	0.00	0.00	0.00	0.00	0.00	0.00	0.00
12	-1	0.00	0.00	0.00	0.00	0.00	0.00	0.00	0.00	0.00
12	0	0.00	0.00	0.00	0.01	0.00	0.01	0.01	0.00	0.01
12	1	0.00	0.00	0.00	0.00	0.00	0.00	0.00	0.00	0.00
12	2	0.00	0.00	0.00	0.00	0.00	0.00	0.00	0.00	0.00
12	3	0.00	0.00	0.00	0.00	0.00	0.00	0.00	0.00	0.00
12	4	0.00	0.00	0.00	0.00	0.00	0.00	0.00	0.00	0.00
12	5	0.00	0.00	0.00	0.00	0.00	0.00	0.00	0.00	0.00
12	6	0.00	0.00	0.00	0.00	0.00	0.00	0.00	0.00	0.00
12	7	0.00	0.00	0.00	0.00	0.00	0.00	0.00	0.00	0.00
12	8	0.00	0.00	0.00	0.00	0.00	0.00	0.00	0.00	0.00
12	9	0.00	0.00	0.00	0.00	0.00	0.00	0.00	0.00	0.00
12	10	0.00	0.00	0.00	0.00	0.00	0.00	0.00	0.00	0.00
12	11	0.00	0.00	0.00	0.00	0.00	0.00	0.00	0.00	0.00
12	12	0.00	0.00	0.00	0.00	0.00	0.00	0.00	0.00	0.00
14	-14	0.00	0.00	0.00	0.00	0.00	0.00	0.00	0.00	0.00
14	-13	0.00	0.00	0.00	0.00	0.00	0.00	0.00	0.00	0.00
14	-12	0.00	0.00	0.00	0.00	0.00	0.00	0.00	0.00	0.00
14	-11	0.00	0.00	0.00	0.00	0.00	0.00	0.00	0.00	0.00
14	-10	0.00	0.00	0.00	0.00	0.00	0.00	0.00	0.00	0.00
14	-9	0.00	0.00	0.00	0.00	0.00	0.00	0.00	0.00	0.00
14	-8	0.00	0.00	0.00	0.00	0.00	0.00	0.00	0.00	0.00
14	-7	0.00	0.00	0.00	0.00	0.00	0.00	0.00	0.00	0.00
14	-6	0.00	0.00	0.00	0.00	0.00	0.00	0.00	0.00	0.00
14	-5	0.00	0.00	0.00	0.00	0.00	0.00	0.00	0.00	0.00
14	-4	0.00	0.00	0.00	0.00	0.00	0.00	0.00	0.00	0.00
14	-3	0.00	0.00	0.00	0.00	0.00	0.00	0.00	0.00	0.00
14	-2	0.00	0.00	0.00	0.00	0.00	0.00	0.00	0.00	0.00
14	-1	0.00	0.00	0.00	0.00	0.00	0.00	0.00	0.00	0.00
14	0	0.00	0.00	0.00	0.00	0.00	0.00	0.00	0.00	0.00
14	1	0.00	0.00	0.00	0.00	0.00	0.00	0.00	0.00	0.00
14	2	0.00	0.00	0.00	0.00	0.00	0.00	0.00	0.00	0.00
14	3	0.00	0.00	0.00	0.00	0.00	0.00	0.00	0.00	0.00
14	4	0.00	0.00	0.00	0.00	0.00	0.00	0.00	0.00	0.00
14	5	0.00	0.00	0.00	0.00	0.00	0.00	0.00	0.00	0.00
14	6	0.00	0.00	0.00	0.00	0.00	0.00	0.00	0.00	0.00
14	7	0.00	0.00	0.00	0.00	0.00	0.00	0.00	0.00	0.00
14	8	0.00	0.00	0.00	0.00	0.00	0.00	0.00	0.00	0.00
14	9	0.00	0.00	0.00	0.00	0.00	0.00	0.00	0.00	0.00
14	10	0.00	0.00	0.00	0.00	0.00	0.00	0.00	0.00	0.00
14	11	0.00	0.00	0.00	0.00	0.00	0.00	0.00	0.00	0.00
14	12	0.00	0.00	0.00	0.00	0.00	0.00	0.00	0.00	0.00
14	13	0.00	0.00	0.00	0.00	0.00	0.00	0.00	0.00	0.00

14	14	0.00	0.00	0.00	0.00	0.00	0.00	0.00	0.00	0.00

7. Additional ac magnetic data for complexes 1-Dy and 2-Dy

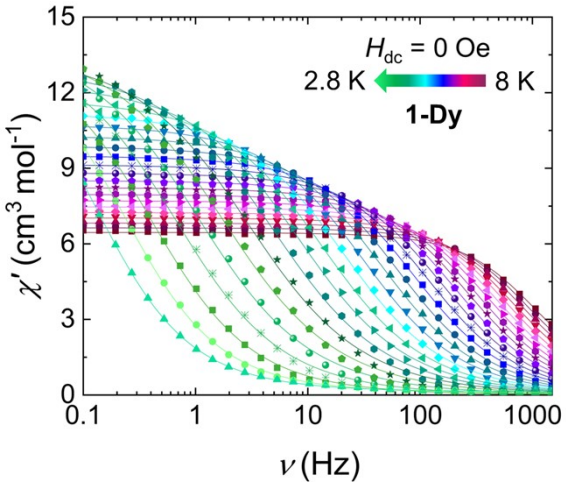

Fig. S28: Frequency-dependence of χ' as a function of temperature in the 8 to 2.8 K temperature range, in the absence of an applied field (H_{dc} = 0 Oe) for **1-Dy**. Solid lines represent best fits to the generalized Debye model.

Table S20. Fitting parameters obtained from CCFit-2[54] using a generalized Debye model for the ac data of **1-Dy** in the absence of a static dc field (H_{dc} = 0 Oe) in the temperature region of 2.8 to 8 K (Fig. 3A and S28).

T (K)	τ (s)	α	χ_s (cm^3 mol^{-1})	χ_t (cm^3 mol^{-1})
2.8	1.23	2.75 x 10^{-1}	1.36 x 10^{-1}	14.7
3	6.68 x 10^{-1}	2.78 x 10^{-1}	8.21 x 10^{-2}	13.9
3.2	3.89 x 10^{-1}	3.01 x 10^{-1}	5.42 x 10^{-2}	13.8
3.4	2.38 x 10^{-1}	3.24 x 10^{-1}	6.78 x 10^{-21}	13.9
3.6	1.51 x 10^{-1}	3.46 x 10^{-1}	8.40 x 10^{-19}	14.1
3.8	9.21 x 10^{-2}	3.55 x 10^{-1}	8.29 x 10^{-19}	14.0
4	5.37 x 10^{-2}	3.52 x 10^{-1}	3.36 x 10^{-15}	13.6
4.2	3.16 x 10^{-2}	3.42 x 10^{-1}	1.84 x 10^{-16}	13.0
4.4	1.90 x 10^{-2}	3.30 x 10^{-1}	1.24 x 10^{-16}	12.4
4.6	1.17 x 10^{-2}	3.15 x 10^{-1}	1.43 x 10^{-17}	11.7
4.8	7.60 x 10^{-3}	3.05 x 10^{-1}	6.65 x 10^{-19}	11.2
5	5.11 x 10^{-3}	2.95 x 10^{-1}	8.49 x 10^{-20}	10.7
5.2	3.52 x 10^{-3}	2.85 x 10^{-1}	1.94 x 10^{-21}	10.3
5.4	2.50 x 10^{-3}	2.76 x 10^{-1}	4.18 x 10^{-18}	9.87
5.6	1.81 x 10^{-3}	2.69 x 10^{-1}	2.26 x 10^{-18}	9.49
5.8	1.34 x 10^{-3}	2.62 x 10^{-1}	1.55 x 10^{-16}	9.13
6	1.02 x 10^{-3}	2.55 x 10^{-1}	4.25 x 10^{-23}	8.81
6.2	7.85 x 10^{-4}	2.50 x 10^{-1}	1.95 x 10^{-18}	8.51
6.4	6.15 x 10^{-4}	2.45 x 10^{-1}	3.12 x 10^{-20}	8.23
6.6	4.91 x 10^{-4}	2.39 x 10^{-1}	6.87 x 10^{-21}	7.96
6.8	3.96 x 10^{-4}	2.33 x 10^{-1}	6.73 x 10^{-3}	7.71
7	3.28 x 10^{-4}	2.23 x 10^{-1}	7.57 x 10^{-2}	7.47
7.2	2.76 x 10^{-4}	2.12 x 10^{-1}	1.56 x 10^{-1}	7.24
7.4	2.34 x 10^{-4}	2.04 x 10^{-1}	2.06 x 10^{-1}	7.03
7.6	2.00 x 10^{-4}	1.94 x 10^{-1}	2.79 x 10^{-1}	6.82
7.8	1.75 x 10^{-4}	1.82 x 10^{-1}	3.68 x 10^{-1}	6.63
8	1.51 x 10^{-4}	1.76 x 10^{-1}	3.86 x 10^{-1}	6.45

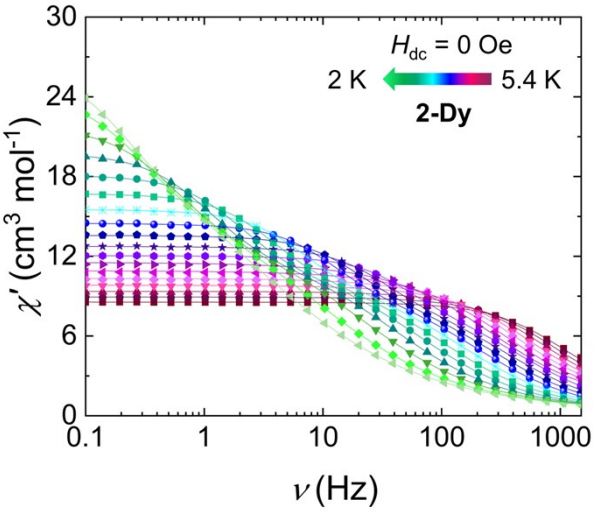

Fig. S29: Frequency-dependence of χ' as a function of temperature in the 2 to 5.4 K temperature range, in the absence of an applied field (H_{dc} = 0 Oe) for **2-Dy**. Solid lines represent best fits to the generalized Debye model.

Table S21. Best-fit parameters obtained from CCFit-2[54] using a generalized Debye model for the ac data for **2-Dy** in the absence of a static dc field (H_{dc} = 0 Oe) in the temperature region of 4.2 to 5.4 K (Fig. 3B and S29).

T (K)	τ (s)	α	χ_s (cm^3 mol^{-1})	χ_t (cm^3 mol^{-1})
4.2	5.98 x 10^{-4}	2.94 x 10^{-1}	0.84	11.5
4.4	4.57 x 10^{-4}	2.63 x 10^{-1}	1.02	10.9
4.6	3.55 x 10^{-4}	2.34 x 10^{-1}	1.19	10.3
4.8	2.81 x 10^{-4}	2.08 x 10^{-1}	1.31	9.82
5	2.26 x 10^{-4}	1.85 x 10^{-1}	1.41	9.36
5.2	1.86 x 10^{-4}	1.63 x 10^{-1}	1.54	8.93
5.4	1.53 x 10^{-4}	1.48 x 10^{-1}	1.59	8.56

Table S22. Best-fit parameters obtained from CCFit-2[54] using a two-term generalized Debye model for the ac data for **2-Dy** in the absence of a static dc field (H_{dc} = 0 Oe) in the temperature region of 2 to 4 K (Fig. 3B and S29).

T (K)	$\chi_{s,TOT}$ (cm^3 mol^{-1})	$\Delta\chi_1$ (cm^3 mol^{-1})	τ_1 (s)	α_1	$\Delta\chi_2$ (cm^3 mol^{-1})	τ_2 (s)	α_2
2	1.54 x 10^{-1}	10.5	7.83 x 10^{-1}	5.53 x 10^{-2}	21.8	5.87 x 10^{-2}	4.84 x 10^{-1}
2.2	2.66 x 10^{-1}	11.6	5.41 x 10^{-1}	1.05 x 10^{-1}	16.6	1.82 x 10^{-2}	4.23 x 10^{-1}
2.4	3.91 x 10^{-1}	8.29	2.87 x 10^{-1}	1.06 x 10^{-1}	13.2	7.08 x 10^{-3}	3.64 x 10^{-1}
2.6	3.79 x 10^{-1}	7.70	1.51 x 10^{-1}	9.20 x 10^{-2}	11.8	3.80 x 10^{-3}	3.32 x 10^{-1}
2.8	3.39 x 10^{-1}	6.92	7.94 x 10^{-2}	7.52 x 10^{-2}	10.9	2.33 x 10^{-3}	3.13 x 10^{-1}
3	3.11 x 10^{-1}	6.27	4.27 x 10^{-2}	6.57 x 10^{-2}	10.2	1.51 x 10^{-3}	2.99 x 10^{-1}
3.2	3.03 x 10^{-1}	5.68	2.36 x 10^{-2}	5.93 x 10^{-2}	9.55	1.03 x 10^{-3}	2.86 x 10^{-1}
3.4	2.40 x 10^{-1}	5.02	1.36 x 10^{-2}	4.86 x 10^{-2}	9.22	7.46 x 10^{-4}	2.86 x 10^{-1}
3.6	2.40 x 10^{-1}	4.58	8.10 x 10^{-3}	4.45 x 10^{-2}	8.76	5.44 x 10^{-4}	2.76 x 10^{-1}
3.8	1.69 x 10^{-1}	3.87	5.07 x 10^{-3}	1.83 x 10^{-2}	8.71	4.24 x 10^{-4}	2.83 x 10^{-1}
4.0	2.37 x 10^{-1}	3.48	3.24 x 10^{-3}	9.87 x 10^{-3}	8.34	3.30 x 10^{-4}	2.70 x 10^{-1}

Table S23. Best-fit parameters of the temperature-dependent relaxation times of the magnetization for **1-Dy** and **2-Dy**, in the absence of a dc field (H_{dc} = 0 Oe).

		1-Dy	2-Dy	
			Process 1	***Process 2***
Raman	C (s^{-1} K^{-n})	4.08×10^{-3}	9.62×10^{-3}	
	n	5.13	6.88	
Orbach	τ_0 (s)	3.30×10^{-7}	1.48×10^{-8}	2.10×10^{-6}
	U_{eff} (cm^{-1})	34	35	14

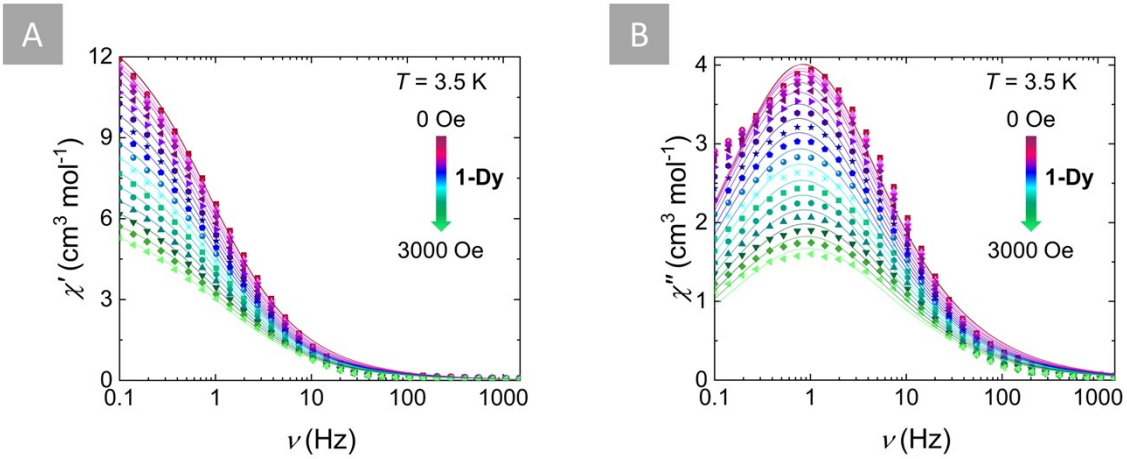

Fig. S30: Field-dependence of the χ' (A) and χ'' (B) magnetic susceptibility of **1-Dy** at 3.5 K in the field range of 0 to 3000 Oe. The solid lines represent the best fit to the generalized Debye model.

Table S24. Best-fit parameters obtained from CCFit-2[54] using a generalized Debye model for the ac data of **1-Dy** in the field range of 0 to 3000 Oe at 3.5 K (Fig. S30).

H (Oe)	τ (s)	α	χ_s (cm^3 mol^{-1})	χ_t (cm^3 mol^{-1})
0	1.88×10^{-1}	3.34×10^{-1}	2.27×10^{-14}	13.9
100	1.92×10^{-1}	3.35×10^{-1}	3.08×10^{-15}	13.9
200	1.95×10^{-1}	3.33×10^{-1}	1.24×10^{-16}	13.7
300	1.99×10^{-1}	3.31×10^{-1}	6.27×10^{-17}	13.5
400	2.03×10^{-1}	3.30×10^{-1}	2.42×10^{-17}	13.4
600	2.10×10^{-1}	3.30×10^{-1}	4.60×10^{-18}	13.0
800	2.13×10^{-1}	3.32×10^{-1}	1.48×10^{-18}	12.6
1000	2.13×10^{-1}	3.33×10^{-1}	1.57×10^{-18}	12.2
1200	2.10×10^{-1}	3.35×10^{-1}	2.51×10^{-18}	11.6
1400	2.08×10^{-1}	3.39×10^{-1}	7.23×10^{-18}	11.0
1600	2.03×10^{-1}	3.42×10^{-1}	2.53×10^{-17}	10.3
1800	2.01×10^{-1}	3.45×10^{-1}	5.03×10^{-17}	9.71
2000	1.95×10^{-1}	3.49×10^{-1}	2.49×10^{-16}	9.05
2200	1.89×10^{-1}	3.52×10^{-1}	3.25×10^{-16}	8.41
2400	1.84×10^{-1}	3.55×10^{-1}	1.04×10^{-15}	7.80
2600	1.79×10^{-1}	3.61×10^{-1}	1.57×10^{-23}	7.23
2800	1.73×10^{-1}	3.62×10^{-1}	2.66×10^{-18}	6.67
3000	1.69×10^{-1}	3.67×10^{-1}	8.85×10^{-19}	6.17

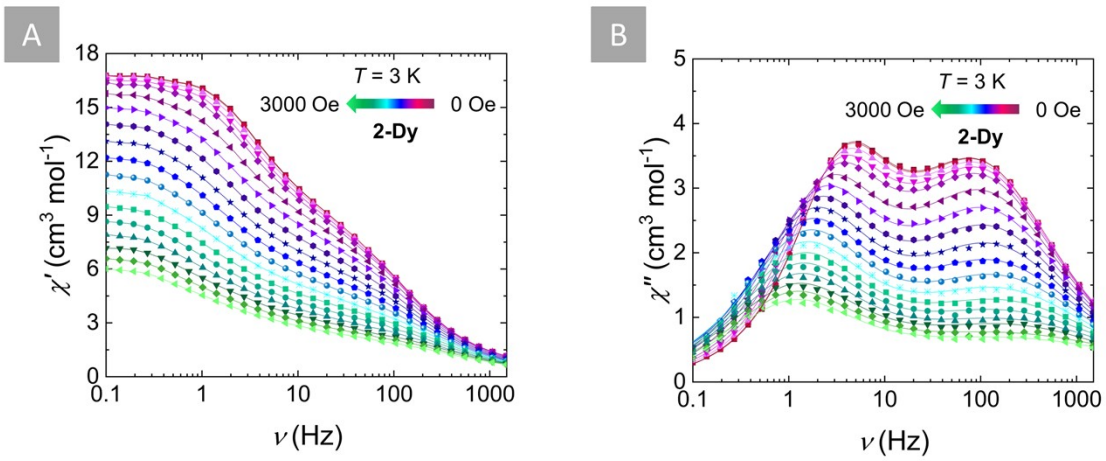

Fig. S31: Field-dependence of the χ' (A) and χ'' (B) magnetic susceptibility of **2-Dy** at 3 K in the field range of 0 to 3000 Oe. The solid lines represent the best fit to the two-term generalized Debye model.

Table S25. Best-fit parameters obtained from CCFit-2[54] using a two-term generalized Debye model for the ac data of **2-Dy** in the field range of 0 to 3000 Oe at 3 K (Fig. S31).

H (Oe)	$\chi_{s,TOT}$ (cm³ mol⁻¹)	$\Delta\chi_1$ (cm³ mol⁻¹)	τ_1 (s)	α_1	$\Delta\chi_2$ (cm³ mol⁻¹)	τ_2 (s)	α_2
0	2.99 x 10^{-1}	6.29	4.31 x 10^{-2}	6.36 x 10^{-2}	10.3	1.52 x 10^{-3}	3.01 x 10^{-1}
100	3.20 x 10^{-1}	6.35	4.35 x 10^{-2}	6.92 x 10^{-2}	10.2	1.51 x 10^{-3}	2.97 x 10^{-1}
200	2.95 x 10^{-1}	6.49	4.59 x 10^{-2}	8.98 x 10^{-2}	10.0	1.47 x 10^{-3}	2.98 x 10^{-1}
300	2.71 x 10^{-1}	6.48	4.98 x 10^{-2}	1.01 x 10^{-1}	9.88	1.45 x 10^{-3}	3.02 x 10^{-1}
400	2.64 x 10^{-1}	6.57	5.47 x 10^{-2}	1.18 x 10^{-1}	9.62	1.42 x 10^{-3}	3.03 x 10^{-1}
600	1.90 x 10^{-1}	6.64	6.54 x 10^{-2}	1.41 x 10^{-1}	9.08	1.33 x 10^{-3}	3.13 x 10^{-1}
800	1.63 x 10^{-1}	6.68	7.50 x 10^{-2}	1.60 x 10^{-1}	8.34	1.24 x 10^{-3}	3.18 x 10^{-1}
1000	1.02 x 10^{-1}	6.51	8.42 x 10^{-2}	1.68 x 10^{-1}	7.70	1.17 x 10^{-3}	3.33 x 10^{-1}
1200	4.78 x 10^{-2}	6.35	9.23 x 10^{-2}	1.82 x 10^{-1}	7.00	1.08 x 10^{-3}	3.47 x 10^{-1}
1400	5.07 x 10^{-3}	6.09	1.01 x 10^{-1}	1.90 x 10^{-1}	6.41	1.02 x 10^{-3}	3.66 x 10^{-1}
1600	6.86 x 10^{-13}	5.88	1.07 x 10^{-1}	2.04 x 10^{-1}	5.70	9.30 x 10^{-4}	3.73 x 10^{-1}
1800	5.65 x 10^{-15}	5.60	1.15 x 10^{-1}	2.18 x 10^{-1}	5.11	8.74 x 10^{-4}	3.86 x 10^{-1}
2000	1.37 x 10^{-18}	5.20	1.19 x 10^{-1}	2.20 x 10^{-1}	4.61	8.16 x 10^{-4}	3.98 x 10^{-1}
2200	1.40 x 10^{-13}	4.88	1.23 x 10^{-1}	2.31 x 10^{-1}	4.12	7.51 x 10^{-4}	4.06 x 10^{-1}
2400	8.26 x 10^{-14}	4.53	1.28 x 10^{-1}	2.38 x 10^{-1}	3.72	7.13 x 10^{-4}	4.21 x 10^{-1}
2600	3.18 x 10^{-16}	4.21	1.32 x 10^{-1}	2.49 x 10^{-1}	3.36	6.74 x 10^{-4}	4.33 x 10^{-1}
2800	2.74 x 10^{-16}	3.75	1.37 x 10^{-1}	2.37 x 10^{-1}	3.14	6.76 x 10^{-4}	4.54 x 10^{-1}
3000	8.83 x 10^{-17}	3.45	1.40 x 10^{-1}	2.43 x 10^{-1}	2.86	6.46 x 10^{-4}	4.64 x 10^{-1}

Fit of the field-dependent relaxation times for 1-Dy and 2-Dy:

To further investigate the relaxation dynamics in **1-Dy** and **2-Dy** the extracted relaxation times from the field-dependent ac susceptibility (χ' and χ'') can be fit to the following eq. (S7):

$$\tau^{-1} = \tau_{QTM}^{-1} + \tau_{Raman}^{-1} + \tau_{Direct}^{-1} + \tau_{Orbach}^{-1}$$

$$\tau^{-1} = \frac{B_1}{1 + B_2 H^2} + \frac{1 + C_1 H^2}{1 + C_2 H^2} C T^n + A T H^m + \tau_0^{-1} exp\left(\frac{-U_{eff}}{k_B T}\right) \quad \text{(S7)}$$

For **1-Dy**, the inclusion of all four relaxation mechanisms did not provide a satisfactory fit and therefore some simplifications of this equation had to be taken into account. This is expected

given that the relaxation times do not exhibit a significant field dependence which in addition to the superposition of the ac signal (Fig. S30), signifies that the relaxation of the magnetization is indeed mediated by thermally activated processes. As such, the direct and QTM terms, which are clearly field-dependent contributions, can be exempt from the fit. Therefore, the QTM and direct terms were fixed to zero and only the Raman and Orbach contributions were taken into account. In order to achieve the best fit parameters, the terms C1 and C2 were fixed to be zero as the fit could not provide any meaningful values for these parameters (C1 < 10^{-8} and C2 = 0). As such, for **1-Dy**, the field-dependent relaxation times (Fig. S32) were fit to a combination of Ramman and Orbach processes according to eq.(S8):

$$\tau^{-1} = \tau_{Raman}^{-1} + \tau_{Orbach}^{-1}$$

$$\tau^{-1} = \frac{1 + C_1 \mathrm{H}^2}{1 + C_2 \mathrm{H}^2} C T^n + \tau_0^{-1} exp(\frac{-U_{eff}}{k_B T}) \quad \text{(S8)}$$

For **2-Dy**, the relaxation times for two distinct processes were analyzed. In the low-frequency range a very small field-dependent shift of the ac susceptibility peak is observed without however an improvement of the signal with the increase of the applied field (Fig. S31). On the contrary, at higher frequencies the peak maxima show no field-dependence or improvement with the increase of the applied field. Similarly to **1-Dy**, for both Process 1 and 2 of **2-Dy**, the relaxation times do not exhibit a significant field-dependence which in addition to the non-improvement of the ac signal, signifies that the relaxation of the magnetization is indeed mediated by thermally activated processes and therefore direct and QTM contributions can be excluded from the fit. For Process 1 (at the low-frequency region) the best-fit can be achieved with a combination of Raman and Orbach to eq.(S8) (Fig. S33A), while for Process 2 the best-fit can be achieved for an Orbach-only process based on eq.(S9) (Fig. S33B):

$$\tau^{-1} = \tau_{Orbach}^{-1}$$

$$\tau^{-1} = \tau_0^{-1} exp(\frac{-U_{eff}}{k_B T}) \quad \text{(S9)}$$

It is important to note that in order to achieve a satisfactory fit for Process 1 of **2-Dy** it was necessary to include the C_1 and C_2 parameters, while for **1-Dy** these were pointing towards zero and were not contributing to the overall fit (hence they were ultimately fixed to zero). The best-fit parameters for the field-dependent τ for both **1-Dy** and **2-Dy** are in good agreement with the best-fit parameters of the temperature-dependent τ and can be found in Table S25.

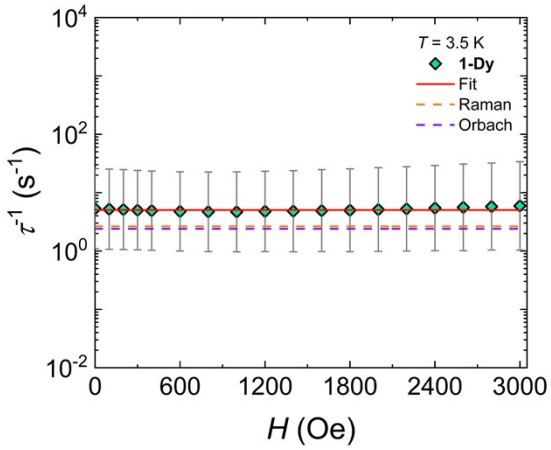

Fig. S32: Field-dependence of the relaxation times (τ^{-1}) for **1-Dy** at a fixed temperature of 3.5 K with the respective estimated standard deviations (gray bars). These estimated standard deviations of the relaxation times have been calculated from the α-parameters of the generalized Debye fits with the log-normal distribution.[54] The relaxation times were obtained from the generalized Debye model (Table S23). The solid red line represents the fit to eq.(S8), while the dashed orange and purple lines represent the individual components of the magnetic relaxation for Raman and Orbach processes, respectively.

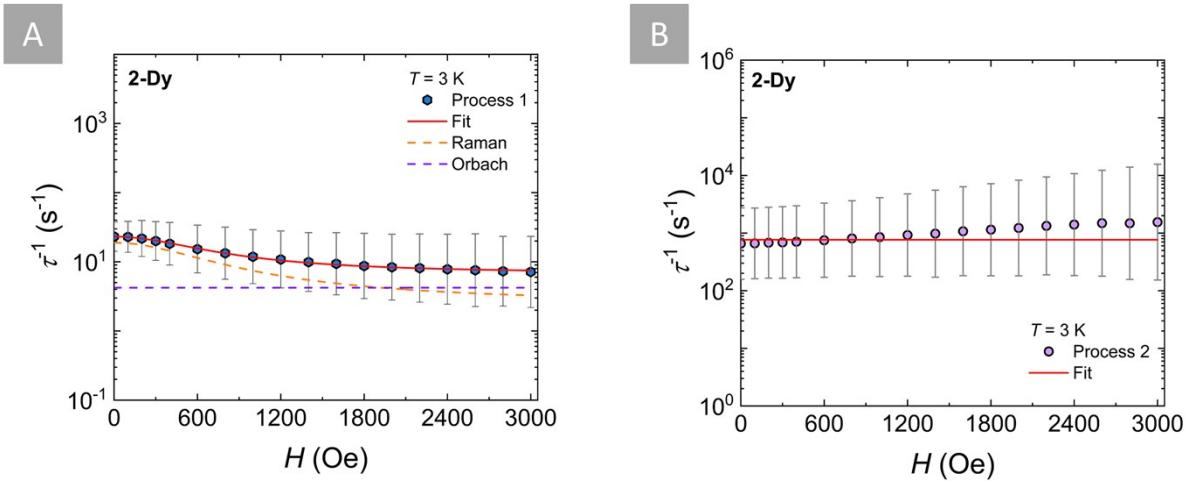

Fig. S33: Field-dependence of the relaxation times (τ^{-1}) for both processes **2-Dy** at a fixed temperature of 3 K with the respective estimated standard deviations (gray bars). These estimated standard deviations of the relaxation times have been calculated from the α-parameters of the generalized Debye fits with the log-normal distribution.[54] The relaxation times were obtained from the generalized Debye model (Table S24). For Process 1 (A) the solid red line represents the fit to eq.(S8), while the dashed orange and purple lines represent the individual components of the magnetic relaxation for Raman and Orbach processes, respectively. For Process 2 (B) the solid red line represents the fit to eq.(S9).

Table S26. Best-fit parameters of the field-dependent relaxation times of the magnetization for **1-Dy** and **2-Dy**.

		1-Dy	2-Dy	
			Process 1	***Process 2***
Raman	C (s^{-1} K^{-n})	7.24×10^{-3}	8.91×10^{-3}	
	n	5.37	6.97	
	C_1 (Oe^{-2})	-	3.13×10^{-7}	
	C_2 (Oe^{-2})	-	2.34×10^{-6}	
Orbach	τ_0 (s)	1.44×10^{-7}	1.21×10^{-8}	2.10×10^{-6}
	U_{eff} (cm^{-1})	31.0	35.0	13.4

8. References

1 R. M. Versteegen, R. Rossin, W. ten Hoeve, H. M. Janssen and M. S. Robillard, *Angew. Chem. Int. Ed.*, 2013, **52**, 14112–14116.

2 R. I. Ishmetova, N. I. Latosh, I. N. Ganebnykh, N. K. Ignatenko, S. G. Tolshchina and G. L. Rusinov, *Russ. J. Org. Chem.*, 2009, **45**, 1102–1107.

3 K. V. Domasevitch, I. A. Gural'skiy, P. V. Solntsev, E. B. Rusanov, H. Krautscheid, J. A. K. Howard and A. N. Chernega, *Dalton Trans.*, 2007, 3140–3148.

4 M. D. Helm, A. Plant and J. P. A. Harrity, *Org. Biomol. Chem.*, 2006, **4**, 4278–4280.

5 M. D. Coburn, G. A. Buntain, B. W. Harris, M. A. Hiskey, K.-Y. Lee and D. G. Ott, *J. Heterocycl. Chem.*, 1991, **28**, 2049–2050.

6 S. Demir, J. M. Zadrozny, M. Nippe and J. R. Long, *J. Am. Chem. Soc.*, 2012, **134**, 18546–18549.

7 G. M. Sheldrick, *SADABS - Bruker/Siemens Area Detector Absorption Correction Program, University of Göttingen: Göttingen, Germany*, 1996.

8 G. M. Sheldrick, *Acta Crystallogr. Sect. Found. Adv.*, 2015, **71**, 3–8.

9 G. M. Sheldrick, *Acta Crystallogr. Sect. C Struct. Chem.*, 2015, **71**, 3–8.

10 A. L. Spek, *Acta Crystallogr. A*, 1990, **46**, 34–34.

11 L. J. Farrugia, *J. Appl. Crystallogr.*, 1999, **32**, 837–838.

12 K. Brandenburg, *Acta Crystallogr. A*, 1996, **52**, 562–562.

13 C. F. Macrae, P. R. Edgington, P. McCabe, E. Pidcock, G. P. Shields, R. Taylor, M. Towler and J. van de Streek, *J. Appl. Crystallogr.*, 2006, **39**, 453–457.

14 Y. He, W. Wu, G. Zhao, Y. Liu and Y. Li, *Macromolecules*, 2008, **41**, 9760–9766.

15 J.-L. Bredas, *Mater. Horiz.*, 2013, **1**, 17–19.

16 Gaussian 16, Revision C.01, M. J. Frisch, G. W. Trucks, H. B. Schlegel, G. E. Scuseria, M. A. Robb, J. R. Cheeseman, G. Scalmani, V. Barone, G. A. Petersson, H. Nakatsuji, X. Li, M. Caricato, A. V. Marenich, J. Bloino, B. G. Janesko, R. Gomperts, B. Mennucci, H. P. Hratchian, J. V. Ortiz, A. F. Izmaylov, J. L. Sonnenberg, D. Williams-Young, F. Ding, F. Lipparini, F. Egidi, J. Goings, B. Peng, A. Petrone, T. Henderson, D. Ranasinghe, V. G. Zakrzewski, J. Gao, N. Rega, G. Zheng, W. Liang, M. Hada, M. Ehara, K. Toyota, R. Fukuda, J. Hasegawa, M. Ishida, T. Nakajima, Y. Honda, O. Kitao, H. Nakai, T. Vreven, K. Throssell, J. A. Montgomery, Jr., J. E. Peralta, F. Ogliaro, M. J. Bearpark, J. J. Heyd, E. N. Brothers, K. N. Kudin, V. N. Staroverov, T. A. Keith, R. Kobayashi, J. Normand, K. Raghavachari, A. P. Rendell, J. C. Burant, S. S. Iyengar, J. Tomasi, M. Cossi, J. M. Millam, M. Klene, C. Adamo, R. Cammi, J. W. Ochterski, R. L. Martin, K. Morokuma, O. Farkas, J. B. Foresman, and D. J. Fox, Gaussian, Inc., Wallingford CT, Gaussian 16, Revision C.01, (version Gaussian 16, Revision C.01,) 2016.

17 B. O. Roos, P. R. Taylor and P. E. M. Sigbahn, *Chem. Phys.*, 1980, **48**, 157–173.

18 B. O. Roos, *Multiconfigurational Quantum Chemistry*, Wiley-Blackwell, 2016.

19 I. Fdez. Galván, M. Vacher, A. Alavi, C. Angeli, F. Aquilante, J. Autschbach, J. J. Bao, S. I. Bokarev, N. A. Bogdanov, R. K. Carlson, L. F. Chibotaru, J. Creutzberg, N. Dattani, M. G. Delcey, S. S. Dong, A. Dreuw, L. Freitag, L. M. Frutos, L. Gagliardi, F. Gendron, A. Giussani, L. González, G. Grell, M.

Guo, C. E. Hoyer, M. Johansson, S. Keller, S. Knecht, G. Kovačević, E. Källman, G. Li Manni, M. Lundberg, Y. Ma, S. Mai, J. P. Malhado, P. Å. Malmqvist, P. Marquetand, S. A. Mewes, J. Norell, M. Olivucci, M. Oppel, Q. M. Phung, K. Pierloot, F. Plasser, M. Reiher, A. M. Sand, I. Schapiro, P. Sharma, C. J. Stein, L. K. Sørensen, D. G. Truhlar, M. Ugandi, L. Ungur, A. Valentini, S. Vancoillie, V. Veryazov, O. Weser, T. A. Wesołowski, P.-O. Widmark, S. Wouters, A. Zech, J. P. Zobel and R. Lindh, *J. Chem. Theory Comput.*, 2019, **15**, 5925–5964.
20 N. Mavragani, D. Errulat, D. A. Gálico, A. A. Kitos, A. Mansikkamäki and M. Murugesu, *Angew. Chem.*, 2021, **133**, 24408–24415.
21 P. Å. Malmqvist, B. O. Roos and B. Schimmelpfennig, *Chem. Phys. Lett.*, 2002, **357**, 230–240.
22 W. Kutzelnigg and W. Liu, *J. Chem. Phys.*, 2005, **123**, 241102.
23 D. Peng and M. Reiher, *Theor. Chem. Acc.*, 2012, **131**, 1081.
24 M. Filatov, *J. Chem. Phys.*, 2006, **125**, 107101.
25 B. O. Roos, R. Lindh, P.-Å. Malmqvist, V. Veryazov, P.-O. Widmark and A. C. Borin, *J. Phys. Chem. A*, 2008, **112**, 11431–11435.
26 B. O. Roos, R. Lindh, P.-Å. Malmqvist, V. Veryazov and P.-O. Widmark, *J. Phys. Chem. A*, 2004, **108**, 2851–2858.
27 L. Ungur and L. F. Chibotaru, *Chem. – Eur. J.*, 2017, **23**, 3708–3718.
28 L. Ungur, M. Thewissen, J.-P. Costes, W. Wernsdorfer and L. F. Chibotaru, *Inorg. Chem.*, 2013, **52**, 6328–6337.
29 L. F. Chibotaru and L. Ungur, *J. Chem. Phys.*, 2012, **137**, 064112.
30 N. F. Chilton, R. P. Anderson, L. D. Turner, A. Soncini and K. S. Murray, *J. Comput. Chem.*, 2013, **34**, 1164–1175.
31 N. Mavragani, A. A. Kitos, J. Hrubý, S. Hill, A. Mansikkamäki, J. O. Moilanen and M. Murugesu, *Inorg. Chem. Front.*, 2023, **10**, 4197–4208.
32 T. R. Cundari and W. J. Stevens, *J. Chem. Phys.*, 1993, **98**, 5555–5565.
33 F. Weigend and R. Ahlrichs, *Phys. Chem. Chem. Phys.*, 2005, **7**, 3297–3305.
34 B. P. Pritchard, D. Altarawy, B. Didier, T. D. Gibson and T. L. Windus, *J. Chem. Inf. Model.*, 2019, **59**, 4814–4820.
35 D. Feller, *J. Comput. Chem.*, 1996, **17**, 1571–1586.
36 K. L. Schuchardt, B. T. Didier, T. Elsethagen, L. Sun, V. Gurumoorthi, J. Chase, J. Li and T. L. Windus, *J. Chem. Inf. Model.*, 2007, **47**, 1045–1052.
37 S. Grimme, S. Ehrlich and L. Goerigk, *J. Comput. Chem.*, 2011, **32**, 1456–1465.
38 S. Grimme, J. Antony, S. Ehrlich and H. Krieg, *J. Chem. Phys.*, 2010, **132**, 154104.
39 F. Neese, *WIREs Comput. Mol. Sci.*, 2022, **12**, e1606.
40 T. Yanai, D. P. Tew and N. C. Handy, *Chem. Phys. Lett.*, 2004, **393**, 51–57.
41 F. Weigend, *Phys. Chem. Chem. Phys.*, 2006, **8**, 1057–1065.
42 C. van Wüllen, *J. Chem. Phys.*, 1998, **109**, 392–399.
43 R. Maurice, C. de Graaf and N. Guihéry, *Phys. Chem. Chem. Phys.*, 2013, **15**, 18784–18804.
44 R. F. W. Bader and R. F. Bader, *Atoms in Molecules: A Quantum Theory*, Clarendon Press, 1990.
45 T. A. Keith, AIMAll (Version 19.10.12) (version Version 19.10. 12) TK Gristmill Software, Overland Park KS, USA 2019.
46 *ADF2022.1, 2022. https://www.scm.com (accessed 2024-07-03)*, 2022.
47 G. te Velde, F. M. Bickelhaupt, E. J. Baerends, C. Fonseca Guerra, S. J. A. van Gisbergen, J. G. Snijders and T. Ziegler, *J. Comput. Chem.*, 2001, **22**, 931–967.
48 AMS 2022.1; SCM, Theoretical Chemistry (version 2022.1) SCM, Vrije Universiteit 2022.
49 P. J. Stephens, F. J. Devlin, C. F. Chabalowski and M. J. Frisch, Ab Initio Calculation of Vibrational Absorption and Circular Dichroism Spectra Using Density Functional Force Fields, https://pubs.acs.org/doi/pdf/10.1021/j100096a001, (accessed 3 July 2024).
50 E. van Lenthe, E. J. Baerends and J. G. Snijders, *J. Chem. Phys.*, 1994, **101**, 9783–9792.
51 E. van Lenthe, E. J. Baerends and J. G. Snijders, *J. Chem. Phys.*, 1993, **99**, 4597–4610.
52 E. van Lenthe, A. Ehlers and E.-J. Baerends, *J. Chem. Phys.*, 1999, **110**, 8943–8953.

53 E. Van Lenthe and E. J. Baerends, *J. Comput. Chem.*, 2003, **24**, 1142–1156.
54 D. Reta and N. F. Chilton, *Phys. Chem. Chem. Phys.*, 2019, **21**, 23567–23575.

9. XYZ coordinates for the optimized geometries

Optimized geometries of Gd complexes at the B3LYP/def2-TZVPP level of theory

Optimized geometry of **1-Gd^{wTHF}**

Gd	3.47313	0.14158	-0.02971
C	-0.00261	1.35136	0.32830
C	-0.13127	2.77762	0.69594
H	-0.60953	3.33103	-0.10695
H	0.84272	3.21725	0.88626
H	-0.73573	2.86467	1.59583
C	5.42869	-2.68753	-0.74603
H	6.25352	-2.17285	-0.25846
H	5.50560	-2.48305	-1.81235
C	5.34803	-4.09227	-0.45405
H	5.67378	-4.67366	-1.31854
H	6.07035	-4.35113	0.32375
C	4.02434	-4.40443	-0.04471
H	3.54581	-5.12833	-0.70627
H	4.02350	-4.88706	0.93535
C	3.37705	-3.21830	-0.04181
H	2.83558	-2.99604	0.88177
H	2.61343	-3.17197	-0.82221
C	3.17446	0.88701	2.62297
C	3.79290	-0.34088	2.65420
C	5.10049	-0.18933	2.19621
C	5.28093	1.14359	1.84393
C	4.08387	1.81920	2.09974
C	1.84742	1.20314	3.26558
H	1.08850	0.45867	3.03863
H	1.47125	2.17458	2.95256
H	1.95031	1.23356	4.35383
C	3.15967	-1.57219	3.28453
H	3.18525	-1.51166	4.37561
H	3.68262	-2.48706	3.00617
H	2.11305	-1.68140	2.99636
C	6.18420	-1.22050	2.32326
H	7.00053	-1.04935	1.62129
H	5.81019	-2.23262	2.16517
H	6.62168	-1.19936	3.32547
C	6.60800	1.78385	1.53857
H	7.18548	1.22380	0.80182
H	7.21916	1.83626	2.44365
H	6.49594	2.79692	1.16601
C	3.87044	3.31641	2.02721
H	4.69244	3.81321	1.51980
H	3.79696	3.75009	3.02743
H	2.95415	3.58323	1.49715
C	4.54234	2.05044	-1.72507
C	3.15271	2.08292	-1.94360
C	2.80422	0.89352	-2.52734
C	3.91126	0.11405	-2.67748
C	5.00871	0.80294	-2.17613

C	5.35549	3.26308	-1.40150
H	5.49653	3.86526	-2.30430
H	6.34536	3.01353	-1.02737
H	4.86689	3.90095	-0.66765
C	2.23164	3.26285	-1.79701
H	2.35665	3.95806	-2.63187
H	2.42196	3.82941	-0.88506
H	1.19006	2.95210	-1.79297
C	1.44211	0.53656	-3.10117
H	1.34390	0.89368	-4.12931
H	0.62866	0.98211	-2.53049
H	1.28434	-0.53993	-3.11626
C	3.93825	-1.18717	-3.44633
H	3.40106	-1.99825	-2.94668
H	4.95606	-1.52560	-3.62474
H	3.47236	-1.06040	-4.42488
C	6.46879	0.42696	-2.29340
H	6.60332	-0.62615	-2.52797
H	7.02089	0.63559	-1.37677
H	6.94974	0.99952	-3.09036
N	1.12167	0.69796	0.21712
N	-1.18956	0.72018	0.11976
O	4.20914	-2.09856	-0.28181
C	0.04585	-1.21822	-0.29103
C	0.07842	-2.77717	-0.69868
H	0.53299	-3.35028	0.10247
H	-0.93900	-3.10718	-0.86235
H	0.65769	-2.88107	-1.61186
N	-1.13673	-0.63438	-0.20125
N	1.20246	-0.60527	-0.08891
Gd	-3.51313	-0.18165	0.01703
C	-5.41344	2.68987	0.74745
H	-6.23976	2.17631	0.26070
H	-5.49062	2.48629	1.81411
C	-5.33278	4.09462	0.45547
H	-5.65914	4.67640	1.31954
H	-6.05506	4.35361	-0.32245
C	-4.00909	4.40678	0.04612
H	-3.53029	5.13081	0.70748
H	-4.00893	4.88986	-0.93389
C	-3.36180	3.22065	0.04323
H	-2.81579	2.99678	-0.87655
H	-2.60566	3.17373	0.82777
C	-3.15921	-0.88466	-2.62155
C	-3.77765	0.34323	-2.65278
C	-5.08524	0.19168	-2.19479
C	-5.26568	-1.14125	-1.84251
C	-4.06862	-1.81686	-2.09832
C	-1.83217	-1.20080	-3.26417
H	-1.06349	-0.47697	-3.00640
H	-1.47445	-2.18773	-2.98085
H	-1.92868	-1.19233	-4.35320
C	-3.14442	1.57453	-3.28311
H	-3.16411	1.50873	-4.37380
H	-3.67129	2.48861	-3.01025
H	-2.10003	1.68635	-2.98841
C	-6.16895	1.22284	-2.32184
H	-6.98437	1.05391	-1.61833
H	-5.79383	2.23468	-2.16633
H	-6.60746	1.19877	-3.32337

C	-6.59275	-1.78150	-1.53716
H	-7.17684	-1.21199	-0.81318
H	-7.19658	-1.84762	-2.44627
H	-6.48087	-2.78868	-1.14935
C	-3.85519	-3.31406	-2.02579
H	-4.69997	-3.81526	-1.56182
H	-3.73489	-3.73930	-3.02482
H	-2.96545	-3.58724	-1.45556
C	-4.52709	-2.04810	1.72649
C	-3.13746	-2.08058	1.94502
C	-2.78897	-0.89118	2.52876
C	-3.89601	-0.11171	2.67890
C	-4.99346	-0.80060	2.17755
C	-5.34024	-3.26074	1.40292
H	-5.47143	-3.86950	2.30272
H	-6.33444	-3.01104	1.04038
H	-4.85808	-3.89303	0.65986
C	-2.21640	-3.26051	1.79843
H	-2.33179	-3.94763	2.64140
H	-2.41640	-3.83688	0.89491
H	-1.17579	-2.94862	1.77951
C	-1.42686	-0.53422	3.10259
H	-1.33587	-0.87932	4.13537
H	-0.61510	-0.99184	2.53971
H	-1.26380	0.54145	3.10393
C	-3.92300	1.18951	3.44775
H	-3.38710	1.99945	2.94551
H	-4.94074	1.52704	3.62823
H	-3.45469	1.06223	4.42501
C	-6.45354	-0.42462	2.29481
H	-6.58925	0.63353	2.50429
H	-7.01088	-0.65724	1.38726
H	-6.92823	-0.97852	3.10862
O	-4.19389	2.10091	0.28323

Optimized geometry of **1-Gd^{woTHF}**

Gd	3.52747	0.00535	0.05464
C	-0.02984	0.00697	1.32042
C	-0.05624	0.02471	2.81142
H	0.38481	0.95061	3.18086
H	0.53028	-0.80362	3.20683
H	-1.07716	-0.05218	3.17331
C	3.29719	-2.67566	0.70353
C	3.26721	-2.64223	-0.71572
C	4.50983	-2.15179	-1.17668
C	5.33209	-1.89957	-0.03052
C	4.56124	-2.20994	1.13421
C	2.19308	-3.16828	1.58672
H	1.21152	-2.93930	1.17309
H	2.24514	-2.72923	2.58306
H	2.24042	-4.25282	1.71442
C	2.13149	-3.10237	-1.57520
H	2.20646	-4.17172	-1.78953
H	2.11386	-2.58613	-2.53503
H	1.16905	-2.94040	-1.09323
C	4.95273	-2.04768	-2.60476
H	5.69842	-1.26538	-2.74543
H	4.11928	-1.83464	-3.27503
H	5.40360	-2.98235	-2.94931

C	6.79782	-1.61211	-0.05733
H	7.08336	-0.99959	-0.91111
H	7.36407	-2.54539	-0.13561
H	7.13598	-1.11135	0.84760
C	5.06208	-2.16224	2.54659
H	5.79925	-1.37201	2.69283
H	5.54532	-3.10135	2.82922
H	4.25470	-1.99659	3.26051
C	5.13851	2.01716	0.57041
C	3.92396	2.45520	1.15895
C	3.00700	2.74003	0.11861
C	3.63755	2.47040	-1.12139
C	4.95584	2.02311	-0.86083
C	6.43184	1.80297	1.29211
H	6.90874	2.76083	1.51897
H	7.13842	1.22598	0.70051
H	6.29550	1.28877	2.24467
C	3.68502	2.63415	2.62752
H	3.96209	3.63845	2.95849
H	4.27154	1.93411	3.22408
H	2.63581	2.49287	2.88868
C	1.61896	3.26738	0.29138
H	1.58867	4.35541	0.19347
H	1.21499	3.02306	1.27264
H	0.93841	2.86256	-0.45771
C	3.03313	2.67271	-2.47706
H	1.94836	2.57135	-2.45244
H	3.41729	1.95841	-3.20691
H	3.25263	3.66995	-2.86725
C	6.02508	1.79945	-1.88424
H	5.62803	1.37419	-2.80639
H	6.80793	1.13580	-1.52200
H	6.50707	2.74343	-2.15426
N	1.15013	0.00678	0.71460
N	-1.17720	-0.00259	0.66463
C	0.02983	-0.00715	-1.32071
C	0.05623	-0.02486	-2.81172
H	-0.38486	-0.95073	-3.18118
H	-0.53026	0.80351	-3.20711
H	1.07715	0.05201	-3.17360
N	-1.15014	-0.00699	-0.71490
N	1.17719	0.00241	-0.66493
Gd	-3.52748	-0.00537	-0.05483
C	-3.29682	2.67571	-0.70333
C	-3.26711	2.64209	0.71592
C	-4.50986	2.15171	1.17659
C	-5.33193	1.89972	0.03023
C	-4.56083	2.21018	-1.13431
C	-2.19250	3.16835	-1.58625
H	-1.21104	2.93919	-1.17249
H	-2.24444	2.72949	-2.58267
H	-2.23969	4.25293	-1.71376
C	-2.13151	3.10203	1.57568
H	-2.20647	4.17134	1.79018
H	-2.11407	2.58562	2.53542
H	-1.16899	2.94010	1.09384
C	-4.95304	2.04753	2.60458
H	-5.69898	1.26543	2.74500
H	-4.11977	1.83415	3.27496
H	-5.40368	2.98228	2.94917

C	-6.79769	1.61237	0.05671
H	-7.08346	0.99986	0.91041
H	-7.36388	2.54569	0.13488
H	-7.13568	1.11166	-0.84831
C	-5.06140	2.16265	-2.54679
H	-5.79856	1.37246	-2.69327
H	-5.54455	3.10180	-2.82941
H	-4.25388	1.99705	-3.26057
C	-5.13862	-2.01717	-0.57029
C	-3.92405	-2.45542	-1.15863
C	-3.00719	-2.74009	-0.11815
C	-3.63784	-2.47017	1.12174
C	-4.95608	-2.02284	0.86097
C	-6.43187	-1.80303	-1.29214
H	-6.90885	-2.76090	-1.51878
H	-7.13844	-1.22581	-0.70075
H	-6.29541	-1.28910	-2.24483
C	-3.68499	-2.63470	-2.62714
H	-3.96215	-3.63904	-2.95792
H	-4.27136	-1.93471	-3.22390
H	-2.63574	-2.49361	-2.88822
C	-1.61918	-3.26759	-0.29070
H	-1.58901	-4.35561	-0.19270
H	-1.21506	-3.02338	-1.27192
H	-0.93868	-2.86277	0.45845
C	-3.03357	-2.67224	2.47751
H	-1.94878	-2.57106	2.45295
H	-3.41767	-1.95771	3.20716
H	-3.25326	-3.66936	2.86792
C	-6.02540	-1.79895	1.88423
H	-5.62841	-1.37360	2.80636
H	-6.80816	-1.13529	1.52182
H	-6.50749	-2.74286	2.15434

Optimized geometry of **2-Gd^{wTHF}**

C	-0.23829	-0.54700	1.13507
C	-0.25513	0.51812	-1.24153
C	-1.42846	1.23416	-3.17582
H	-1.91159	0.27497	-3.34747
H	-1.14592	1.68547	-4.12088
H	-2.09781	1.89666	-2.63241
C	-1.36427	-1.49575	2.99696
H	-2.00559	-0.63902	3.19219
H	-1.04648	-1.94286	3.93254
H	-1.89002	-2.22738	2.38894
C	2.96605	1.97071	-2.62078
H	2.44293	2.59434	-1.90077
H	2.24602	1.30792	-3.09150
C	3.79191	2.77944	-3.62270
H	3.75175	2.31886	-4.60949
H	3.42925	3.80076	-3.71487
C	5.21718	2.70276	-3.06260
H	5.37370	3.45660	-2.29107
H	5.98144	2.83120	-3.82610
C	5.23493	1.31494	-2.45466
H	5.37780	0.54884	-3.21733
H	5.96465	1.17489	-1.66441
C	-3.12603	2.72694	0.51309
C	-3.50946	2.15217	1.75193

C	-4.86874	1.76602	1.66308
C	-5.33408	2.12133	0.35084
C	-4.24537	2.70602	-0.35167
C	-1.78057	3.31701	0.22876
H	-0.97572	2.70050	0.62844
H	-1.67866	4.30374	0.68746
H	-1.60164	3.43982	-0.83815
C	-2.64266	2.07464	2.97045
H	-2.60483	3.03854	3.48476
H	-1.61437	1.80706	2.72851
H	-3.01995	1.35117	3.69283
C	-5.71971	1.24292	2.78068
H	-6.14671	2.06140	3.36649
H	-5.15154	0.62248	3.47454
H	-6.55504	0.64697	2.41456
C	-6.75359	2.12400	-0.11999
H	-7.18286	3.12529	-0.01787
H	-7.37962	1.44697	0.45501
H	-6.84310	1.85265	-1.17260
C	-4.34830	3.29800	-1.72555
H	-4.73904	2.59145	-2.46307
H	-3.38503	3.65469	-2.08504
H	-5.02569	4.15531	-1.73155
C	-3.80198	-2.14869	-1.70493
C	-3.62623	-2.71451	-0.41577
C	-4.76556	-2.41113	0.36304
C	-5.67112	-1.67099	-0.45817
C	-5.05583	-1.49593	-1.74031
C	-2.84627	-2.32004	-2.84443
H	-1.81240	-2.14500	-2.54515
H	-3.07800	-1.65124	-3.67245
H	-2.89304	-3.33777	-3.24080
C	-2.46399	-3.56963	-0.01942
H	-2.43053	-4.47974	-0.62271
H	-2.52578	-3.88301	1.02099
H	-1.50833	-3.06481	-0.16117
C	-5.06753	-2.88384	1.75368
H	-5.59244	-2.12771	2.34021
H	-4.16400	-3.15338	2.29897
H	-5.70770	-3.76993	1.74099
C	-7.09449	-1.37337	-0.11192
H	-7.70688	-2.27152	-0.23709
H	-7.52113	-0.60408	-0.75035
H	-7.21446	-1.05706	0.92444
C	-5.69628	-0.85357	-2.93445
H	-6.27581	-1.57769	-3.51302
H	-4.95814	-0.42571	-3.61370
H	-6.38190	-0.05516	-2.65022
C	4.82697	0.58225	2.24050
C	3.52344	0.52383	2.80124
C	2.77729	1.60641	2.27389
C	3.59803	2.32147	1.37074
C	4.86930	1.69752	1.34605
C	6.03580	-0.17014	2.69978
H	6.68640	-0.46670	1.87617
H	5.77407	-1.06621	3.25499
H	6.63852	0.45709	3.36349
C	3.04795	-0.44319	3.84274
H	3.07426	0.00175	4.84118
H	3.67180	-1.33494	3.87554

H	2.02353	-0.76611	3.65826
C	1.39357	2.00434	2.67784
H	1.41709	2.83581	3.38768
H	0.86493	1.18387	3.15788
H	0.79928	2.33693	1.82586
C	3.21344	3.58281	0.66088
H	2.16770	3.57162	0.34857
H	3.82267	3.74964	-0.22662
H	3.34113	4.45747	1.30482
C	6.12255	2.25220	0.74503
H	6.67099	2.84658	1.48217
H	5.91759	2.90948	-0.09786
H	6.80625	1.47126	0.40918
C	2.75164	-2.87594	0.17597
C	2.45393	-2.51471	-1.15877
C	3.64961	-2.09981	-1.79030
C	4.69935	-2.17864	-0.83946
C	4.13480	-2.67429	0.38678
C	1.81310	-3.48839	1.16799
H	0.77324	-3.33841	0.88365
H	1.94197	-3.07358	2.16779
H	1.97352	-4.56758	1.24283
C	1.12302	-2.62107	-1.83256
H	0.30312	-2.46808	-1.13237
H	0.97597	-3.60859	-2.27889
H	1.01702	-1.88737	-2.63177
C	3.76239	-1.75471	-3.24340
H	3.43954	-2.59360	-3.86367
H	4.78871	-1.53093	-3.52559
H	3.14623	-0.89761	-3.52352
C	6.16504	-1.99573	-1.09188
H	6.66739	-2.96018	-1.20841
H	6.66640	-1.48115	-0.27033
H	6.35398	-1.42585	-1.99956
C	4.90755	-3.19445	1.55703
H	4.39373	-3.02183	2.50233
H	5.89721	-2.75149	1.62703
H	5.04517	-4.27635	1.46556
Gd	-3.75745	0.05151	-0.00704
Gd	3.32339	-0.14677	0.14946
N	-1.41021	-0.33341	0.57166
N	-1.41678	0.18349	-0.71563
N	0.92244	0.36043	-0.64818
N	0.92741	-0.25491	0.57063
O	-0.19997	1.05571	-2.45857
O	-0.15518	-1.08154	2.34782
O	3.91959	1.16084	-1.87418

Optimized geometry of **2-Gd^{woTHF}**

C	-0.07124	-0.03666	-1.26131
C	-0.03978	-0.00960	1.35139
C	1.13146	0.01933	3.41345
H	1.74438	-0.83967	3.15226
H	0.84126	-0.02992	4.45710
H	1.67575	0.94046	3.21834
C	1.04652	-0.06889	-3.35216
H	1.64794	0.80729	-3.12351
H	0.72938	-0.04621	-4.38884
H	1.61514	-0.97462	-3.15332

C	3.01285	2.68200	-0.67045
C	4.11926	2.21423	-1.41603
C	5.17134	1.92005	-0.50231
C	4.69162	2.19677	0.82287
C	3.36453	2.67196	0.70433
C	1.70914	3.18552	-1.20427
H	1.56496	2.92849	-2.25195
H	1.64865	4.27406	-1.13090
H	0.86159	2.78594	-0.64726
C	4.25104	2.14284	-2.90822
H	4.95969	2.88933	-3.27494
H	3.30368	2.33467	-3.40828
H	4.61809	1.17270	-3.25352
C	6.58496	1.62641	-0.89160
H	7.09083	2.54732	-1.19712
H	6.64952	0.94076	-1.73720
H	7.15873	1.20349	-0.07107
C	5.51117	2.14009	2.07680
H	6.02047	3.09016	2.25887
H	6.28307	1.37258	2.02603
H	4.90096	1.93580	2.95715
C	2.49666	3.18362	1.81194
H	2.84504	2.84981	2.78889
H	1.45724	2.87323	1.69780
H	2.49841	4.27649	1.83560
C	3.10377	-2.67583	0.74456
C	3.33000	-2.68745	-0.65660
C	4.63292	-2.19730	-0.90360
C	5.22661	-1.88880	0.36607
C	4.26335	-2.17545	1.37881
C	1.86692	-3.20079	1.40294
H	0.95959	-2.78643	0.96253
H	1.84653	-2.98578	2.46959
H	1.80036	-4.28614	1.29615
C	2.37002	-3.23117	-1.66867
H	2.35694	-4.32395	-1.64457
H	2.64317	-2.94467	-2.68357
H	1.34705	-2.90037	-1.48610
C	5.33234	-2.14400	-2.22871
H	6.08160	-1.35330	-2.26384
H	4.63763	-1.97522	-3.05207
H	5.85174	-3.08222	-2.44072
C	6.66654	-1.57550	0.61845
H	7.20736	-2.48653	0.89213
H	6.80177	-0.87413	1.44228
H	7.15825	-1.16328	-0.25891
C	4.52871	-2.07832	2.85147
H	5.18925	-2.88236	3.18596
H	3.61434	-2.15715	3.43698
H	5.01748	-1.14078	3.12585
C	-5.26802	1.95517	0.45130
C	-4.75337	2.17540	-0.87123
C	-3.41368	2.61493	-0.74332
C	-3.08837	2.65470	0.63588
C	-4.22303	2.24039	1.37492
C	-6.69475	1.67327	0.80148
H	-6.78880	1.10146	1.72429
H	-7.21053	1.12714	0.01395
H	-7.24343	2.60771	0.95158
C	-5.54282	2.11134	-2.14359

H	-5.95978	3.08987	-2.39736
H	-6.37952	1.41830	-2.07051
H	-4.92914	1.80188	-2.99070
C	-2.51364	3.00886	-1.87421
H	-2.65836	4.05697	-2.14937
H	-2.70051	2.41565	-2.76987
H	-1.46293	2.88612	-1.61539
C	-1.78657	3.10840	1.21853
H	-0.95205	2.89663	0.55108
H	-1.57902	2.62474	2.17261
H	-1.78542	4.18720	1.39483
C	-4.33161	2.18250	2.86904
H	-4.61074	3.15345	3.28693
H	-3.38748	1.89670	3.33483
H	-5.08967	1.46948	3.19442
C	-4.03027	-2.22862	-1.42326
C	-3.06462	-2.67693	-0.48947
C	-3.63394	-2.62458	0.80671
C	-4.96166	-2.14477	0.68781
C	-5.21471	-1.90691	-0.70971
C	-3.84831	-2.14997	-2.90902
H	-2.83668	-1.84268	-3.17803
H	-4.53958	-1.44017	-3.36350
H	-4.02726	-3.11728	-3.38571
C	-1.69233	-3.17193	-0.81917
H	-1.33116	-2.75928	-1.76036
H	-1.67533	-4.26061	-0.91556
H	-0.97347	-2.91349	-0.04171
C	-2.95730	-3.03967	2.07742
H	-3.09174	-4.10756	2.26887
H	-3.35573	-2.51000	2.94311
H	-1.88413	-2.85125	2.04372
C	-5.97906	-2.06814	1.78533
H	-6.49252	-3.02554	1.91094
H	-6.74551	-1.32168	1.58167
H	-5.52670	-1.82543	2.74746
C	-6.54441	-1.57929	-1.31224
H	-6.44950	-1.00770	-2.23492
H	-7.17557	-1.01246	-0.63038
H	-7.08855	-2.49503	-1.56109
Gd	3.46140	0.00324	0.00063
Gd	-3.57853	-0.00428	0.05330
N	1.10264	-0.04810	-0.66199
N	1.11908	0.01991	0.72287
N	-1.21902	-0.04830	0.74302
N	-1.23420	-0.00451	-0.62300
O	-0.10014	0.00017	2.67721
O	-0.16612	-0.06054	-2.58518

Optimized geometry of **2-^{tr}Gd^{woTHF}**

C	0.09866	0.01913	1.30343
C	-0.09977	0.02280	-1.30113
C	0.89025	0.05201	-3.45405
H	1.46767	0.95871	-3.28384
H	0.51256	0.03269	-4.47028
H	1.50664	-0.82469	-3.26506
C	-0.89167	0.03628	3.45633
H	-1.47071	0.94294	3.29163
H	-0.51396	0.01154	4.47244

H	-1.50637	-0.84040	3.26189
C	3.04714	-2.69209	-0.54592
C	3.34239	-2.56895	0.83563
C	4.67617	-2.11687	0.96832
C	5.21838	-1.96662	-0.35126
C	4.19491	-2.31166	-1.28174
C	1.75819	-3.19945	-1.11208
H	0.89589	-2.80651	-0.57454
H	1.70003	-4.28887	-1.05034
H	1.64017	-2.93426	-2.16176
C	2.42088	-2.90752	1.96672
H	2.61693	-3.91306	2.34823
H	1.37752	-2.87824	1.65713
H	2.53232	-2.21965	2.80550
C	5.42648	-1.97601	2.25769
H	5.79537	-2.94507	2.60430
H	4.79848	-1.57506	3.05455
H	6.29150	-1.32288	2.15761
C	6.64948	-1.70678	-0.70134
H	7.16279	-2.64600	-0.92730
H	7.19053	-1.23476	0.11488
H	6.75555	-1.07463	-1.58441
C	4.37129	-2.36440	-2.76976
H	4.99584	-1.54933	-3.14060
H	3.41848	-2.31694	-3.29646
H	4.85628	-3.29390	-3.07979
C	3.44121	2.69414	-0.65308
C	3.05788	2.62446	0.70986
C	4.14541	2.11317	1.45638
C	5.22347	1.88190	0.55784
C	4.77457	2.22889	-0.76306
C	2.59640	3.23206	-1.76715
H	1.54241	2.98614	-1.63462
H	2.91082	2.84830	-2.73828
H	2.66387	4.32153	-1.82466
C	1.74845	3.07940	1.27139
H	1.76242	4.15142	1.48468
H	1.50812	2.56664	2.20152
H	0.92963	2.90735	0.57367
C	4.18085	1.91762	2.94200
H	4.93066	1.18323	3.23513
H	3.21855	1.57907	3.32867
H	4.42485	2.84783	3.46163
C	6.63237	1.56017	0.94097
H	7.17282	2.47595	1.19822
H	7.18124	1.08491	0.13082
H	6.68491	0.90877	1.81227
C	5.62963	2.24495	-1.99441
H	6.17884	3.18643	-2.08215
H	5.03859	2.13975	-2.90458
H	6.37272	1.44700	-1.98875
C	-5.23151	-1.95736	0.33136
C	-4.22222	-2.30321	1.27746
C	-3.06615	-2.69143	0.55872
C	-3.34182	-2.57150	-0.82706
C	-4.67170	-2.11418	-0.97968
C	-6.66589	-1.68865	0.66055
H	-7.19207	-1.21374	-0.16374
H	-6.78072	-1.05545	1.54167
H	-7.18842	-2.62449	0.87927

C	-4.41879	-2.35049	2.76319
H	-4.89799	-3.28360	3.07139
H	-5.05711	-1.54021	3.12049
H	-3.47413	-2.28972	3.30329
C	-1.78814	-3.20453	1.14441
H	-1.73252	-4.29391	1.07971
H	-1.68755	-2.94386	2.19704
H	-0.91538	-2.81245	0.62330
C	-2.40671	-2.91829	-1.94436
H	-1.36745	-2.89112	-1.62121
H	-2.50502	-2.23388	-2.78757
H	-2.60119	-3.92494	-2.32382
C	-5.40209	-1.97275	-2.28049
H	-5.75844	-2.94276	-2.63732
H	-4.76420	-1.56396	-3.06560
H	-6.27301	-1.32603	-2.19149
C	-3.46246	2.68738	0.68276
C	-3.03133	2.63476	-0.66636
C	-4.09169	2.13269	-1.45728
C	-5.20007	1.88941	-0.60106
C	-4.79870	2.22071	0.73983
C	-2.65834	3.21184	1.83273
H	-1.59699	2.98747	1.72241
H	-2.99161	2.79895	2.78562
H	-2.74652	4.29826	1.91502
C	-1.70227	3.09521	-1.17445
H	-0.90486	2.89059	-0.46067
H	-1.69953	4.17398	-1.35067
H	-1.44112	2.61243	-2.11488
C	-4.07205	1.94985	-2.94483
H	-4.29574	2.88450	-3.46560
H	-4.81146	1.21899	-3.27151
H	-3.09658	1.61246	-3.29799
C	-6.59431	1.57120	-1.03736
H	-7.12748	2.48965	-1.30011
H	-7.16977	1.08382	-0.25331
H	-6.61532	0.93196	-1.91888
C	-5.69752	2.22666	1.93952
H	-5.14050	2.10608	2.86906
H	-6.44503	1.43417	1.89654
H	-6.24318	3.17096	2.01926
Gd	3.51927	0.00676	-0.11402
Gd	-3.52011	0.00760	0.11447
N	1.21649	-0.00890	0.59224
N	1.11188	0.04408	-0.77849
N	-1.21743	-0.01102	-0.59012
N	-1.11306	0.03860	0.78075
O	-0.27599	0.03608	-2.61735
O	0.27467	0.02744	2.61963

Optimized geometry of **3-GdCl^{wTHF}**

Gd	2.21573	-2.53663	1.40695
C	-0.00074	0.50730	1.17403
C	3.45012	-5.04448	-0.87160
H	3.89683	-5.36862	0.06205
H	4.20409	-4.53049	-1.46677
C	2.77855	-6.17260	-1.66567
H	3.35590	-6.40451	-2.55784
H	2.70414	-7.08226	-1.07537

C	1.37819	-5.62122	-2.01589
H	1.13024	-5.74790	-3.06740
H	0.61018	-6.12425	-1.43189
C	1.45533	-4.15104	-1.63190
H	0.52354	-3.72988	-1.27207
H	1.83040	-3.53397	-2.45082
C	-0.07869	-3.07904	2.98203
C	0.02706	-4.16997	2.08006
C	1.21901	-4.86511	2.36903
C	1.87491	-4.18572	3.44489
C	1.06044	-3.06789	3.81257
C	-1.27374	-2.19062	3.09954
H	-1.65747	-1.89194	2.12556
H	-1.05731	-1.28915	3.66683
H	-2.08869	-2.70886	3.61289
C	-1.01520	-4.54631	1.07238
H	-1.89267	-4.98576	1.55415
H	-0.64309	-5.28050	0.36019
H	-1.37024	-3.68218	0.50661
C	1.63711	-6.19529	1.82910
H	2.72112	-6.29890	1.77704
H	1.23499	-6.37672	0.83536
H	1.27815	-7.00308	2.47342
C	3.01822	-4.75145	4.22566
H	3.82518	-5.11776	3.58896
H	2.68093	-5.60433	4.82265
H	3.44137	-4.02509	4.91302
C	1.28982	-2.14865	4.97312
H	2.33967	-2.10762	5.25672
H	0.73287	-2.47681	5.85491
H	0.96941	-1.12971	4.75408
C	4.52194	-1.64852	2.43044
C	3.88493	-0.42310	2.11772
C	3.82913	-0.30945	0.71073
C	4.43214	-1.45867	0.13835
C	4.86778	-2.29613	1.19242
C	5.07029	-2.01235	3.77195
H	6.01485	-1.48583	3.94435
H	5.27689	-3.07567	3.86069
H	4.40128	-1.72783	4.58251
C	3.50823	0.62033	3.12245
H	4.40087	1.08642	3.54853
H	2.93660	0.20969	3.95531
H	2.91292	1.41306	2.67612
C	3.30810	0.84899	-0.07634
H	4.11718	1.51537	-0.38760
H	2.60398	1.45085	0.49653
H	2.80670	0.51896	-0.98539
C	4.61057	-1.67207	-1.33414
H	3.65999	-1.80097	-1.85870
H	5.22248	-2.54706	-1.54285
H	5.10987	-0.81659	-1.79295
C	5.76435	-3.49280	1.10358
H	5.88314	-3.83793	0.07987
H	5.40758	-4.33570	1.69948
H	6.76211	-3.25034	1.47898
N	0.66168	-0.61945	1.01699
N	-0.66155	1.17400	0.24998
O	2.40538	-4.10133	-0.54736
C	0.00074	-0.50730	-1.17403

N	-0.66168	0.61945	-1.01699
N	0.66155	-1.17400	-0.24998
Gd	-2.21573	2.53663	-1.40695
C	-3.45012	5.04448	0.87160
H	-3.89683	5.36862	-0.06205
H	-4.20409	4.53049	1.46677
C	-2.77855	6.17260	1.66567
H	-3.35590	6.40451	2.55784
H	-2.70414	7.08226	1.07537
C	-1.37819	5.62122	2.01589
H	-1.13024	5.74790	3.06740
H	-0.61018	6.12425	1.43189
C	-1.45533	4.15104	1.63190
H	-0.52354	3.72988	1.27207
H	-1.83040	3.53397	2.45082
C	0.07869	3.07904	-2.98203
C	-0.02706	4.16997	-2.08006
C	-1.21901	4.86511	-2.36903
C	-1.87491	4.18572	-3.44489
C	-1.06044	3.06789	-3.81257
C	1.27374	2.19062	-3.09954
H	1.65747	1.89194	-2.12556
H	1.05731	1.28915	-3.66683
H	2.08869	2.70886	-3.61289
C	1.01520	4.54631	-1.07238
H	1.89267	4.98576	-1.55415
H	0.64309	5.28050	-0.36019
H	1.37024	3.68218	-0.50661
C	-1.63711	6.19529	-1.82910
H	-2.72112	6.29890	-1.77704
H	-1.23499	6.37672	-0.83536
H	-1.27815	7.00308	-2.47342
C	-3.01822	4.75145	-4.22566
H	-3.82518	5.11776	-3.58896
H	-2.68093	5.60433	-4.82265
H	-3.44137	4.02509	-4.91302
C	-1.28982	2.14865	-4.97312
H	-2.33967	2.10762	-5.25672
H	-0.73287	2.47681	-5.85491
H	-0.96941	1.12971	-4.75408
C	-4.52194	1.64852	-2.43044
C	-3.88493	0.42310	-2.11772
C	-3.82913	0.30945	-0.71073
C	-4.43214	1.45867	-0.13835
C	-4.86778	2.29613	-1.19242
C	-5.07029	2.01235	-3.77195
H	-6.01485	1.48583	-3.94435
H	-5.27689	3.07567	-3.86069
H	-4.40128	1.72783	-4.58251
C	-3.50823	-0.62033	-3.12245
H	-4.40087	-1.08642	-3.54853
H	-2.93660	-0.20969	-3.95531
H	-2.91292	-1.41306	-2.67612
C	-3.30810	-0.84899	0.07634
H	-4.11718	-1.51537	0.38760
H	-2.60398	-1.45085	-0.49653
H	-2.80670	-0.51896	0.98539
C	-4.61057	1.67207	1.33414
H	-3.65999	1.80097	1.85870
H	-5.22248	2.54706	1.54285

H	-5.10987	0.81659	1.79295
C	-5.76435	3.49280	-1.10358
H	-5.88314	3.83793	-0.07987
H	-5.40758	4.33570	-1.69948
H	-6.76211	3.25034	-1.47898
O	-2.40538	4.10133	0.54736
Cl	0.00451	1.18041	2.75927
Cl	-0.00451	-1.18041	-2.75927

Optimized geometry of **3-GdCl^{woTHF}**

Gd	2.22074	-2.09646	1.84572
C	-0.13181	0.76201	1.02999
C	-0.05043	-2.98594	3.12535
C	0.08313	-3.82996	1.99067
C	1.27959	-4.57205	2.12537
C	1.88641	-4.20226	3.36795
C	1.06221	-3.19821	3.97245
C	-1.19331	-2.05959	3.40550
H	-1.68679	-1.73980	2.48922
H	-0.87245	-1.16381	3.93759
H	-1.95245	-2.54441	4.02455
C	-0.89354	-3.94920	0.86183
H	-1.60402	-4.76085	1.03797
H	-0.39842	-4.15911	-0.08650
H	-1.47578	-3.03832	0.73524
C	1.76781	-5.64789	1.20281
H	2.85413	-5.73956	1.22030
H	1.46663	-5.46611	0.17073
H	1.36272	-6.62412	1.48269
C	3.02557	-4.91065	4.02490
H	3.74458	-5.29449	3.30309
H	2.65662	-5.77139	4.59120
H	3.55659	-4.27370	4.72955
C	1.27712	-2.58775	5.32438
H	2.33413	-2.53198	5.58461
H	0.78790	-3.17487	6.10630
H	0.86691	-1.57917	5.38506
C	4.64981	-1.44046	2.58624
C	4.12781	-0.19002	2.16838
C	3.96610	-0.22780	0.76183
C	4.37599	-1.50158	0.29466
C	4.80408	-2.26442	1.40887
C	5.15331	-1.76596	3.95726
H	6.15714	-1.35752	4.10507
H	5.21804	-2.83858	4.12531
H	4.52394	-1.34157	4.74015
C	3.84171	0.98030	3.05939
H	4.70554	1.64609	3.13194
H	3.59845	0.66703	4.07510
H	3.00762	1.57777	2.69085
C	3.48513	0.89966	-0.09394
H	4.31732	1.50910	-0.45503
H	2.81914	1.56513	0.45424
H	2.95320	0.53870	-0.97428
C	4.39213	-1.94826	-1.13556
H	3.56095	-1.52797	-1.70272
H	4.33519	-3.03341	-1.22295
H	5.31160	-1.63784	-1.63848
C	5.48262	-3.59760	1.35510

H	5.06070	-4.24463	0.58533
H	5.42142	-4.12571	2.30428
H	6.54474	-3.48174	1.12150
N	0.65042	-0.28775	1.16051
N	-0.79285	1.10553	-0.05455
C	0.13181	-0.76201	-1.02999
N	-0.65042	0.28775	-1.16051
N	0.79285	-1.10553	0.05455
Gd	-2.22074	2.09646	-1.84572
C	0.05043	2.98594	-3.12535
C	-0.08313	3.82996	-1.99067
C	-1.27959	4.57205	-2.12537
C	-1.88641	4.20226	-3.36795
C	-1.06221	3.19821	-3.97245
C	1.19331	2.05959	-3.40550
H	1.68679	1.73980	-2.48922
H	0.87245	1.16381	-3.93759
H	1.95245	2.54441	-4.02455
C	0.89354	3.94920	-0.86183
H	1.60402	4.76085	-1.03797
H	0.39842	4.15911	0.08650
H	1.47578	3.03832	-0.73524
C	-1.76781	5.64789	-1.20281
H	-2.85413	5.73956	-1.22030
H	-1.46663	5.46611	-0.17073
H	-1.36272	6.62412	-1.48269
C	-3.02557	4.91065	-4.02490
H	-3.74458	5.29449	-3.30309
H	-2.65662	5.77139	-4.59120
H	-3.55659	4.27370	-4.72955
C	-1.27712	2.58775	-5.32438
H	-2.33413	2.53198	-5.58461
H	-0.78790	3.17487	-6.10630
H	-0.86691	1.57917	-5.38506
C	-4.64981	1.44046	-2.58624
C	-4.12781	0.19002	-2.16838
C	-3.96610	0.22780	-0.76183
C	-4.37599	1.50158	-0.29466
C	-4.80408	2.26442	-1.40887
C	-5.15331	1.76596	-3.95726
H	-6.15714	1.35752	-4.10507
H	-5.21804	2.83858	-4.12531
H	-4.52394	1.34157	-4.74015
C	-3.84171	-0.98030	-3.05939
H	-4.70554	-1.64609	-3.13194
H	-3.59845	-0.66703	-4.07510
H	-3.00762	-1.57777	-2.69085
C	-3.48513	-0.89966	0.09394
H	-4.31732	-1.50910	0.45503
H	-2.81914	-1.56513	-0.45424
H	-2.95320	-0.53870	0.97428
C	-4.39213	1.94826	1.13556
H	-3.56095	1.52797	1.70272
H	-4.33519	3.03341	1.22295
H	-5.31160	1.63784	1.63848
C	-5.48262	3.59760	-1.35510
H	-5.06070	4.24463	-0.58533
H	-5.42142	4.12571	-2.30428
H	-6.54474	3.48174	-1.12150
Cl	-0.30564	1.77809	2.40216

Cl	0.30564	-1.77809	-2.40216

Optimized geometry of **4-GdOH^{wTHF}**

Gd	3.52072	0.22171	-0.00031
C	-0.03266	1.26717	0.34062
C	5.40665	-2.69439	-0.82648
H	6.23384	-2.19735	-0.32472
H	5.48499	-2.46121	-1.88699
C	5.31940	-4.10604	-0.57216
H	5.64045	-4.66716	-1.45168
H	6.04041	-4.39021	0.19791
C	3.99472	-4.42255	-0.16941
H	3.51200	-5.12938	-0.84552
H	3.99073	-4.92615	0.80002
C	3.35333	-3.23374	-0.13376
H	2.79946	-3.03242	0.78628
H	2.60336	-3.16997	-0.94326
C	3.17466	0.79955	2.64047
C	3.78704	-0.43177	2.63785
C	5.09475	-0.27444	2.18219
C	5.28135	1.06655	1.86552
C	4.08800	1.74095	2.14110
C	1.85006	1.10486	3.29326
H	1.13989	0.29167	3.16810
H	1.39818	2.00972	2.89161
H	1.98473	1.25321	4.36834
C	3.14853	-1.67641	3.23585
H	3.13976	-1.62524	4.32706
H	3.69200	-2.58131	2.96416
H	2.11281	-1.79584	2.91364
C	6.17350	-1.31397	2.27995
H	6.99058	-1.12798	1.58216
H	5.79525	-2.31936	2.09146
H	6.61203	-1.32444	3.28151
C	6.61118	1.70822	1.57551
H	7.18310	1.16856	0.81972
H	7.22506	1.72600	2.48019
H	6.50454	2.73456	1.23915
C	3.88191	3.24059	2.10906
H	4.65585	3.74208	1.53573
H	3.90648	3.65408	3.12088
H	2.91592	3.50955	1.67881
C	4.54255	2.07245	-1.67680
C	3.15281	2.11763	-1.89235
C	2.79764	0.94605	-2.50727
C	3.90060	0.16545	-2.67988
C	5.00212	0.83522	-2.16183
C	5.36214	3.27196	-1.32200
H	5.51645	3.88589	-2.21548
H	6.34643	3.00840	-0.94392
H	4.86672	3.90345	-0.58809
C	2.23781	3.29773	-1.71283
H	2.37749	4.01970	-2.52242
H	2.41672	3.82695	-0.77677
H	1.19456	2.99502	-1.72208
C	1.43302	0.61134	-3.08849
H	1.34753	0.97494	-4.11533
H	0.62516	1.06730	-2.51898
H	1.25843	-0.46256	-3.10881

C	3.92011	-1.11479	-3.48339
H	3.38236	-1.93569	-3.00062
H	4.93548	-1.45138	-3.67769
H	3.44607	-0.95995	-4.45378
C	6.46016	0.45533	-2.29126
H	6.58566	-0.58604	-2.57735
H	7.01214	0.61090	-1.36367
H	6.95096	1.06164	-3.05658
N	1.14689	0.68014	0.23350
N	-1.19256	0.66558	0.12381
O	4.19066	-2.11208	-0.34486
C	0.03266	-1.26717	-0.34062
N	-1.14689	-0.68014	-0.23350
N	1.19256	-0.66558	-0.12381
Gd	-3.52072	-0.22171	0.00031
C	-5.40665	2.69439	0.82648
H	-6.23384	2.19735	0.32472
H	-5.48499	2.46121	1.88699
C	-5.31940	4.10604	0.57216
H	-5.64045	4.66716	1.45168
H	-6.04041	4.39021	-0.19791
C	-3.99472	4.42255	0.16941
H	-3.51200	5.12938	0.84552
H	-3.99073	4.92615	-0.80002
C	-3.35333	3.23374	0.13376
H	-2.79946	3.03242	-0.78628
H	-2.60336	3.16997	0.94326
C	-3.17466	-0.79955	-2.64046
C	-3.78704	0.43177	-2.63785
C	-5.09475	0.27444	-2.18219
C	-5.28135	-1.06655	-1.86552
C	-4.08800	-1.74095	-2.14110
C	-1.85006	-1.10486	-3.29326
H	-1.13989	-0.29167	-3.16810
H	-1.39818	-2.00972	-2.89161
H	-1.98473	-1.25321	-4.36834
C	-3.14853	1.67641	-3.23585
H	-3.13976	1.62524	-4.32706
H	-3.69200	2.58131	-2.96416
H	-2.11281	1.79584	-2.91364
C	-6.17350	1.31397	-2.27995
H	-6.99058	1.12798	-1.58216
H	-5.79525	2.31936	-2.09146
H	-6.61203	1.32444	-3.28151
C	-6.61118	-1.70822	-1.57551
H	-7.18310	-1.16856	-0.81972
H	-7.22506	-1.72600	-2.48019
H	-6.50454	-2.73456	-1.23915
C	-3.88191	-3.24059	-2.10906
H	-4.65585	-3.74208	-1.53573
H	-3.90648	-3.65408	-3.12088
H	-2.91592	-3.50955	-1.67881
C	-4.54255	-2.07245	1.67680
C	-3.15281	-2.11763	1.89235
C	-2.79764	-0.94605	2.50727
C	-3.90060	-0.16545	2.67988
C	-5.00212	-0.83522	2.16183
C	-5.36214	-3.27196	1.32200
H	-5.51645	-3.88589	2.21548
H	-6.34643	-3.00840	0.94392

H	-4.86672	-3.90345	0.58809
C	-2.23781	-3.29773	1.71283
H	-2.37749	-4.01970	2.52242
H	-2.41672	-3.82695	0.77677
H	-1.19456	-2.99502	1.72209
C	-1.43302	-0.61134	3.08849
H	-1.34753	-0.97494	4.11533
H	-0.62516	-1.06730	2.51898
H	-1.25843	0.46256	3.10881
C	-3.92011	1.11479	3.48339
H	-3.38236	1.93569	3.00062
H	-4.93548	1.45138	3.67769
H	-3.44607	0.95995	4.45378
C	-6.46016	-0.45533	2.29126
H	-6.58566	0.58604	2.57735
H	-7.01214	-0.61090	1.36367
H	-6.95096	-1.06164	3.05658
O	-4.19066	2.11208	0.34486
O	-0.01256	2.55387	0.69174
H	-0.92298	2.87270	0.74460
O	0.01256	-2.55387	-0.69174
H	0.92298	-2.87270	-0.74460

Optimized geometry of **5-GdNH$_2$^{wTHF}**

Gd	3.52088	0.21913	-0.00411
C	-0.03170	1.27241	0.32116
H	0.84060	2.95565	0.99218
H	-0.85246	2.96409	1.06996
C	5.40461	-2.71071	-0.78545
H	6.23391	-2.20710	-0.29330
H	5.48338	-2.49539	-1.85001
C	5.31637	-4.11822	-0.50939
H	5.63818	-4.69296	-1.38001
H	6.03779	-4.39061	0.26479
C	3.99153	-4.42751	-0.10165
H	3.50766	-5.14406	-0.76687
H	3.98874	-4.91801	0.87479
C	3.35097	-3.23784	-0.08426
H	2.78705	-3.02094	0.82487
H	2.60374	-3.18332	-0.88729
C	3.17557	0.83788	2.62746
C	3.78706	-0.39378	2.64376
C	5.09483	-0.24443	2.18558
C	5.28235	1.09139	1.84824
C	4.08951	1.77081	2.11353
C	1.85127	1.15418	3.27562
H	1.07150	0.45347	2.98949
H	1.50773	2.15657	3.02676
H	1.94239	1.10925	4.36421
C	3.14773	-1.62859	3.26095
H	3.15075	-1.56485	4.35182
H	3.68183	-2.53983	2.99312
H	2.10872	-1.74343	2.94866
C	6.17284	-1.28311	2.29923
H	6.98861	-1.11079	1.59668
H	5.79164	-2.29045	2.12972
H	6.61277	-1.27560	3.30030
C	6.61261	1.72754	1.54823
H	7.19258	1.16126	0.81856

H	7.21814	1.78035	2.45728
H	6.50774	2.73951	1.17074
C	3.88451	3.26993	2.05840
H	4.75099	3.77673	1.64292
H	3.71705	3.67857	3.05737
H	3.02478	3.56044	1.44806
C	4.54383	2.04307	-1.70908
C	3.15409	2.08592	-1.92515
C	2.79801	0.90526	-2.52189
C	3.90039	0.12128	-2.68256
C	5.00245	0.79817	-2.17503
C	5.36433	3.24731	-1.37291
H	5.48500	3.86943	-2.26568
H	6.36172	2.98777	-1.02744
H	4.88954	3.86966	-0.61709
C	2.23997	3.26931	-1.76374
H	2.32775	3.94371	-2.62046
H	2.47834	3.85976	-0.87780
H	1.19971	2.96814	-1.69013
C	1.43307	0.56261	-3.09771
H	1.35390	0.89778	-4.13470
H	0.62802	1.03995	-2.54231
H	1.25428	-0.51062	-3.08731
C	3.91886	-1.17121	-3.46624
H	3.38619	-1.98473	-2.96601
H	4.93395	-1.50875	-3.66020
H	3.43927	-1.03208	-4.43627
C	6.46020	0.41528	-2.29876
H	6.58472	-0.63211	-2.56152
H	7.01330	0.59236	-1.37588
H	6.94869	1.00495	-3.07862
N	1.14736	0.68274	0.22279
N	-1.19204	0.66819	0.11372
O	4.18910	-2.12018	-0.31272
C	0.03170	-1.27241	-0.32116
H	-0.84060	-2.95565	-0.99218
H	0.85246	-2.96409	-1.06996
N	-1.14736	-0.68274	-0.22279
N	1.19204	-0.66819	-0.11372
Gd	-3.52088	-0.21913	0.00411
C	-5.40461	2.71071	0.78545
H	-6.23391	2.20710	0.29330
H	-5.48338	2.49539	1.85001
C	-5.31637	4.11822	0.50939
H	-5.63818	4.69296	1.38001
H	-6.03779	4.39061	-0.26479
C	-3.99153	4.42751	0.10165
H	-3.50766	5.14406	0.76687
H	-3.98874	4.91801	-0.87479
C	-3.35097	3.23784	0.08426
H	-2.78705	3.02094	-0.82487
H	-2.60374	3.18332	0.88729
C	-3.17557	-0.83788	-2.62746
C	-3.78706	0.39378	-2.64376
C	-5.09483	0.24443	-2.18558
C	-5.28235	-1.09139	-1.84824
C	-4.08951	-1.77081	-2.11353
C	-1.85127	-1.15418	-3.27562
H	-1.07150	-0.45347	-2.98949
H	-1.50773	-2.15657	-3.02676

H	-1.94239	-1.10925	-4.36421
C	-3.14773	1.62859	-3.26095
H	-3.15075	1.56485	-4.35182
H	-3.68183	2.53983	-2.99312
H	-2.10872	1.74343	-2.94866
C	-6.17284	1.28311	-2.29923
H	-6.98861	1.11079	-1.59668
H	-5.79164	2.29045	-2.12972
H	-6.61277	1.27560	-3.30030
C	-6.61261	-1.72754	-1.54823
H	-7.19258	-1.16126	-0.81856
H	-7.21814	-1.78035	-2.45728
H	-6.50774	-2.73951	-1.17074
C	-3.88451	-3.26993	-2.05840
H	-4.75099	-3.77673	-1.64292
H	-3.71705	-3.67857	-3.05737
H	-3.02478	-3.56044	-1.44806
C	-4.54383	-2.04307	1.70908
C	-3.15409	-2.08592	1.92515
C	-2.79801	-0.90526	2.52189
C	-3.90039	-0.12128	2.68256
C	-5.00245	-0.79817	2.17503
C	-5.36433	-3.24731	1.37291
H	-5.48500	-3.86943	2.26568
H	-6.36172	-2.98777	1.02744
H	-4.88954	-3.86966	0.61709
C	-2.23997	-3.26931	1.76374
H	-2.32775	-3.94371	2.62046
H	-2.47834	-3.85976	0.87780
H	-1.19971	-2.96814	1.69013
C	-1.43307	-0.56261	3.09771
H	-1.35390	-0.89778	4.13470
H	-0.62802	-1.03995	2.54231
H	-1.25428	0.51062	3.08731
C	-3.91886	1.17121	3.46624
H	-3.38619	1.98473	2.96601
H	-4.93395	1.50875	3.66020
H	-3.43927	1.03208	4.43627
C	-6.46020	-0.41528	2.29876
H	-6.58472	0.63211	2.56152
H	-7.01330	-0.59236	1.37588
H	-6.94869	-1.00495	3.07862
O	-4.18910	2.12018	0.31272
N	0.02751	-2.60731	-0.62250
N	-0.02751	2.60731	0.62250

Optimized geometry of neutral Rtz ligand at the B3LYP/def2-TZVPP level of theory

Optimized geometry of **dtz**

C	0.00119	0.49806	1.16111
N	0.66614	-0.64258	0.99005
N	-0.66469	1.16086	0.21783
C	-0.00119	-0.49806	-1.16111
N	-0.66614	0.64258	-0.99005
N	0.66469	-1.16086	-0.21783
H	0.00269	0.90900	2.11826
H	-0.00269	-0.90900	-2.11826

Optimized geometry of **dcltz**

C	0.00145	0.49682	1.15781
N	0.66736	-0.64435	0.99003
N	-0.66577	1.16214	0.21651
C	-0.00145	-0.49682	-1.15781
N	-0.66736	0.64435	-0.99003
N	0.66577	-1.16214	-0.21651
Cl	0.00337	1.17224	2.73186
Cl	-0.00337	-1.17224	-2.73186

Optimized geometry of **dmtz**

C	1.35148	0.05964	0.01137
C	2.82840	-0.00696	-0.00302
H	3.17293	-0.69216	0.76906
H	3.26585	0.97654	0.15312
H	3.16770	-0.39540	-0.96374
N	0.64431	1.15654	0.00868
N	0.73864	-1.15492	0.00823
C	-1.29132	-0.00114	-0.01234
C	-2.90255	-0.03651	0.00433
H	-3.27117	0.97081	-0.16135
H	-3.24761	-0.71460	-0.77170
H	-3.22896	-0.40648	0.97406
N	-0.65434	-1.15943	-0.00839
N	-0.69644	1.18225	-0.00873

Optimized geometry of **dmeotz**

C	-1.26900	0.28405	0.00012
C	1.26901	0.28405	-0.00011
C	3.32667	-0.87296	0.00005
H	3.09092	-1.45978	0.88658
H	4.37201	-0.58201	0.00026
H	3.09123	-1.45948	-0.88678
C	-3.32664	-0.87297	-0.00003
H	-3.09147	-1.45922	-0.88713
H	-4.37199	-0.58205	0.00057
H	-3.09060	-1.46007	0.88624
N	-0.66362	-0.89086	-0.00003
N	0.66361	-0.89088	-0.00008
N	0.64705	1.48360	-0.00010
N	-0.64708	1.48360	-0.00004
O	2.59573	0.36072	0.00010
O	-2.59574	0.36071	0.00013

Optimized geometry of **dmeotz**$_{\textbf{trans}}$

C	1.23026	0.31405	0.00032
C	-1.23037	-0.31316	0.00035
C	-3.50312	0.34168	-0.00046
H	-3.41203	0.96672	0.88638
H	-4.45147	-0.18565	-0.00092
H	-3.41124	0.96687	-0.88711
C	3.50291	-0.34238	-0.00042
H	3.41139	-0.96747	0.88632
H	4.45154	0.18446	-0.00066
H	3.41092	-0.96740	-0.88717
N	0.34697	1.31524	0.00023
N	-0.92147	0.98650	0.00021
N	-0.34657	-1.31498	0.00022
N	0.92121	-0.98635	0.00018
O	-2.50534	-0.68949	-0.00008

O	2.50558	0.68930	-0.00012

Optimized geometry of **dohtz**

C	-0.03266	1.26717	0.34062
N	1.14689	0.68014	0.23350
N	-1.19256	0.66558	0.12381
C	0.03266	-1.26717	-0.34062
N	-1.14689	-0.68014	-0.23350
N	1.19256	-0.66558	-0.12381
O	-0.03330	2.55521	0.68771
H	-0.95218	2.85218	0.72721
O	0.03330	-2.55521	-0.68771
H	0.95218	-2.85218	-0.72721

Optimized geometry of **dnh$_2$tz**

C	1.31268	-0.00229	0.00677
H	3.12809	0.86618	-0.20520
H	3.14049	-0.84533	-0.20826
N	0.69060	1.16415	0.00549
N	0.70222	-1.17780	0.00556
C	-1.31268	0.00229	-0.00674
H	-3.12805	-0.86616	0.20530
H	-3.14046	0.84530	0.20832
N	-0.69060	-1.16415	-0.00546
N	-0.70222	1.17780	-0.00553
N	-2.68094	-0.00666	-0.06342
N	2.68092	0.00666	0.06331

Optimized geometry of radical Rtz ligand at the B3LYP/def2-TZVPP level of theory

Optimized geometry of **dtz**

C	0.00152	0.49626	1.15634
N	0.67554	-0.63873	1.03384
N	-0.67395	1.18999	0.25080
C	-0.00152	-0.49626	-1.15634
N	-0.67554	0.63873	-1.03384
N	0.67395	-1.18999	-0.25080
H	0.00248	0.90551	2.11044
H	-0.00248	-0.90551	-2.11044

Optimized geometry of **dcltz**

C	0.00146	0.48622	1.13310
N	0.67510	-0.63692	1.03616
N	-0.67346	1.19049	0.25366
C	-0.00146	-0.48622	-1.13310
N	-0.67510	0.63692	-1.03616
N	0.67346	-1.19049	-0.25366
Cl	0.00344	1.18887	2.77049
Cl	-0.00344	-1.18887	-2.77049

Optimized geometry of **dmtz**

C	1.35157	0.06040	0.01085
C	2.82855	-0.00477	-0.00402
H	3.18189	-0.61719	0.82738
H	3.26562	0.99238	0.06563
H	3.17125	-0.48188	-0.92473
N	0.64334	1.15662	0.00832
N	0.73991	-1.15475	0.00799

C	-1.29118	-0.00295	-0.01198
C	-2.90236	-0.03988	0.00522
H	-3.28527	0.54485	-0.83127
H	-3.22289	-1.07630	-0.06821
H	-3.25910	0.40546	0.93433
N	-0.65307	-1.16062	-0.00816
N	-0.69745	1.18102	-0.00865

Optimized geometry of **dmeotz**

C	-1.25340	0.30331	0.00005
C	1.25336	0.30331	0.00067
C	3.30331	-0.88740	-0.00081
H	3.05579	-1.48385	0.88027
H	4.36708	-0.64487	-0.00177
H	3.05409	-1.48284	-0.88210
C	-3.30319	-0.88745	0.00033
H	-3.05483	-1.48430	-0.88025
H	-4.36698	-0.64501	0.00015
H	-3.05469	-1.48242	0.88214
N	-0.69713	-0.89188	0.00006
N	0.69705	-0.89193	0.00052
N	0.69435	1.50365	0.00005
N	-0.69438	1.50367	-0.00013
O	2.62836	0.35426	0.00057
O	-2.62838	0.35426	-0.00099

Optimized geometry of **dmeotz$_{trans}$**

C	1.21421	0.31157	-0.00004
C	-1.21426	-0.31144	0.00004
C	-3.49177	0.34693	-0.00007
H	-3.39488	0.98548	0.88084
H	-4.46485	-0.14655	-0.00027
H	-3.39453	0.98553	-0.88091
C	3.49169	-0.34727	0.00004
H	3.39423	-0.98573	0.88091
H	4.46484	0.14610	0.00019
H	3.39448	-0.98565	-0.88092
N	0.38146	1.34065	0.00003
N	-0.96333	0.98310	0.00006
N	-0.38123	-1.34048	-0.00002
N	0.96315	-0.98301	-0.00005
O	-2.53587	-0.69451	0.00008
O	2.53600	0.69455	-0.00005

Optimized geometry of **dohtz**

C	-0.03266	1.26717	0.34062
N	1.14689	0.68014	0.23350
N	-1.19256	0.66558	0.12381
C	0.03266	-1.26717	-0.34062
N	-1.14689	-0.68014	-0.23350
N	1.19256	-0.66558	-0.12381
O	-0.07411	2.58268	0.69294
H	-1.02052	2.77744	0.70245
O	0.07411	-2.58268	-0.69294
H	1.02052	-2.77744	-0.70245

Optimized geometry of **dnh$_2$tz**

C	1.31247	-0.00244	0.02420
H	3.07912	0.84895	-0.33060

H	3.09138	-0.82476	-0.34367
N	0.69061	1.16407	0.01446
N	0.70194	-1.17789	0.01506
C	-1.31247	0.00244	-0.02424
H	-3.07913	-0.84898	0.33063
H	-3.09139	0.82477	0.34372
N	-0.69061	-1.16407	-0.01450
N	-0.70194	1.17789	-0.01510
N	-2.71671	-0.00605	-0.09175
N	2.71671	0.00605	0.09184

Optimized geometries of neutral dRbpym at the B3LYP/def2-TZVPP level of theory

Optimized geometry of **dNMe2bpym**

N	-0.09240	1.61780	0.80308
N	0.97166	-0.37607	1.47830
N	1.44160	2.15228	4.08380
C	0.23544	0.33574	0.62037
C	1.37917	0.21623	2.58710
H	1.98442	-0.38651	3.25195
C	1.06057	1.54973	2.90500
C	0.31459	2.21108	1.91156
H	0.04201	3.25305	2.01941
C	1.30601	3.58988	4.21158
H	0.27062	3.89653	4.06167
H	1.93139	4.14077	3.49732
H	1.59404	3.88317	5.21771
C	2.42572	1.49464	4.92075
H	3.40099	1.39057	4.42804
H	2.08550	0.50048	5.21133
H	2.56030	2.07537	5.82955
N	0.09240	-1.61780	-0.80308
N	-0.97166	0.37607	-1.47830
N	-1.44160	-2.15228	-4.08380
C	-0.23544	-0.33574	-0.62037
C	-1.37917	-0.21623	-2.58710
H	-1.98442	0.38651	-3.25195
C	-1.06057	-1.54973	-2.90500
C	-0.31459	-2.21108	-1.91156
H	-0.04201	-3.25305	-2.01941
C	-1.30601	-3.58988	-4.21158
H	-0.27062	-3.89653	-4.06167
H	-1.93139	-4.14077	-3.49732
H	-1.59404	-3.88317	-5.21771
C	-2.42572	-1.49464	-4.92075
H	-3.40099	-1.39057	-4.42804
H	-2.08550	-0.50048	-5.21133
H	-2.56030	-2.07537	-5.82955

Optimized geometry of **dOEtbpym**

O	-4.74674	-0.53788	0.00013
O	4.74680	0.53779	-0.00004
N	-1.25428	-1.30639	0.00025
N	1.46652	-1.04971	-0.00025
N	-1.46660	1.04984	-0.00016
N	1.25425	1.30648	0.00023
C	-0.74319	-0.06691	0.00003
C	0.74312	0.06703	-0.00001
C	-2.79101	0.93509	-0.00013
H	-3.35566	1.85856	-0.00029
C	2.56791	1.42149	0.00021
H	2.99354	2.41949	0.00040
C	-3.41557	-0.30975	0.00008
C	3.41551	0.30988	-0.00004
C	-2.56793	-1.42140	0.00027
H	-2.99361	-2.41937	0.00046
C	2.79093	-0.93498	-0.00027

H	3.35557	-1.85843	-0.00049
C	-5.62650	0.59011	-0.00013
H	-5.43115	1.20164	-0.88601
H	-5.43123	1.20196	0.88555
C	5.62658	-0.59026	-0.00012
H	5.43135	-1.20179	-0.88602
H	5.43115	-1.20206	0.88556
C	-7.04402	0.06780	-0.00010
H	-7.74682	0.90130	-0.00027
H	-7.22991	-0.54082	0.88423
H	-7.22983	-0.54114	-0.88421
C	7.04413	-0.06809	0.00011
H	7.74687	-0.90165	0.00004
H	7.22998	0.54053	0.88444
H	7.23015	0.54083	-0.88398

Optimized geometry of **dMebpym**

N	-1.36496	-1.18410	-0.01284
N	1.36493	-1.18410	0.01286
N	-1.36495	1.18425	-0.01245
N	1.36498	1.18425	0.01247
C	-0.74864	0.00016	-0.00528
C	0.74864	0.00013	0.00530
C	-2.69126	1.17170	-0.01464
H	-3.18335	2.14002	-0.02700
C	2.69126	1.17168	0.01465
H	3.18335	2.14001	0.02703
C	-3.44365	0.00007	-0.00738
C	3.44365	0.00001	0.00738
C	-2.69115	-1.17168	-0.01501
H	-3.18296	-2.14015	-0.02776
C	2.69115	-1.17169	0.01503
H	3.18297	-2.14016	0.02778
C	-4.94212	-0.00015	0.01972
H	-5.31555	-0.02944	1.04607
H	-5.34685	-0.86868	-0.49971
H	-5.34570	0.89681	-0.44961
C	4.94212	-0.00015	-0.01979
H	5.34670	-0.87324	0.49202
H	5.31550	-0.02042	-1.04637
H	5.34590	0.89262	0.45733

Optimized geometry of **dFbpym**

N	0.66496	-1.20444	1.16896
C	-0.05062	-0.16722	0.72742
N	-0.84993	0.59613	1.47728
C	-0.94214	0.30099	2.76643
H	-1.58635	0.91035	3.38984
C	-0.23134	-0.75965	3.29899
C	0.57604	-1.50355	2.45780
H	1.15056	-2.34272	2.83272
F	-0.32364	-1.06004	4.60279
N	-0.66496	1.20444	-1.16896
C	0.05062	0.16722	-0.72742
N	0.84993	-0.59613	-1.47728
C	0.94214	-0.30099	-2.76643
H	1.58635	-0.91035	-3.38984
C	0.23134	0.75965	-3.29899
C	-0.57604	1.50355	-2.45780
H	-1.15056	2.34272	-2.83272
F	0.32364	1.06004	-4.60279

Optimized geometries of radical dRbpym•⁻ at the B3LYP/def2-TZVPP level of theory

Optimized geometry of **dNMe2bpym•⁻**

N	-0.13467	1.60586	0.80905

N	0.93591	-0.40067	1.48835
N	1.35285	2.13105	4.16272
C	0.21945	0.33180	0.63431
C	1.32770	0.20101	2.63635
H	1.91506	-0.40838	3.30975
C	0.99395	1.52592	2.94097
C	0.26014	2.20181	1.95898
H	-0.03001	3.23720	2.07548
C	1.33576	3.57631	4.21284
H	0.34444	3.95541	3.96943
H	2.05350	4.04405	3.52007
H	1.57513	3.89878	5.22654
C	2.43358	1.52328	4.90726
H	3.39429	1.53614	4.36806
H	2.19942	0.48639	5.14327
H	2.55988	2.05799	5.84908
N	0.13467	-1.60586	-0.80905
N	-0.93591	0.40067	-1.48835
N	-1.35285	-2.13105	-4.16272
C	-0.21945	-0.33180	-0.63431
C	-1.32770	-0.20101	-2.63635
H	-1.91506	0.40838	-3.30975
C	-0.99395	-1.52592	-2.94097
C	-0.26014	-2.20181	-1.95898
H	0.03001	-3.23720	-2.07548
C	-1.33576	-3.57631	-4.21284
H	-0.34444	-3.95541	-3.96943
H	-2.05350	-4.04405	-3.52007
H	-1.57513	-3.89878	-5.22654
C	-2.43358	-1.52328	-4.90726
H	-3.39429	-1.53614	-4.36806
H	-2.19942	-0.48639	-5.14327
H	-2.55988	-2.05799	-5.84908

Optimized geometry of **dOEtbpym**•⁻

O	-4.79092	-0.55253	0.00020
O	4.79101	0.55259	-0.00045
N	-1.26250	-1.32631	-0.00003
N	1.48367	-1.07722	-0.00013
N	-1.48369	1.07746	0.00013
N	1.26250	1.32659	0.00003
C	-0.71236	-0.06215	0.00010
C	0.71234	0.06228	0.00005
C	-2.79432	0.93534	0.00015
H	-3.37512	1.85483	0.00020
C	2.56552	1.42463	-0.00012
H	3.00085	2.42359	-0.00007
C	-3.42237	-0.31139	0.00012
C	3.42236	0.31147	-0.00026
C	-2.56550	-1.42456	-0.00001
H	-3.00057	-2.42362	-0.00008
C	2.79424	-0.93532	-0.00028
H	3.37497	-1.85487	-0.00039
C	-5.63470	0.57323	-0.00005
H	-5.43989	1.19642	-0.88322
H	-5.44009	1.19668	0.88298
C	5.63464	-0.57335	0.00020
H	5.43998	-1.19696	-0.88270
H	5.43951	-1.19625	0.88350
C	-7.06911	0.08501	-0.00012
H	-7.75988	0.93036	-0.00030
H	-7.26557	-0.52366	0.88325
H	-7.26540	-0.52389	-0.88338
C	7.06918	-0.08554	0.00036
H	7.75971	-0.93111	0.00084
H	7.26555	0.52352	0.88349
H	7.26598	0.52286	-0.88312

Optimized geometry of **dMebpym**•⁻

N	-1.37842	-1.20564	-0.02481
N	1.37844	-1.20569	0.02479
N	-1.37855	1.20603	-0.02484
N	1.37853	1.20597	0.02480
C	-0.71584	0.00014	-0.01040
C	0.71584	0.00009	0.01030
C	-2.68926	1.17436	-0.02259
H	-3.19476	2.14281	-0.03893
C	2.68921	1.17441	0.02262
H	3.19462	2.14290	0.03900
C	-3.45970	0.00000	-0.01150
C	3.45970	-0.00001	0.01155
C	-2.68883	-1.17473	-0.02256
H	-3.19392	-2.14337	-0.03904
C	2.68888	-1.17468	0.02259
H	3.19406	-2.14328	0.03909
C	-4.95678	-0.00017	0.03515
H	-5.35625	-0.02072	1.05852
H	-5.37256	-0.87060	-0.48100
H	-5.36987	0.89170	-0.44495
C	4.95678	-0.00012	-0.03512
H	5.37189	-0.87556	0.47294
H	5.35624	-0.01139	-1.05864
H	5.37054	0.88700	0.45321

Optimized geometry of **dFbpym**$^{\bullet-}$

N	0.68080	-1.22528	1.17918
C	-0.04821	-0.15967	0.69527
N	-0.86548	0.61255	1.49391
C	-0.94350	0.30294	2.76699
H	-1.58669	0.90916	3.40281
C	-0.23355	-0.76323	3.30960
C	0.57778	-1.50515	2.45753
H	1.15150	-2.34525	2.84541
F	-0.32818	-1.07143	4.64603
N	-0.68080	1.22528	-1.17918
C	0.04821	0.15967	-0.69527
N	0.86548	-0.61255	-1.49391
C	0.94350	-0.30294	-2.76699
H	1.58669	-0.90916	-3.40281
C	0.23355	0.76323	-3.30960
C	-0.57778	1.50515	-2.45753
H	-1.15150	2.34525	-2.84541
F	0.32818	1.07143	-4.64603

XYZ coordinates of **1-Dy** utilized in the CASSCF calculations.

C	-0.01275	-0.54777	1.19536
C	-0.04597	-1.14730	2.57047
H	0.48987	-0.50613	3.25990
H	0.41655	-2.13054	2.57476
H	-1.07655	-1.24350	2.90690
C	3.25449	5.03202	-0.88979
H	4.18060	4.52595	-1.15749
H	3.46044	5.61196	0.00720
C	2.71939	5.80264	-1.97729
H	2.43942	6.79627	-1.61561
H	3.49426	6.00213	-2.71919
C	1.59302	5.12547	-2.50981
H	0.72751	5.78295	-2.59925
H	1.77576	4.76081	-3.52274
C	1.38651	4.08889	-1.62901
H	1.45973	3.12285	-2.12517
H	0.38976	4.08715	-1.17975
C	3.78299	0.51183	0.50331
C	4.39065	1.66200	0.12583
C	4.78684	2.34636	1.27175
C	4.39734	1.57287	2.38173
C	3.76689	0.42557	1.87168
C	3.34239	-0.56790	-0.47635

H	3.04832	-0.13852	-1.43129
H	2.50221	-1.14613	-0.09664
H	4.15516	-1.27182	-0.67063
C	4.76244	2.00993	-1.29422
H	5.27108	1.16899	-1.76844
H	5.44664	2.85354	-1.33350
H	3.89968	2.24957	-1.92104
C	5.68237	3.57561	1.35264
H	6.70513	3.28779	1.60663
H	5.34909	4.27485	2.11929
H	5.72293	4.11509	0.40993
C	4.88246	1.70657	3.78156
H	4.18646	1.28325	4.50289
H	5.07219	2.73944	4.06260
H	5.82742	1.16766	3.90103
C	3.32436	-0.80656	2.63788
H	2.63771	-1.40810	2.04999
H	2.84335	-0.55761	3.58325
H	4.18476	-1.43728	2.87675
C	0.10820	4.10038	2.05593
C	-0.00203	3.00771	2.88729
C	1.15042	2.98471	3.72089
C	1.91088	4.12769	3.39734
C	1.26459	4.79336	2.37948
C	-1.00259	4.50581	1.11222
H	-1.37271	3.65957	0.53176
H	-0.68615	5.27989	0.41411
H	-1.85473	4.90801	1.66618
C	-1.22429	2.15514	3.04232
H	-2.01313	2.71817	3.54896
H	-1.02538	1.27202	3.64473
H	-1.63003	1.82942	2.08830
C	1.39140	2.05882	4.88704
H	0.71853	2.28981	5.71708
H	2.40612	2.14463	5.26342
H	1.22768	1.01070	4.63205
C	3.05804	4.66972	4.20847
H	3.47169	3.92115	4.87601
H	2.71807	5.50361	4.82801
H	3.87292	5.04901	3.59070
C	1.60657	6.18363	1.90763
H	1.08695	6.92983	2.51435
H	1.30928	6.35440	0.87294
H	2.67206	6.39465	1.99211
Dy	2.12453	2.46526	1.30546
N	0.65234	0.59522	1.03583
N	-0.66481	-1.17749	0.21795
O	2.29853	4.02129	-0.55722
C	0.01275	0.54777	-1.19536
C	0.04597	1.14730	-2.57047
H	-0.48987	0.50613	-3.25990
H	-0.41655	2.13054	-2.57476
H	1.07655	1.24350	-2.90690
N	-0.65234	-0.59522	-1.03583
N	0.66481	1.17749	-0.21795
C	-3.25449	-5.03202	0.88979
H	-4.18060	-4.52595	1.15749
H	-3.46044	-5.61196	-0.00720
C	-2.71939	-5.80264	1.97729
H	-2.43942	-6.79627	1.61561
H	-3.49426	-6.00213	2.71919
C	-1.59302	-5.12547	2.50981
H	-0.72751	-5.78295	2.59925
H	-1.77576	-4.76081	3.52274
C	-1.38651	-4.08889	1.62901
H	-1.45973	-3.12285	2.12517
H	-0.38976	-4.08715	1.17975
C	-3.78299	-0.51183	-0.50331
C	-4.39065	-1.66200	-0.12583
C	-4.78684	-2.34636	-1.27175
C	-4.39734	-1.57287	-2.38173

C	-3.76689	-0.42557	-1.87168
C	-3.34239	0.56790	0.47635
H	-3.04832	0.13852	1.43129
H	-2.50221	1.14613	0.09664
H	-4.15516	1.27182	0.67063
C	-4.76244	-2.00993	1.29422
H	-5.27108	-1.16899	1.76844
H	-5.44664	-2.85354	1.33350
H	-3.89968	-2.24957	1.92104
C	-5.68237	-3.57561	-1.35264
H	-6.70513	-3.28779	-1.60663
H	-5.34909	-4.27485	-2.11929
H	-5.72293	-4.11509	-0.40993
C	-4.88246	-1.70657	-3.78156
H	-4.18646	-1.28325	-4.50289
H	-5.07219	-2.73944	-4.06260
H	-5.82742	-1.16766	-3.90103
C	-3.32436	0.80656	-2.63788
H	-2.63771	1.40810	-2.04999
H	-2.84335	0.55761	-3.58325
H	-4.18476	1.43728	-2.87675
C	-0.10820	-4.10038	-2.05593
C	0.00203	-3.00771	-2.88729
C	-1.15042	-2.98471	-3.72089
C	-1.91088	-4.12769	-3.39734
C	-1.26459	-4.79336	-2.37948
C	1.00259	-4.50581	-1.11222
H	1.37271	-3.65957	-0.53176
H	0.68615	-5.27989	-0.41411
H	1.85473	-4.90801	-1.66618
C	1.22429	-2.15514	-3.04232
H	2.01313	-2.71817	-3.54896
H	1.02538	-1.27202	-3.64473
H	1.63003	-1.82942	-2.08830
C	-1.39140	-2.05882	-4.88704
H	-0.71853	-2.28981	-5.71708
H	-2.40612	-2.14463	-5.26342
H	-1.22768	-1.01070	-4.63205
C	-3.05804	-4.66972	-4.20847
H	-3.47169	-3.92115	-4.87601
H	-2.71807	-5.50361	-4.82801
H	-3.87292	-5.04901	-3.59070
C	-1.60657	-6.18363	-1.90763
H	-1.08695	-6.92983	-2.51435
H	-1.30928	-6.35440	-0.87294
H	-2.67206	-6.39465	-1.99211
Dy	-2.12453	-2.46526	-1.30546
O	-2.29853	-4.02129	0.55722

XYZ coordinates of **2-Dy** utilized in the CASSCF calculations.

C	-0.26809	-1.38479	0.50596
C	-0.28828	1.11489	-0.23650
C	-1.39525	3.15499	-0.78697
H	-2.12014	2.62937	-1.40246
H	-1.07806	4.06324	-1.28914
H	-1.82777	3.39449	0.17649
C	-1.29645	-3.44235	1.19868
H	-1.84194	-3.03271	2.04469
H	-0.90775	-4.42433	1.44578
H	-1.95158	-3.51044	0.33241
C	2.72602	3.05672	-1.19622
H	1.87626	3.05256	-0.53005
H	2.40037	2.75452	-2.19063
C	3.50088	4.36471	-1.18594
H	3.40576	4.82597	-2.17200
H	2.99726	5.06350	-0.51533
C	4.82776	4.13359	-0.82335
H	5.07816	4.61299	0.12684
H	5.55155	4.52877	-1.53617
C	4.95598	2.70588	-0.71022
H	5.50854	2.28507	-1.55707

H	5.47559	2.37950	0.17822
C	-3.56533	0.77800	2.53570
C	-4.37200	-0.37914	2.54180
C	-5.59855	-0.05867	1.92327
C	-5.54999	1.29651	1.53507
C	-4.29332	1.81361	1.91348
C	-2.17720	0.88733	3.09313
H	-1.57602	1.61129	2.54574
H	-1.64893	-0.06211	3.05432
H	-2.18692	1.20556	4.13870
C	-3.99232	-1.71493	3.10724
H	-4.55724	-1.93834	4.01579
H	-2.93875	-1.74670	3.37516
H	-4.19393	-2.53981	2.41746
C	-6.75216	-0.99401	1.71591
H	-6.42429	-2.00042	1.45304
H	-7.42358	-0.65004	0.93576
H	-7.34891	-1.09261	2.62706
C	-6.64289	2.05405	0.84229
H	-6.29010	2.57788	-0.04680
H	-7.05690	2.82005	1.50409
H	-7.46402	1.41022	0.55231
C	-3.81491	3.21735	1.69342
H	-4.35663	3.91953	2.33321
H	-3.97277	3.56037	0.66883
H	-2.76187	3.32221	1.94239
C	-3.32456	-0.18081	-2.56084
C	-3.67255	-1.48960	-2.15554
C	-5.02072	-1.47615	-1.75625
C	-5.51738	-0.16270	-1.90240
C	-4.45866	0.64668	-2.38334
C	-2.01636	0.20872	-3.18822
H	-2.00862	-0.04413	-4.25135
H	-1.17947	-0.31362	-2.73290
H	-1.82064	1.27680	-3.11582
C	-2.80745	-2.72132	-2.24339
H	-3.14148	-3.49452	-1.55254
H	-1.76058	-2.50432	-2.03390
H	-2.84874	-3.15641	-3.24510
C	-5.83465	-2.69222	-1.38591
H	-6.05389	-3.29334	-2.27131
H	-6.78527	-2.41583	-0.93739
H	-5.31583	-3.34766	-0.68311
C	-6.95674	0.25586	-1.82635
H	-7.46385	-0.01518	-2.75683
H	-7.06470	1.32872	-1.70860
H	-7.49904	-0.23331	-1.02250
C	-4.57588	2.09743	-2.75259
H	-3.61619	2.51630	-3.04897
H	-4.97016	2.71234	-1.94002
H	-5.25282	2.23352	-3.59897
C	4.78848	-0.86486	2.13557
C	3.47833	-1.26486	2.46487
C	2.72662	-0.09694	2.65475
C	3.52961	1.02160	2.42868
C	4.82470	0.54513	2.11276
C	6.02544	-1.73708	2.09675
H	6.71697	-1.43828	1.31243
H	5.78546	-2.78555	1.96091
H	6.56132	-1.64692	3.04605
C	2.97204	-2.67336	2.68282
H	3.64814	-3.40703	2.24747
H	1.98917	-2.82549	2.24059
H	2.89408	-2.90035	3.74905
C	1.32448	-0.04869	3.21206
H	1.34676	0.15124	4.28622
H	0.80438	-0.99384	3.07082
H	0.72693	0.73986	2.75554
C	3.09243	2.45433	2.56966
H	2.09025	2.61151	2.16736
H	3.76516	3.13306	2.04739

H	3.06886	2.76565	3.61719
C	6.11514	1.33490	2.08437
H	6.70356	1.10352	2.97628
H	5.93989	2.40887	2.09969
H	6.74765	1.09776	1.22773
C	3.28795	-2.35272	-1.41931
C	2.73181	-1.37663	-2.25713
C	3.73523	-0.46740	-2.60339
C	4.92837	-0.87225	-1.99151
C	4.63960	-2.04382	-1.25726
C	2.50254	-3.56161	-0.99027
H	2.72913	-3.87765	0.02769
H	2.71594	-4.41367	-1.64200
H	1.43522	-3.36848	-1.03878
C	1.36288	-1.24803	-2.88851
H	0.59941	-1.79575	-2.33683
H	1.36222	-1.64199	-3.90764
H	1.05288	-0.20613	-2.94112
C	3.70285	0.61662	-3.64977
H	3.94822	0.20634	-4.63259
H	4.42844	1.39988	-3.43702
H	2.72347	1.08715	-3.74085
C	6.36515	-0.43554	-2.18989
H	6.91126	-0.40909	-1.24676
H	6.44510	0.55035	-2.64634
H	6.88642	-1.13549	-2.84689
C	5.59514	-3.09388	-0.72159
H	5.15716	-3.64832	0.10390
H	6.54735	-2.68724	-0.39604
H	5.80870	-3.81428	-1.51643
Dy	-3.73681	-0.05205	0.03518
Dy	3.24349	-0.17465	0.05586
N	-1.45320	-0.80665	0.36480
N	-1.45212	0.53909	-0.02601
N	0.89848	0.51827	-0.11204
N	0.90115	-0.79732	0.27931
O	-0.20821	2.38020	-0.61769
O	-0.15188	-2.64909	0.90605
O	3.68124	2.09287	-0.70620